Order Number 9511459

Effect of fines content on liquefaction potential of sands

Erten, Duygu, Ph.D.

Rutgers The State University of New Jersey - New Brunswick, 1994

U·M·I
300 N. Zeeb Rd.
Ann Arbor, MI 48106

EFFECT OF FINES CONTENT ON LIQUEFACTION POTENTIAL OF SANDS

DUYGU ERTEN

A dissertation submitted to the
Graduate School-New Brunswick
Rutgers, The State University of New Jersey
in partial fulfillment of the requirements
for the degree of
Doctor of Philosophy
Graduate Program in Civil and Environmental Engineering

Written under the direction of
Professor Mohamad H. Maher
and approved by

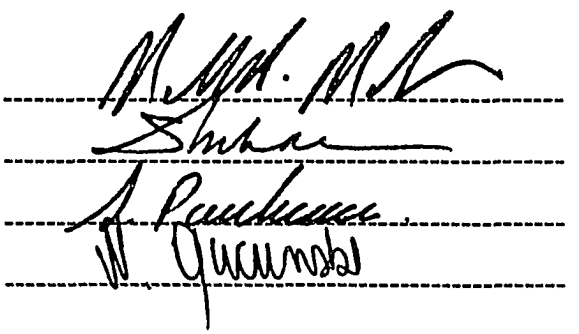

New Brunswick, New Jersey
October, 1994

ABSTRACT OF THE DISSERTATION

EFFECT OF FINES CONTENT ON LIQUEFACTION POTENTIAL OF SAND

By DUYGU ERTEN

Dissertation Director:

Professor Mohamad H. Maher

One of the most dramatic causes of damage to infrastructure during earthquakes is liquefaction of saturated sandy soils. While liquefaction has been reported in numerous earthquakes (Seed, 1968), the phenomenon has been more dramatically illustrated in the Niigata, Japan Earthquake of 1964, the Alaska Earthquake the same year and recently in the Loma Prieta Earthquake of 1989. An understanding of this phenomenon is critical for mitigation against severe damages to buildings and various superstructures during earthquakes.

The purpose of this dissertation is to investigate the effect of fines on liquefaction behavior of sand by using stress and strain controlled consolidated undrained cyclic triaxial tests. It is also aimed to provide a framework for understanding the stress-strain behavior silty sands and offer guidelines for future research. The second purpose of the dissertation is to compare the laboratory test data with a theory based on the density of dissipated energy during cyclic loading. The theory originally is used for pure sand. Here, it is modified to give closer approximations for the experimental findings on silty sand. The model was successsfully predicted the test results.

The resistance of soils with addition of 10% low plasticity and non-plastic fines compared to clean sand has small significance on the pore pressure generation of sand. Though adding 10% low plasticity fines slightly increases the resistance to liquefaction while addition of 10% non-plastic fines decrease the liquefaction potential. As non-plastic fines content increases up to a level of 30%, the liquefaction resistance decreases. There is a level of cyclic shear strain below which, there is little pore water pressure generation in saturated silty soils. This threshold strain level is similar to those observed in sands and is in the order of 0.01 percent.

It is anticipated that the outcome of this research will help engineers better understand the behavior of silty soils under seismic conditions and enable them to come up with a much comprehensive guideline or design against liquefaction of silty soils.

DEDICATION

Annem'e ve Babam'a

The principle of science, the definition, almost, is the following. The test of all knowledge is experiment. Experiment is the sole judge of scientific "truth". But what is the source of knowledge? Where do the laws that are to be tested come from? Experiment, itself, helps to produce these laws, in the sense that it gives us hints. But also needed is the imagination to create from these things the great generalizations-to guess at the wonderful, simple, but very strange patterns beneath them all, and then to experiment to check again whether we have made the right guess.

R. Feynman

ACKNOWLEDGEMENTS

I received much help and support from a number of people and I would like to thank them here. This project would not be completed without the constant guidance and encouragement of my thesis advisor, Dr. M.H. Maher. I thank him for suggesting the topic of this dissertation and valuable criticism of the manuscript during the preparation of this dissertation.

To Dr. N. Gucunski I thank for many friendly conversations and suggestions he has given me at various stages of my work.

To Drs. Y.S.Chae and S. Pamukçu, I like to thank for carefully reading this dissertation and their valuable comments, and their continuing interest in my work.

I also like to thank the Geotech group at Rutgers University, especially Dr.K.S. Ro, D. Brill, F. Jafari, N. Khodatoust, V. Ganji, R.E. Landau and N. Solar. I had numerous helpful discussions with them deepening my understanding of geotechnical engineering.

I like to thank to Civil and Environmental Engineering Department for the financial support they provided me all these years.

I also like to thank to PEO Board for providing me International Peace Scholarship.

Prof. T. Durgunoğlu receives special thanks for initiating my interest to geotechnical engineering. I also like to thank to Prof. E. İnan as being a role model for my academic

inspiration. Prof. A.Ş. Çakmak provided access to the facilities of Civil Engineering Department of Princeton University. I like to thank him here for all the support he gave me.

Finally, I want to thank my family and my husband Mehmet Artun for their constant love and support.

Duygu Erten

August 1994

Piscataway, NJ

TABLE OF CONTENTS

LIST OF ILLUSTRATIONS

FIGURE

LIST OF TABLES

TABLE

LIST OF APPENDICES

NOTATION

A_c	Consolidated Sample Area
a_{max}	Maximum Ground Surface Acceleration
a_p	Horizontal Peak Acceleration of the Ground Surface
B	Pore Pressure Parameter
C_u	Grain Size Distribution
C_v	Coefficient of Consolidation
D_r	Relative Density
Δu	Change in Pore Pressure
E	Elastic Modulus
e_{max}	Maximum Void Ratio
e_{min}	Minimum Void Ratio
$e_{skeleton}$	Skeleton Void Ratio
e_t	Total Void Ratio
ε_p	Volumetric Strain
ε_q	Triaxial Strain
ε_v	Single Amplitude Vertical Strain
G	Shear Modulus
G_s	Specific Gravity
g	Acceleration of Gravity
γ	Unit Weight of Soil
γ_t	Cyclic Threshold Strain
h_n	Total number of layers
h_t	Total height of the specimen
K	Bulk Modulus

μ	Poisson's Ratio
N_c	Number of Equivalent Stress Cycles
n	Number of layers being constant
n_i	First initial layer
n_t	Total number of layers
P_c	Cyclic Load
p'	Mean Effective Stress
q	Deviatoric Stress
ρ_w	Density of Water
r_d	Stress Reduction Factor
τ	Shear Stress τ_{max}
τ_{max}	Maximum Positive Shear Stress
S_r	Desired Cyclic Stress Ratio
σ_{max}	Maximum Allowable Total Stress
$\overline{\sigma}_i$	Initial Effective Stress
σ_c	Confining Pressure
σ_o	Total Stress
$\overline{\sigma}_c$	Effective Stress
σ_{dc}	Cyclic Deviatoric Stress
σ_h	Horizontal Stress
σ_v	Vertical Stress
U_n	% Undercompaction
U_{ni}	% Undercompaction selected for the first layer
U_{nt}	% Undercompaction selected for the final layer

I. INTRODUCTION

1.1 Prelimineries

1.1.1 Liquefaction, Initial Liquefaction, Cyclic Mobility

Liquefaction of soils is a complex problem on which a great deal of research has been done both experimentally and numerically. Liquefaction may be defined as a phenomenon associated with the rise of pore water pressure and loss of shearing resistance in soils. While liquefaction has been reported in numerous earthquakes, the phenomenon has been dramatically illustrated in the Niigata, Japan Earthquake of 1964, the Alaska earthquake the same year, Loma Prieta Earthquake of 1989 and recently in the Northridge Earthquake of 1994. Liquefaction effects in Loma Prieta area involved subsidence and loss of bearing of shallow foundations, with differential settlement, racking and tilting of two to four-story timber structures (O'Rourke et al., 1990). Throughout the marina district in San Francisco, there was direct evidence of soil liquefaction in the form of sand boils. Sand boils were observed on every street where there was damage to buildings and along curb lines, sidewalks and foundation bearing walls.

The liquefaction phenomena cause not only sand boils but flow failures, lateral spreads and various types of deformation. The word liquefaction does not refer to a single phenomenon, but rather to a complex set of interrelated phenomena that can contribute to the occurrence of unacceptable damage to buildings or other facilities during an earthquake. There is considerable disagreement in engineering profession about the use of the word liquefaction. The Committee on Soil Dynamics of the Geotechnical Engineering Division, ASCE defines liquefaction as a changing of state that is independent of initiating

disturbance that could be static, vibratory, sea wave, or shock loading, or a change in ground water pressure. In cohesionless soils, the transformation is from a solid state to a liquefied state as a consequence of increased pore pressure and reduced effective stress.

The word liquefaction was first used by Casagrande (1936) for the response of contractive sand under statically imposed stresses that leads to loss of strength which can cause flow slides. The pore pressure buildup was first investigated by Seed and Lee (1966) in sand subjected to cyclic loading; they extended the original definition to include dynamic loads. Seed (1976) defined initial liquefaction when the residual pore water pressure equaled to the applied confining pressure on completion of any full stress cycle. Initial liquefaction can also be produced by cyclic loading in medium dense and dense sands and is not limited to loose sands.

Casagrande (1975) defined the steady state deformation for liquefaction flow failure. Steady state deformation is the state in which a mass of particles deforming at constant volume, constant normal effective stress, constant rate of strain and constant shear stress. It is achieved only after all particle orientation effects reached a steady state condition and after all possible breakage. Liquefaction is only possible for this concept, when steady state strength is less than the driving shear.

Steady state concept later extended by Castro and Poulos (1977); and Poulos et al., (1985). This behavior is called as flow failure and accompanied by strain softening behavior. Poulos implied that cyclic load tests are unnecessary in determining whether a soil mass is susceptible to liquefaction flow failure and several monotonic tests are required in order to determine the position of the steady state line.

Generally speaking, all of the above conditions, a condition of zero effective stress, cumulative strains due to cyclic loading and steady state failure are described by the term liquefaction.

From the examination of the results of laboratory research on the subject, it is possible to distinguish two different phenomena; liquefaction and cyclic mobility. Casagrande (1975) and Castro (1975) suggested using the term cyclic mobility for the definition of liquefaction based on zero effective stress. Cyclic mobility as defined by Castro is the densification tendencies of a medium to high density soils during cyclic loading. Dilatancy occurs when particles start rolling and sliding over one an other under a constant volume which causes a reduction in pore pressure. If cyclic stresses are large enough, even dilative sands can lose strength and liquefy. Liquefaction flow failure and cyclic mobility are illustrated together in Fig. 1.1. Soils above the steady state line are contractive and susceptible to liquefaction flow failure. Either loaded monotonically or cyclically it will move towards point A and liquefy. Below the steady state line if the specimen is under cyclic loading, it will go to point B, the condition of zero effective stress and liquefy. If it is loaded monotonically then the loading path move towards the steady state line.

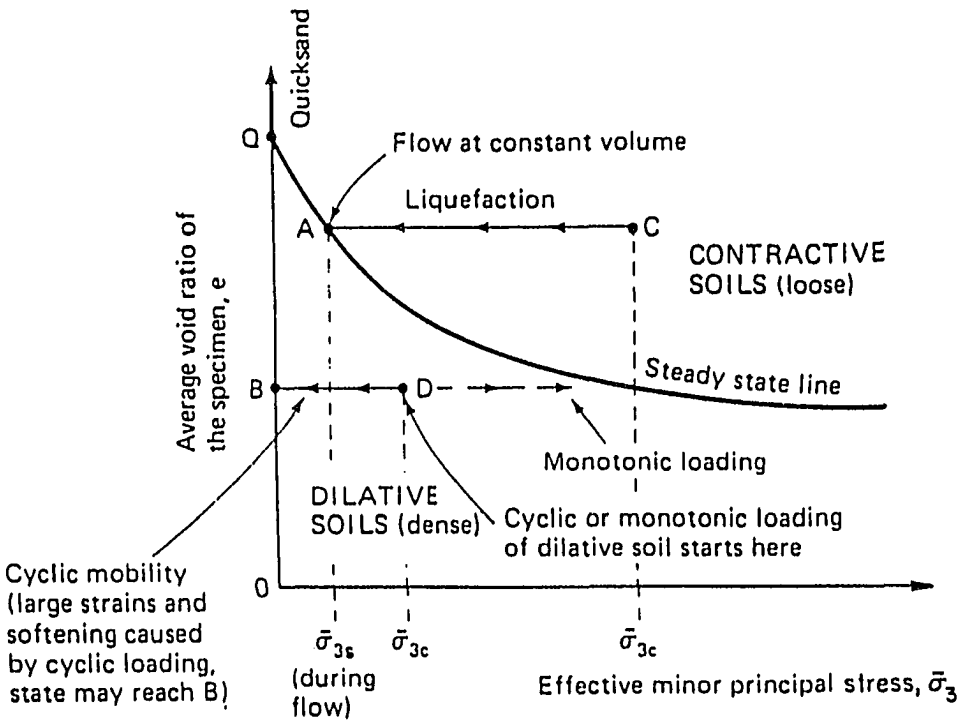

Figure 1.1 Steady State Diagram Showing Liquefaction Potential Based on Undrained Tests of Saturated Sands (after Castro and Poulos, 1976)

1.1.2 Definition

Stress controlled tests were run to a double amplitude strain of 15% or initial liquefaction, whichever occurred first. To represent failure of the soil for stress controlled tests, three criteria are used. These were a) 2.5% double amplitute strain b) 5% double amplitute strain c) initial liquefaction. 5% double amplitude strain was always accompanied by effective stresses being momentarily equal to zero for pure sand samples. Initial liquefaction which is the condition of zero effective stress is only observed for pure sand and could not be reached for silty sand specimens. It is accepted failure when residual shear stresses become excessive, even though $\Delta u \prec \sigma_c$ which means the pore pressure would not develop to the value of confining pressure that would be the case of initial liquefaction. So, it is concluded that the concept of initial liquefaction is not a satisfactory criteria for soils containing fines. The term liquefaction is used here to imply a certain degree of seismically induced softening of silty soils which is commonly defined in terms of the cyclic stress ratio to cause 5% double amplitude axial strain in the course of a certain number of load application. For strain controlled tests, the observed parameter was the pore pressure buildup. Tests were run to 1000 cycles or initial liquefaction whichever occurred first.

1.2 Motivation

There are controversial results on liquefaction of silty sands and the effect of silt content on liquefaction potential. Investigations on liquefaction potential of silty soils are limited, though there is an extensive amount of research done on liquefaction of pure sand. In the context of civil engineering projects for example, in the design and improvement of hydraulic fill properties, more knowledge on behavior of silty sands during earthquakes are needed. It is known that plasticity, the void ratio of the fine fraction and compaction

control the behavior of a fill. These factors all can be controlled during construction. In order to achieve a better seismic resistant construction under seismic loading, effect of fines content should be considered seriously. It is necessary to establish new rules for identification of liquefiable materials particularly for low to non-plastic soils because it is sometimes unsafe to use the available charts that classify liquefiable soils (Ishihara et al., 1980) for the low to non-plastic soils. These charts may also become very conservative for soils containing highly plastic fines. So an investigation of fines (passing #200 sieve), and reevaluating the boundaries for liquefiable soils is extremely important.

1.3 Objectives And Methods

Post earthquake investigations helped to understand the importance of predicting the response of soils under earthquake-type loading. Medium to loose cohesionless soils such as silty soils and fine sands are most commonly susceptible to liquefaction. The damages to buildings and earth structures from earthquakes may be correlated in several ways to the liquefaction which is related to the amount and type of fines in the soil.

Many natural and artificial sand deposits contain finer, more impervious silty layers. Sometimes, the sand itself may contain finer or siltier zones. The effect of these permeability changes, on liquefaction potential, is not yet thoroughly investigated. Mid-Chiba earthquake with a magnitude of 6.1 shook the area of Tokyo Bay in 1980. Recorded time change of pore pressures indicated that, there were differences in the rate of pore water pressure dissipation in different layers due to the fact that layers contained different amount of fines (Ishihara, 1988). The silty sand layer with 27% of fines was less permeable compared to 12% fines in the above layer. So the pore pressure dissipated by two times faster in the layer with 12% fines compared to layer with higher percentage of fines. In the

Chilean earthquake of March 3 1985, the liquefaction analysis on a hydraulic fill showed partial liquefaction might have occurred in the silty sand layer which was underlying pure sand. Boring data showed that the liquefaction of the sandy hydraulic fill was very extensive during this earthquake. But some of the layers which contained sand with higher fines content, did not liquefy or partially liquefied although liquefaction was more extensive for pure sand layers (Poran et al.,1989). It was also found that the presence of the silt or of a suitably fine grained layer at the surface was causing the generation of sand boils which are diagnostic evidence of liquefaction occurrence.

Several factors that control the development of liquefaction may be summarized as follows:

- Medium to loose cohesionless materials such as fine sand, silty sand, and sandy silt are the materials most commonly susceptible to liquefaction.
- Sediments most susceptible to liquefaction are poorly compacted sand fills and sands and silts deposited within the past few hundred years by fluvial, littoral or eolian processes.
- Liquefaction tends to begin at a magnitude threshold of about 5 and an intensity threshold of MMI V-VI. Seed et al., (1976) , used a weighing procedure to represent the equivalent number of uniform cycles, N_{eq} corresponding to different earthquake magnitudes and this earthquake magnitude corresponds to 5 cycles for 8 seconds of shaking.

The purpose of this dissertation is to investigate the effect of fines on liquefaction potential of sand by using stress and strain controlled consolidated undrained cyclic triaxial tests. It is also aimed to provide a framework for understanding the stress-strain behavior of silty sands and offer guidelines for future research. The concept of void ratio instead of relative density is used as a basis for comparison purposes for the whole testing program. The second purpose of the dissertation is to compare the laboratory test data with a theory based on the density of dissipated energy during cyclic loading. The theory originally is used for

pure sand. Here, it is modified to give closer approximations for the experimental findings on silty sand. The model was successfully fitted to the test results, and the main trends and results presented by the model for pure sand have shown to be valid for silty sands. Third objective is to evaluate the potential improvement of soil resistance to liquefaction by adding fines.

1.4 Scope And Outline Of The Dissertation

Chapter 2 of this dissertation presents a review of the previous research done to determine the liquefaction of sands with fines. It also presents previous research related to laboratory liquefaction investigations to evaluate the factors affecting the liquefaction potential and numerical models used to predict pore pressure generation. Chapter 3 describes the materials and equipment used for this research and presents the results of several laboratory tests that give a better insight to understand the engineering properties of the soils used. Chapter 4 presents the results of stress controlled consolidated undrained tests and discusses the stress controlled test results. Chapter 5 describes a soil model for predicting pore pressure build-up, thus leading to the assessment of the liquefaction potential of soils. The model predicts the pore water pressure in terms of the stress ratio and the number of cycles. Modifications to the model are made to improve the predictions for silty sand. Chapter 6 presents the results of strain controlled consolidated undrained tests and discusses the strain controlled test results. A summary of the dissertation, conclusions from test results and future work recommendations are presented in chapter 7. Appendix part contains the test results from cyclic triaxial tests and calibration outline.

II. REVIEW OF THE PREVIOUS RESEARCH

2.1 Introduction

The purpose of this literature survey is to review the existing research related to the cyclic behavior of sandy soils. In particular, cyclic triaxial testing is also reviewed in some detail to have a better understanding of stress conditions. Several models describing soil response under cyclic loading are also reviewed. The main topics of interest are:

1) Cyclic Tests
2) Factors Effecting Liquefaction Potential
3) Liquefaction Pore Pressure Models

2.2 Cyclic Tests

Cyclic tests were developed to simulate the field conditions in the laboratory. A laboratory test specimen of soil represents an element of a foundation, embankment, backfill, or slope. From the laboratory behavior of soil, the behavior of the field element is predicted. These tests also permit the evaluation of the material damping and shear modulus of soil. The shear modulus, G is usually expressed as the secant modulus determined by the extreme point on the hysteresis loop. The damping ratio, λ is defined as the ratio of the energy dissipated per loading cycle (area inside the hysteresis loop) to two times the maximum elastic strain energy stored in the soil element. The cyclic triaxial test is one of the methods developed to simulate the field conditions in the laboratory. Detailed description of the triaxial testing is given in chapter 3. There are a number of laboratory testing devices used for testing soils under cyclic loading beside triaxial device. Each of these devices have

different shearing strain amplitude capabilities. Fig. 2.1 summarizes laboratory techniques and corresponding shearing strain amplitude capabilities.

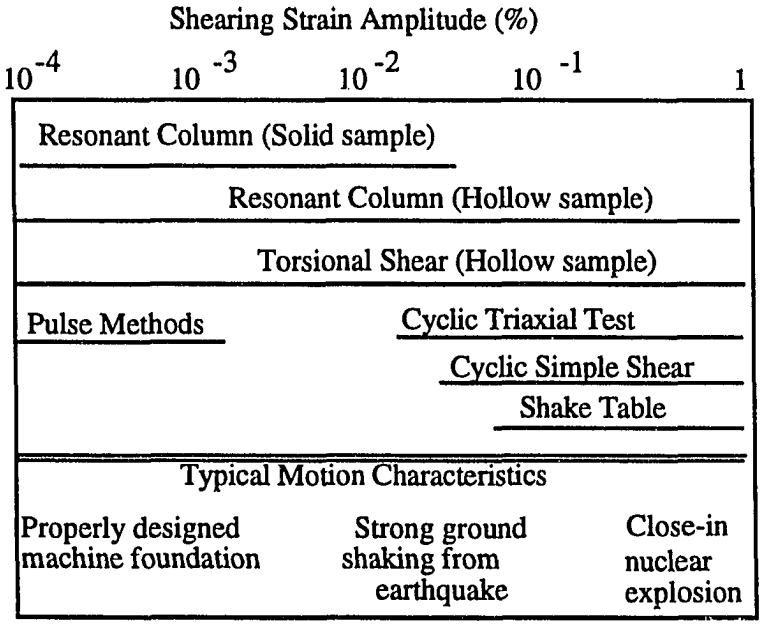

Figure 2.1 Shearing Strain Amplitude Capabilities of Laboratory Apparatus (after Woods, 1978)

2.3 Factors Affecting Liquefaction Potential

There are many factors that effect the results of cyclic triaxial tests. These effects can be investigated in two categories: material characteristics, test parameters and procedures.

2.3.1 Material Parameters Affecting Test Results

2.3.1.1 Effect of Soil Granulometry

Particle size, distribution and shape affect the cyclic strength, liquefaction susceptibility and displacement of soil particles. The grain size distribution is expressed by C_u and indicates the uniformity of the soil. Mean grain size is expressed as D_{50}, D referring to the size of the soil particle and 50 denotes the percent that is smaller. Lee and Fitton (1968), showed a strong dependence of liquefaction potential on mean grain size of the soil. As the mean grain size increases, the resistance to liquefaction also increases. On the other hand, analyses by Martin, Finn and Seed (1978) of the effects of membrane compliance on undrained test results indicate that mean grain size effects may be due almost entirely to the effects of membrane penetration. Data by Wong et al., (1975) as shown in Figs. 2.2 (a) and (b) summarize the effects of particle size on cyclic strength. As mean grain size increases from 0.1 to 30 mm. there is a 30 % increase in cyclic strength to cause 2.5 % strain. The cyclic strength increase is more pronounced for 10% strain. As the mean grain diameter passes 0.2 mm. which is the typical silt size, an increase in cyclic strength is observed. As fines are added to pure sand, the uniformity of the soil changes and the finer particles move into the voids between larger particles. Greater densification tendency in well graded soils increases the pore pressure generation and causes well graded soils act weaker than uniformly graded soils.

Comparison of cyclic loading strengths of uniformly graded and well graded soils can be seen in Fig. 2.3. From these graphs, it is obvious that the presence of fines impedes particle rearrangement during cyclic straining. In addition, the size of the voids of a uniform rounded sand is controlled by its particle size.

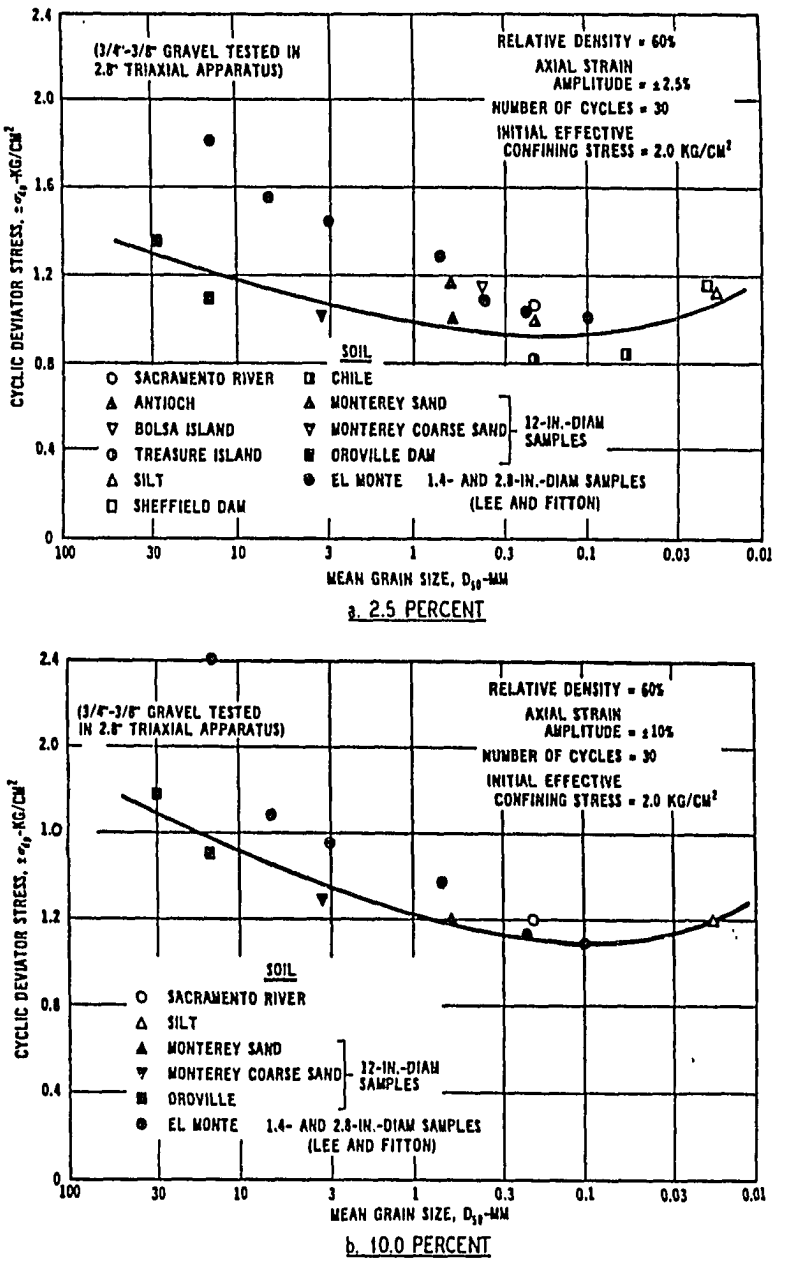

Figure 2.2 Cyclic Deviator Stresses Causing Axial Strain Amplitude For Different Grain Sizes a) 2.5% strainb) 10% strain (after Wong et al., 1975)

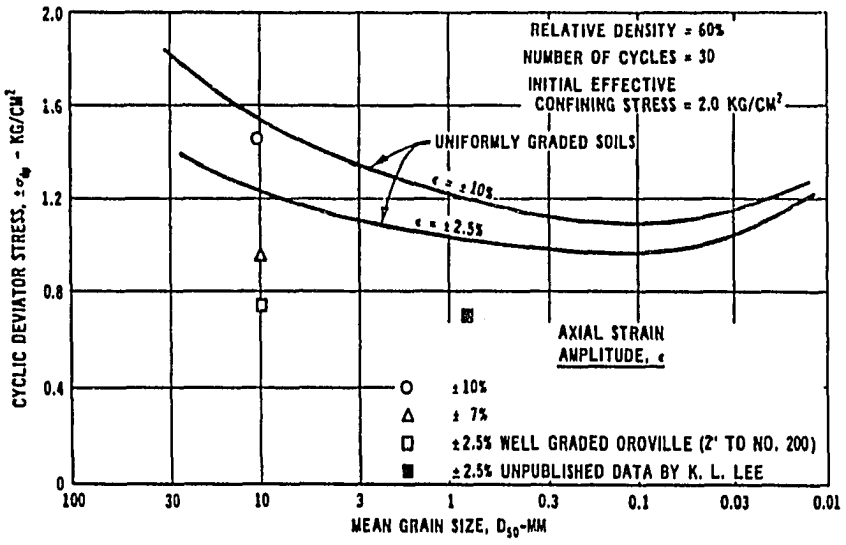

Figure 2.3 Comparison of Cyclic Loading Strengths of Uniformly Graded and Well-graded Soils (after Wong et al., 1975)

The presence of voids in the sand which is less coarser than the other are smaller in size but larger in number and has a more significant effect on the movement of pore water (Shen et al., 1977).

Grain shape (subrounded, subangular and angular) has also has an effect on the results. Castro (1977), Poulos et al., (1985) found that the slope of the steady state line is affected mainly by the shape of a given soil's grains.

2.3.1.2 Void Ratio

To express the denseness and looseness of the materials, the concept of relative density is used. But when the tested soils are made up of different soils which creates different grain

size distributions for different specimens, using relative density will not give reliable results. In view of this, void ratio was used to express the density of sands and silty sands in this investigation.

It is known that the cyclic strength required to cause liquefaction, increase linearly as void ratio decreases. Fig. 2.4 illustrates cyclic strength versus void ratio relationship of tailings sand. It may be seen that cyclic strength increases consistently with increase in the void ratio, although the sands tested came from entirely different mining sources. Compacting the specimen to the same void ratio is extremely important for comparison purposes.

Kuerbis et al., (1988) compared the results of cyclic tests based on the sand skeleton relative density. Sand skeleton relative density is calculated using $e_{skeleton}$ and e_{max} and e_{min}. This void ratio $e_{skeleton}$ can be calculated using the following expression:

$$e_{skeleton} = \frac{\left[V_t G_s \rho_w - (M - M_{silt})\right]}{(M - M_{silt})} \qquad (2.1)$$

where,

V_t = Total volume

G_s = Specific Gravity of soil

ρ_w = Density of water

M= Total mass

M_{silt} = Mass of silt

The relative behavior at different silt contents in terms of ASTM relative density of silty sand has the form similar to that in terms of void ratio i.e. the higher the silt content the

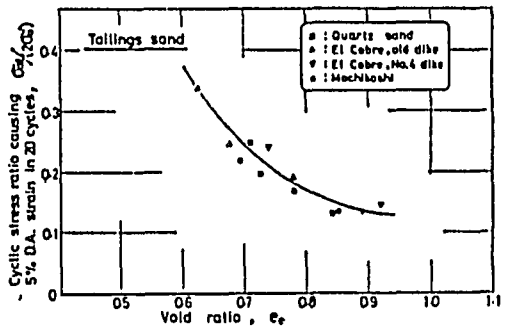

Figure 2.4 Cyclic Strength versus Void Ratio Relationship of Tailings Sands (after Ishihara et al., 1980)

lower is the cyclic resistance for a given relative density. An alternative comparison of cyclic resistance of silty sands as a function of ASTM as well as sand skeleton relative density is shown in Fig. 2.5.

Carrier (1988) simplified the formula for sand skeleton void ratio as follows:

$$e_s = \frac{e_t(SFR+1)+1}{SFR} \qquad (2.2)$$

SFR = sand-to-fines ratio, by dry weight

e_t = total void ratio (conventional definition)

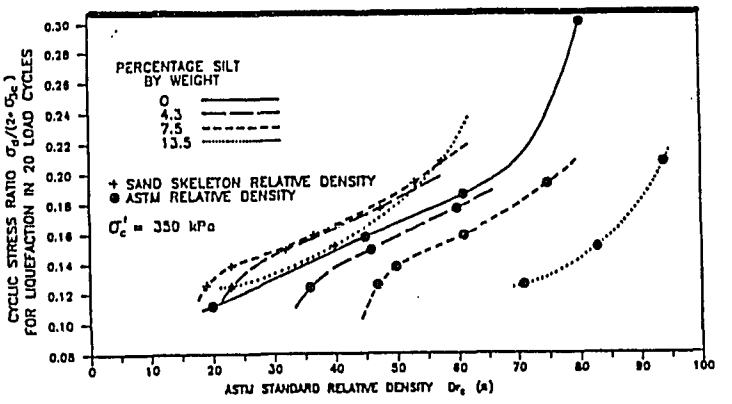

Figure 2.5 Variation of Silty 20/200 Sand Cyclic Strength With Relative Density (after Kuerbis et al., 1988)

Carrier mentions that the silty sand is gap graded, so e_t controls the behavior of the sand. Since gap grading can occur in a hydraulic fill and cause problems, one should be aware of consequences of using silty sand. Furthermore when the amount of fines are increased, and particularly if the fines are plastic, a transition occurs where the sand particles no longer control the behavior but are suspended in a matrix of fines. So the controlling void ratio is defined as:

$$e_f = e_t(SFR+1) = e_s SFR - 1 \qquad (2.3)$$

2.3.1.3 Fabric

The arrangement of physical components of a soil in relation to each other is called the fabric of the soil. Two soils can have the same fabrics but may still exhibit different properties due to different fabric stabilities. Fabric and stability together are called the

structure of the soil. In granular cohesionless soils, the interparticle forces are very small, both the fabric and structure of gravels, sands and to some extent silts are the same (Kovacs & Holtz, 1981).

Two soils having the same relative densities and void ratios may have different fabric structure and exhibit different engineering behaviors. Initial water content and method of sample preparation also changes the fabric of the soil. There are several techniques for preparing specimens. Fig. 2.6 makes it possible to see the effect of specimen preparation technique on cyclic soil strength by comparing test results for specimens prepared by wet tamping and dry tamping methods (Silver et al., 1976). It is seen that the specimens prepared by dry tamping method are much stronger than specimens prepared using the wet tamping method. The increase of the number of cycles with respect to decreasing stress ratio is more pronounced for specimens prepared by wet tamping. For samples prepared by pluviating dry sand through air for example, grains are packed with their longer axes in the horizontal plane, whereas in moist tamping the orientation of the grains is essentially random, in view of the capillary forces holding the grains together. In this case, the sample tends to have a more random fabric (Ladd, 1977). It is obvious that the choice of specimen preparation technique is important in determining the cyclic strength and stress-strain properties of sands.

Kaufman (1981), studied the effect of fines on cyclic shear resistance of the soil and found that the addition of silty fines affects the fabric and grain structure of the compacted soil specimens.

2.3.1.4 Plasticity Index

Plasticity index directly affects the results of liquefaction tests. Lee and Fitton (1969) have found that when soils contained large amount of plastic fines, their cyclic stress increase. They also performed cyclic triaxial tests on sands, silts, silty sands and coarse silty sands. They observed that clayey fines have tendency to increase the strength where silty fines have a tendency to decrease compared to sand alone.

Tsuchida (1970) studied the effect of amounts of fines especially cohesive fines and found that they slow the progress of particle rearrangement during cyclic straining.

Shen et al., (1977) presented the results of cyclic triaxial tests with two different types of standard Ottowa sand and plastic fines passing #200 sieve. Specimens prepared were controlled by dry density, all being packed to a dry density of 1.70 g/cm^3. His findings show that, for a given void ratio of the sand, where sand to sand contact is possible, the presence of plastic fines in the voids, would increase the resistance to liquefaction under cyclic loading and samples containing a small percentage of fines will liquefy.

Ishihara et al.(1980), found that the cyclic strength of fine grained tailings having a plasticity index in the order of 15 to 20 were shown to have much higher cyclic strength as compared to the non plastic tailings. Figs. 2.7 (a) and (b) shows the cyclic strength vs. void ratio relationship of low and high plasticity tailings.

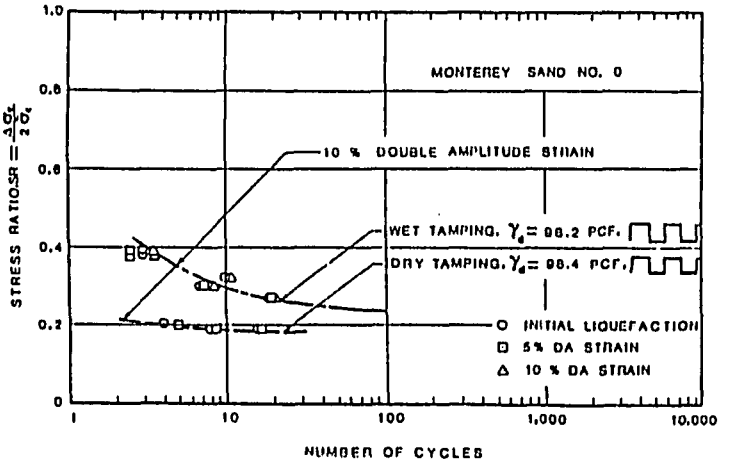

Figure 2.6 Effect of Sample Preparation Technique on Cyclic Strength of Test Sand (Silver, 1976).

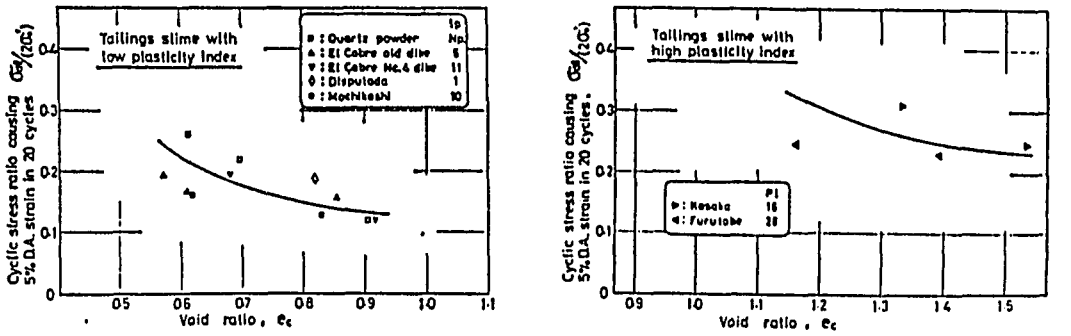

Figure 2.7 a) Cyclic Strength Versus Void Ratio Relationship of Low Plasticity Tailings Slimes b) Cyclic Strength Versus Void Ratio Relationship of High Plasticity Tailings Slimes (after Ishihara et al., 1980).

2.3.2 Test Parameters and Procedures Affecting Test Results

2.3.2.1 Effect of Cyclic Prestraining

Once a specimen is liquefied, it is more susceptible to liquefaction even though it might be reconsolidated and have a denser structure So previous strain history should be taken into consideration when dealing with soils (Finn et al., 1970). On the other hand when a specimen is subjected to small strains (<0.01%) prior to cyclic loading, consolidated and stresses are reapplied, it is more resistant to liquefaction. This increase in liquefaction resistance can be attributed to particle rearrangement within the specimen and increased interlocking of particles.

In particular, the liquefaction potential of saturated undrained granular bodies, as well as their tendency toward densification under drained conditions, may be altered dramatically by suitable prestraining which results in a change of granular fabric (Finn 1970, Ishihara 1975, Nemat-Nasser 1982).

2.3.2.2 Degree of Saturation (Capillary Effect)

It is widely recognized that 100% saturation is necessary to obtain reliable results from liquefaction tests. It may be seen from Fig. 2.8 that a slight reduction in degree of saturation results in a significant increase in the stress ratio to cause initial liquefaction in a given number of cycles, a fact that reinforces the necessity for full saturation in liquefaction testing.

2.3.2.3 Effect of Backpressure

Soils that are or will be saturated in the field should be tested in the laboratory under saturated conditions. Saturated specimens and pore pressure lines are necessary for accurate pore pressure and volume change measurements (Brandon et al., 1990). An elevated backpressure is used to produce complete saturation in various types of laboratory test specimens. After increasing the backpressure, the degree of saturation is monitored during and at the end of the process by measuring the B value. Back pressures have a significant effect on the liquefaction resistance of the tested sand. The higher the applied back pressure, the higher the liquefaction resistance of sand (Xia and Hu, 1991). Fig. 2.9 shows the liquefaction resistance of the five sets of samples. If soils are saturated using backpressure, the back pressure value should be increased to the same value for all the samples for comparison purposes.

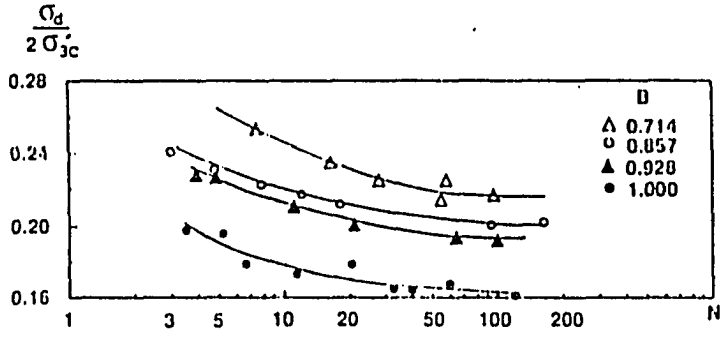

Figure 2.8 Effect of Degree of Saturation (after Xia and Hu, 1991)

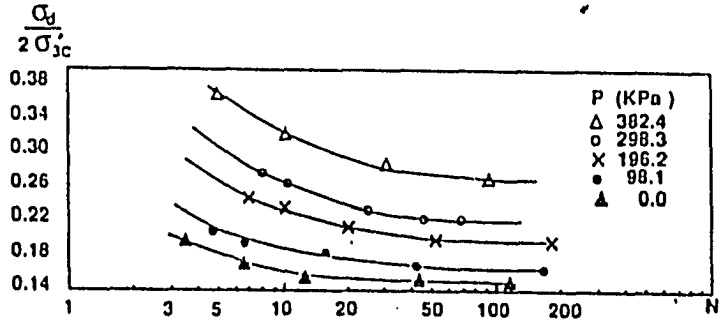

Figure 2.9 Effect of Back Pressure (after Xia and Hu, 1991)

2.3.2.4 Confining Pressure

Typical effects of confining stress are showed in Fig. 2.10. As the confining stress is increased, the value of peak cyclic stress is required to fail the sample in a given number of cycles.

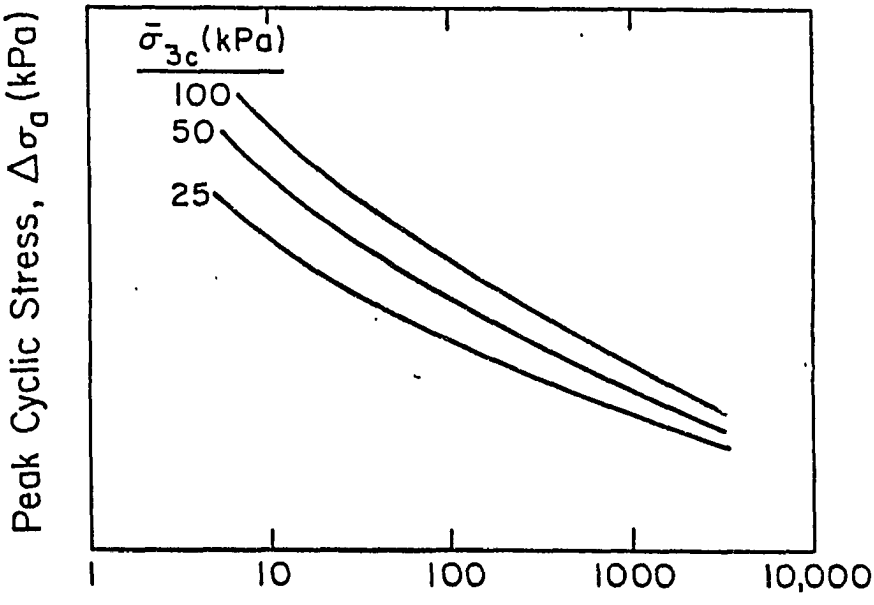

Figure 2.10 Generalized Relationship Between Peak Cyclic Stress and Number of Cycles to Cause Cyclic Mobility Failure (after Holtz and Kovacs, 1981).

Castro and Poulos (1976), Pyke et al., (1978) showed that the stress ratio decreases with increasing confining pressure for various void ratios and soil types. The magnitude of this decrease depends on several factors such as void ratio, type of soil and specimen preparation method.

2.3.2.5 Effect of Loading Frequencies

It can be said that using a range of frequencies between 1 and 60 cpm have minor effects on cyclic strength of cohesionless soils. Lee and Fitton (1969), Lee and Focht (1975), Mulilis (1975) and Wong (1972) have studied the frequency effects over a range of 1 to 60 cpm. Lee and Fitton found that slower frequencies gave slightly lower strengths than higher frequencies (< 10 %). Chang et al., (1982) investigated the frequency effects on the cyclic behavior of sand using both stress and strain controlled tests. Frequency range was from 0.0001 to 1 Hz. The result of the stress controlled tests indicated that using high frequencies increases the number of cycles to cause liquefaction. On the other hand strain controlled tests showed almost no change in the results. So it can be said that, a high frequency test allows less time for a sample to deform than a low frequency test. At frequencies greater than 0.01 Hz., the number of cycles to liquefaction increases with increasing frequency.

2.3.2.6 Effect of Specimen Preparation Method

For cohesionless soils, reconstituted samples are used for testing. There are several methods to prepare a specimen for testing. Mulilis (1977) performed an extensive study on sample preparation techniques which directly effects the results of the tests. Fig. 2.11 indicates several methods used to compact a sample and how the cyclic strengths vary

obtained from the different preparation techniques. Mulilis et al., (1978), also presented results concerning effects using a procedure of undercompaction during specimen preparation.

De Gregorio (1986) investigated the effects of several sample preparation methods on stress strain behavior of Ottowa Sand. From the consideration of all the tests, it appeared that the method of sample preparation, affects the stress-strain behavior, the pore water pressure response, the peak deviator stress, the steady state deviator stress, the steady state effective minor principle stress in load controlled CIU triaxial tests.

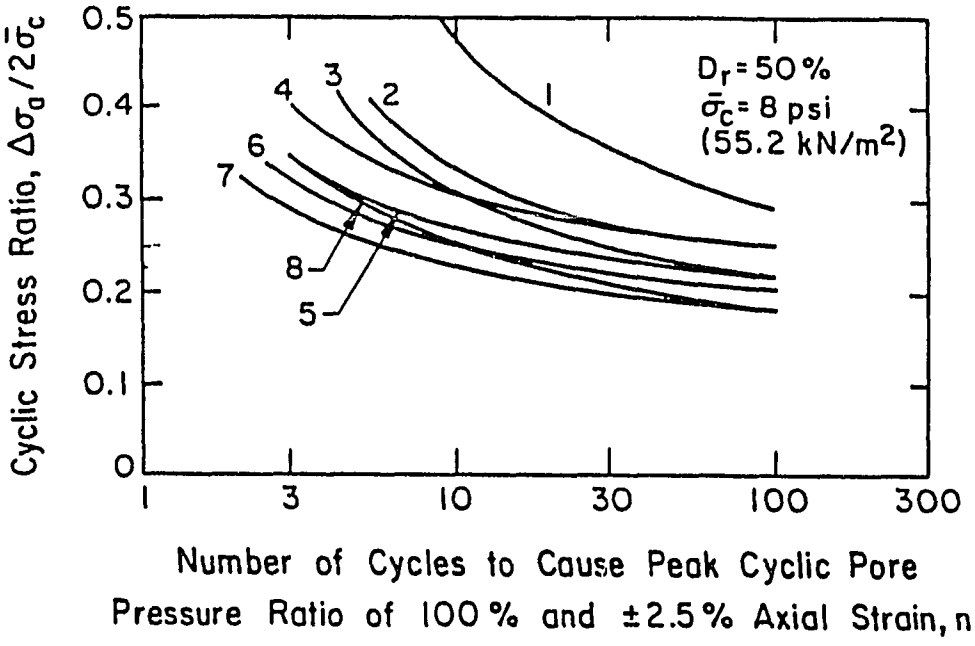

CURVE #	METHOD OF COMPACTION
1	High Frequency vibrations on moist samples
2	Moist Tamping
3	Moist Rodding
4	Low frequency vibrations on dry samples
5	High frequency vibrations on dry samples
6	Pluviated-water
7	Pluviated-air
8	Dry Rodding

Figure 2.11 Cyclic Stress Ratio vs. Number of Cycles for Different Compaction Procedures (after Mulilis, et al., 1977)

2.4 Previous Findings on Effect of Fines Content

Kodera (1964) pointed out that some piers of Arakawa Bridge on clean sands settled during the Kanto Earthquake of 1923 considerably more than those on silty sands, despite the fact that SPT N values for the latter were smaller, probably because the clean sands were sensitive to vibration. According to his findings cleaner sands containing less than 8 percent fines suffered much larger settlements than the silty sands with more than 20 percent fines. Terzaghi and Peck (1967) observed that silty sands can undergo rapid displacements and liquefy.

Shen et al., (1977) performed a laboratory investigation to study the effect of fines (passing #200 sieve) on liquefaction potential of isotropically consolidated Ottowa sands under cyclic triaxial loading. All specimens were statically compacted to a dry density of 0.70 g/cm^3. A cyclic sinusoidal load with frequency of 100 cycles per minute was applied to the specimen by a double acting pneumatic loading system. D_{50} for ASTM C-109 was 0.4 mm and for ASTM C-190, 0.8 mm. Liquefaction of the specimen was defined as the number of cycles required to cause a sudden loss of strength. Test results for specimens with different amounts of fines are shown in Figs. 2.12 (a) and (b). Both figures show the same pattern where specimens containing a relatively small percentage of fines are stronger against liquefaction under cyclic loading. This appears to be true for specimens having sand to sand contact. A maximum obtainable void ratio of 0.85 of the sand structure is reached when the amount of fines reaches 15-17.5% by weight. Beyond this void ratio, they assumed that the resistance to liquefaction of the soil mass is no longer dominated by the packing of the sand particles.

It is also observed that for a given void ratio of the sand structure, the specimens with fines are stronger than the corresponding pure sand specimens, based on a comparison made on the void ratio only. When the same specimens are compared based on a given relative density of the sand structure, the lower the relative density the greater is the strength increase. The difference in stress ratio vs. cycles to failure in Fig. 2.13 (a) and (b) may be attributed to such factors as the size of the voids, the ease of pore water movement in the voids, and the liquefaction potential of the pure sand itself. The presence of fines in the voids tends to retard the movement of water, requiring an increase in cycles to cause liquefaction at a given stress level. But this study did not consider the factors such as size gradation, grain shape, types of fines, etc.

Seed and Idriss (1981), found that recent studies in China have shown that certain types of clayey materials may be vulnerable to severe strength loss as a result of earthquake shaking. These soils have fines less than 15%.

Kaufman (1981) determined the liquefaction potential of silty sand by triaxial tests. The percentage of silt and sand in the specimens, as well as their void ratios, were systematically controlled. The sand gradations were of mean grain size, D_{50}, equal to 0.85 mm, but different from each other in that their coefficients of uniformity, C_u were approximately equal to 2 and 8. Silt was then added so that samples of each sand were formed containing 0, 10, 30, 60 and 100 percent silt, 20 samples all. Testing of the sands containing no silt was previously conducted by Yeh (1981). Test specimens were formed from the remaining 16 samples using a moist tamping method. Specimens were remolded to a predetermined void ratio, based on the condition of 50% relative density for the sand with no fines.

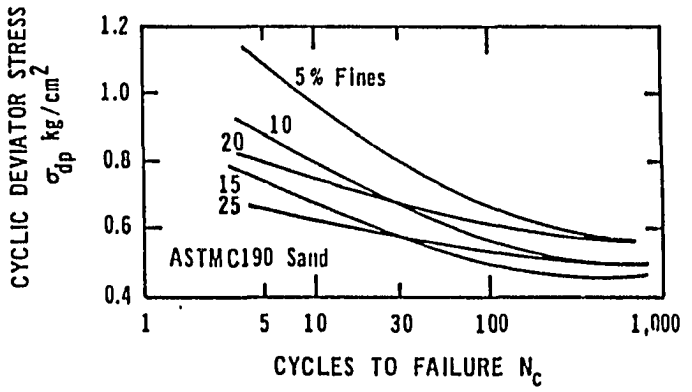

(a)

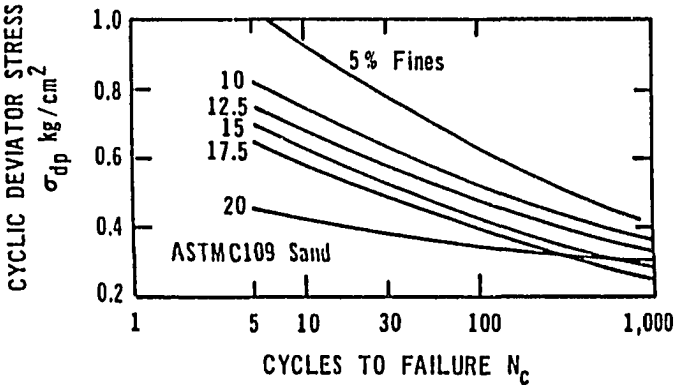

(b)

Figure 2.12 Cyclic Deviator Stress vs. Cycles to Failure a) ASTM C-190 Sand With Fines b) ASTM C-109 Sand With Fines (after Shen et al., 1977).

Thus no matter what the fines content of the specimens were, all specimens originating from any single sand gradation were remolded to a single value of void ratio. The specimens were subjected to cyclic triaxial strength until a condition of total failure was reached as judged by the attainment of 20% double amplitude axial strain. Results showed that the presence of silty fines affect the cyclic shear resistance of a soil. But because of serious effects from membrane compliance, the magnitude of cyclic load required to induce failure in the soil specimen is overestimated. No reliable quantitative means at that time existed for correcting the test results. So, he concluded that the fines strengthen the sand but they may even weaken it (Kaufman, 1981).

Tokimatsu and Yoshimi (1983) indicated that sands containing more than 10% fines, has much greater resistance to liquefaction than clean sands with same SPT N-values. Silty sands containing more than 10% fines with SPT-N values greater than 20, or sandy silts with more than 20% clay would not liquefy. A triangular classification chart for the liquefied soil data is given in Fig. 2.14. It is interesting to note that more than half of all liquefied data fall within a range of fines content less than five percent and that none of the soils containing more than 20% clay has suffered serious strength loss due to liquefaction. It is also noted that soils with more than 60% fines, many of which must contain more than 20% clay, hardly liquefied. Using the fines content as an index parameter for estimating the liquefaction resistance has the following advantages:

1-)The fines content is better correlated than the mean grain size with the degree of damage due to soil liquefaction.

2-)And the fines content is probably better related with soil consistency which in turn is related to undisturbed shear strength of soil.

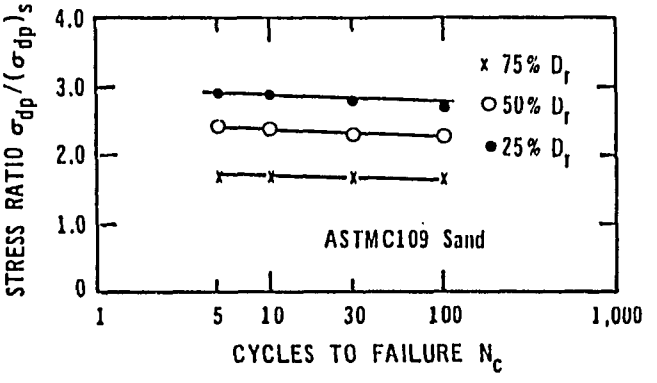

(a)

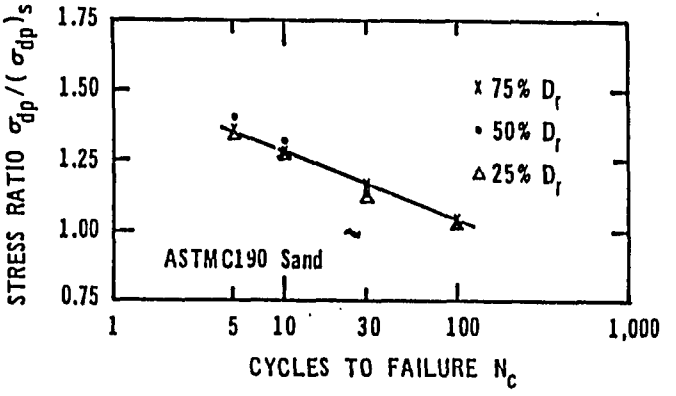

(b)

Figure 2.13 Increase in Cyclic Strength For Specimens With Fines a) ASTM C-190 Sand b) ASTM C-190 Sand (after Shen et. al., 1977).

Sherif, Tien and Pan (1983) conducted liquefaction experiments with torsional shear using sand and low plasticity (PI=4) silt mixtures. C_u value for the sand used was 1.75 mm. and silt was 0.03 mm. Results from tests showed that the addition of less than about 35% fines to sand increases the liquefaction potential of pure sand. Increasing the amount of fines content above this value, decreases the liquefaction potential of the sand. When the amount of fines in the sand-fines mixture reaches a state where sand to sand contact is not a predominant feature, the deformation characteristic of specimen is controlled by the fines leading to reduction in resistance to liquefaction potential.

Tokimatsu and Yoshimi(1983) and Seed et al.,(1984) studied the relationship between the SPT value and the fines content. Their findings say that for a constant SPT value, continuous increase in liquefaction resistance depends on increasing the fine content of the soil.

Tokimatsu and Yoshimi (1983) indicated that sands containing more than 10% fines, has much greater resistance to liquefaction than clean sands with same SPT N-values. Silty sands containing more than 10% fines with SPT-N values greater than 20, or sandy silts with more than 20% clay would not liquefy. A triangular classification chart for the liquefied soil data is given in Fig. 2.14. It is interesting to note that more than half of all liquefied data fall within a range of fines content less than five percent and that none of the soils containing more than 20% clay has suffered serious strength loss due to liquefaction. The above discussion can be summarized as:

1-) Sands with fines have much greater liquefaction resistance than the clean sands with the same SPT N value, and this tendency increases with increasing fines content,

2-) Liquefaction with catastrophic failure would not occur for clean sands with SPT N value greater than 25 and this critical value decreases with increasing fines content.

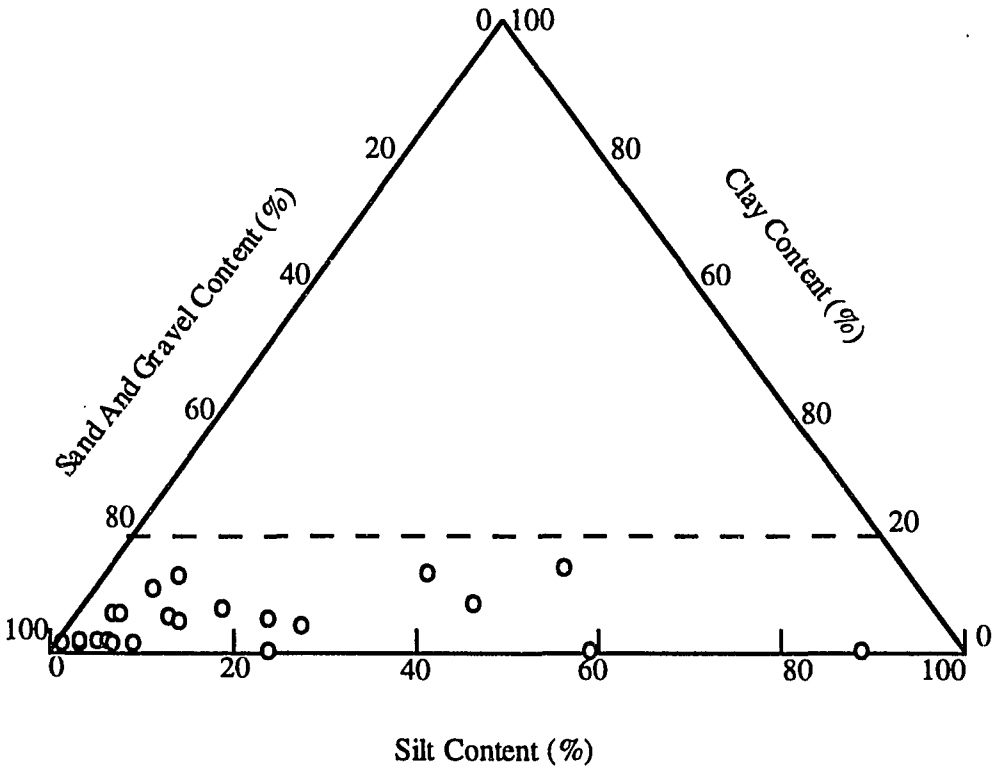

Figure 2.14 Triangular Classification Chart For Liquefied Soils (after Tokimatsu and Yoshimi, 1983).

Seed et al., (1984) presented his field observations as graphs showing silty sand curves containing different amounts of fines between stress ratio causing liquefaction and corrected blow count (Figs. 2.15 and 2.16). The number alongside of each data point is the actual fines content. Clearly there are a number of instances of non liquefaction that lie above these curves. These graphs are useful in confirming the influence of different amount of fines upon the relationship of liquefaction resistance and penetration resistance.

Seed, Tokimatsu, Harder and Chung(1984) presented the same liquefaction resistance curves for sands with different fines content and different N values. Two set of graphs which the amount of fines are smaller than 5% and greater than 5% are given as before. The results are in good agreement with Tokimatsu and Yoshimi (1983). As the percentage of fines increases, resistance to liquefaction decreases for the same SPT N value.

Preliminary analysis using regression methods (Liao, 1986) confirms that there is statistically significant effect of fines and fines content on liquefaction susceptibility of a deposit, and it is clear that ignoring the presence of the fines can be conservative and that fines content should be noted in evaluating the liquefaction potential.

In 1985, The Committee on Earthquake Engineering summarized the areas that still required research on liquefaction and among these needs were the study of soils other than clean sands, including soils with a content of cohesive fines.

Troncoso (1986), found that soils with about same relative density but with different fine content presented very different behavior. He concluded that the silty sand is contractive and therefore, develops high increments of pore pressure leading almost to liquefaction, while clean sand is strongly dilative. Fig. 2.16 summarizes the critical state curves drawn from the results of monothonic triaxial tests for different effective confining stresses for two different samples. Critical state curves of silty sands and of clean sands indicate a higher resistance to liquefaction of the clean material.

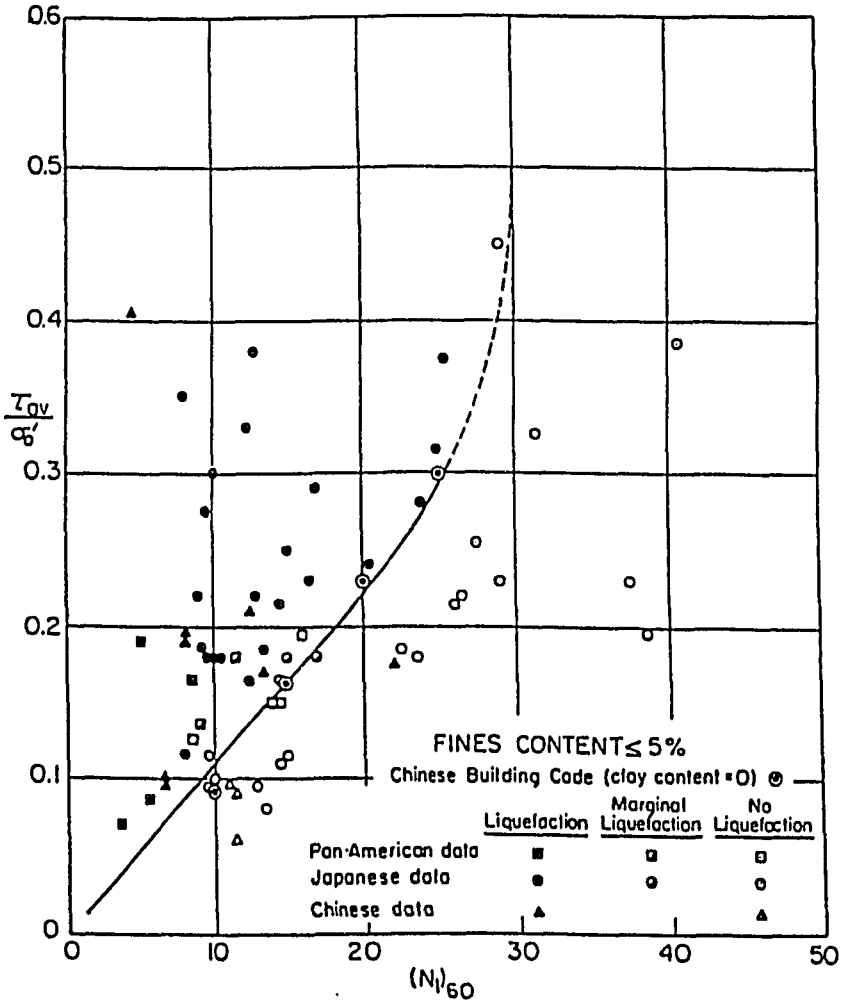

Figure 2.15 Relationships Between Stress Ratio Causing Liquefaction and N Values For Clean Sands For M = 7-1/2 Earthquakes (after Seed et al., 1984).

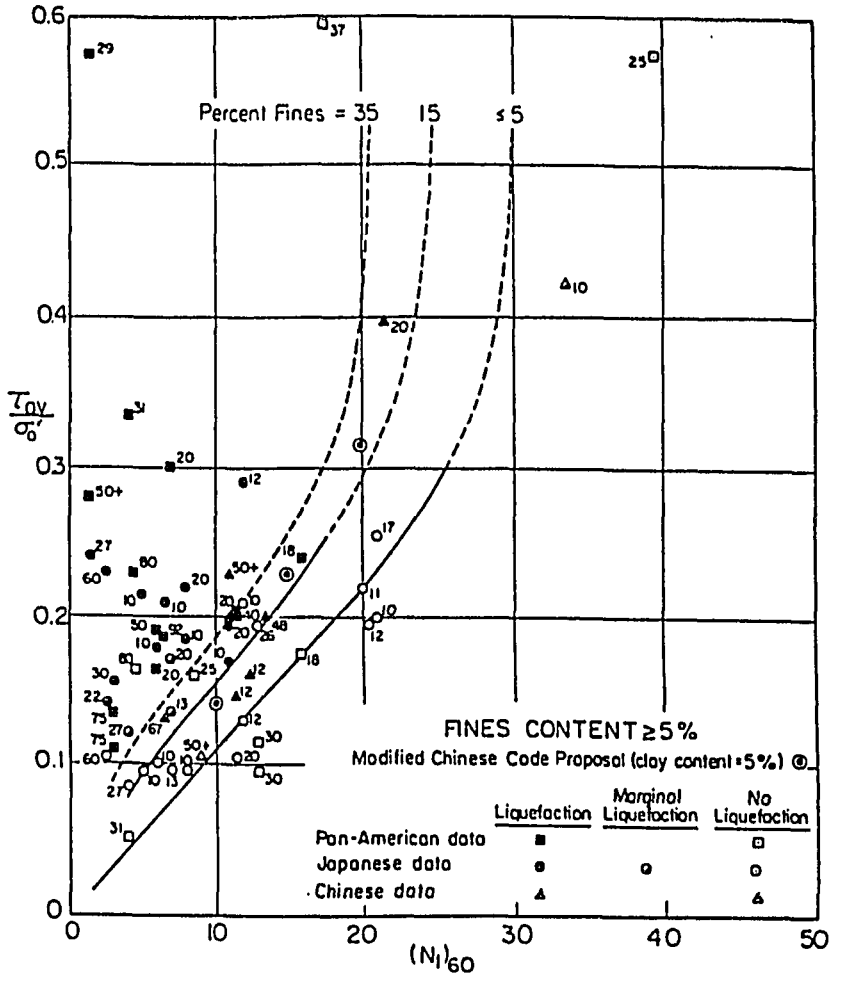

Figure 2.16 Relationships Between Stress Ratio Causing Liquefaction and N Values For Silty Sands For M = 7-1/2 Earthquakes (after Seed et al., 1984).

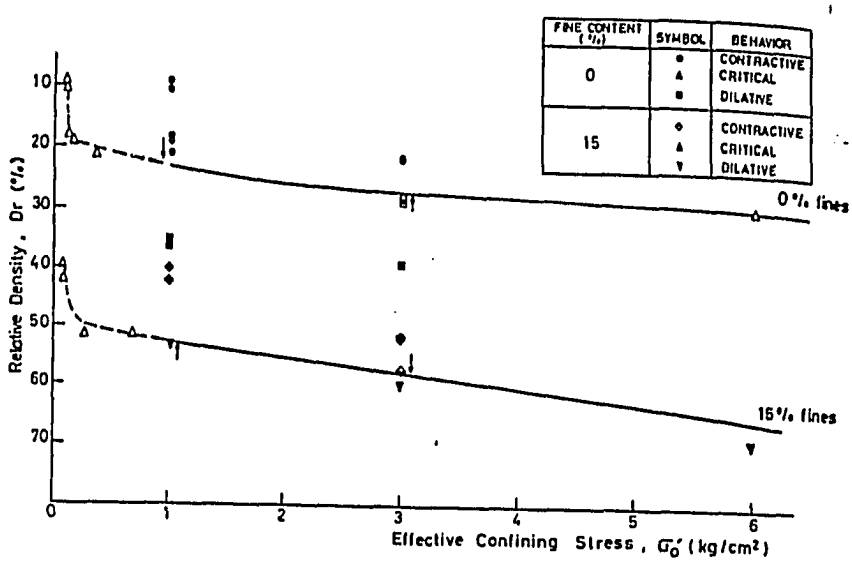

Figure 2.17 Critical State Curves of Tailing Sands (after Troncoso, 1986)

Dobry et al., (1985) conducted undrained strain controlled cyclic torsional tests. The three soils tested were from the same deposit but had different plastic silt contents of 13%, 32% and 63% respectively. The steady lines obtained from these cyclic and monotonic tests were different for the three sands, with the slopes of the lines becoming flatter as the sand become siltier.

Liao (1986) and Liao, Veneziano and Whitman (1988) developed statistical models and studied the effect of soil gradation variables (such as fines content, gravel content) on the liquefaction probability. Liao (1986) presented that if there is a continuous effect of fines content, the increases in liquefaction resistance due to fines content are already at a maximum once fine content exceeds about 12% to 15%. Therefore, with a certain N

value, a soil with fine content value 30% would have no more additional resistance to liquefaction than soil with fine content 15%.

Stewart and Walker (1989), studied the cyclic undrained behavior of non plastic and low plasticity silts. An important finding was the similarity between silts and sands in the magnitude of pore pressure response with varying strain level. This indicates that loose silt deposits which are currently considered safe from liquefaction on the grounds that their grain size distribution curves are outside the generally accepted boundaries for potentially liquefiable soils, should be reevaluated.

As seen from the above observations based on laboratory tests, conclusions drawn on the influence of fines on liquefaction resistance are contradictory and not clear.

2.5 Theoretical Models For Cyclic Behavior Of Sandy Soils

In recent years, numerous approaches and soil models have been proposed in order to predict pore-pressure buildup, thus leading to the assessment of liquefaction potential of soils by several researches such as Ishihara et al., (1975), Martin et al., (1975), Seed et al., (1976) Bazant and Krizek, (1976), Liou et al., (1977), Prevost and Höeg (1977), Ghaboussi and Dikmen, (1978), Zienkiewicz et al., (1978), Nasser and Shokooh (1979), Sherif and Ishibashi (1982). The major problem associated with many of these methods is the determination of material properties. Some of the models are also too complex to understand. A model should predict the pore pressure generation using the basic fundamental concept of liquefaction and also use soil parameters that effect the liquefaction potential.

Ishihara's model was based on a number of postulates or assumptions about the behavior of sand under cyclic loading. Results were used to predict the behavior of sand under triaxial test conditions. But his model is in direct conflict with the critical state model proposed by Schofield and Wroth (1968). The assumption that unloading and reloading within previously established yield loci is elastic and does not result in changes in pore-water pressures or effective stresses is not supported by experimental data.

Martin et al., (1975) developed a theory for evaluating pore pressure buildup and subsequent dissipation in sand deposits both during and following a period of earthquake shaking. The model was developed for the analysis of level ground conditions and its parameters are determined by cyclic shear tests. The model requires reliable data on shear modulus and volume changes. This model today is being used in practice.

Ghaboussi et al., (1977) modified the Ishihara stress path model. The effective stress path for undrained loading is assumed to be a quarter ellipse and major and minor axes of the ellipse are a function of relative density and grain shape. During excitation the pore-water pressures are allowed to diffuse in the Ghaboussi analysis. This has the effect of reducing the elastic traps on pore pressure increases but does not remove their limiting effects on pore pressure development.

Liou et al., (1977) used a Ramberg-Osgood stress-strain law to model the soil. There are inconsistencies involved with the use of elasticity assumptions in this model. More experimental verification of all the basic assumptions used in this model are needed.

Prevost and Höeg (1977), first applied the concept of kinematic hardening in addition to isotropic hardening to soils. Using isotropic theory predicts only elastic behavior during

unloading. This theory undoubtedly predict correct behavior but it is still not known whether it can give quantitative predictions.

Theories of Bazant and Krizek used the endochronic formulation of strains. The residual volumetric strains were expressed by a damage parameter κ. Zienkiewicz et al (1978) found that the damage parameter was related to the length of total strain path in cyclic simple shear tests. Endochronic formulation is not an other pore-water generation model. It is an other way of describing volume change. Any advantages of the method relate only to the convenience of the mathematical formulation. Zienkiewicz et al. took into account the effects of increasing pore-water pressures on the yield criterion, but not on the elastic moduli. The only problem about this method is the stress-strain law used. A non-associative theory of plasticity with isotropic hardening for dynamic response analysis is still been questioned.

The model proposed by Nasser and Shookoh (1978) uses a simple dimensionless analysis and several physically motivated assumptions to predict the pore pressure generation. The model predicts the pore pressure generation in terms of void ratio, number of cycles, confining pressure and other relevant parameters. The model will be explained in chapter 5 in more detail.

III. EXPERIMENTAL PROGRAM

3.1 Introduction

A two stage testing program is completed in order to understand the cyclic undrained behavior of silty soils. All tests are run by a triaxial testing device built by C. K. Chan (1981). The system is a modification and extension of the CKC e/p cyclic triaxial testing system which was initially designed for the purpose of performing cyclic loading to study the liquefaction potential and cyclic mobility of soils (ASTM D-2850). Before starting the testing program, the equipment is checked to see if it meets the required standards.

3.2 Experimental Program

3.2.1 Triaxial Testing Device

The axisymmetric apparatus, known as the triaxial test operates using a simple arrangement. A photograph and a schematic diagram of the automated systems are shown in Figs. 3.1 and 3.2. It consists of a load frame together with a triaxial cell and a loading piston, a volume measuring device with three pressure transducers, a dual pneumatic loading system, a signal conditioning unit, a process interface unit, a microcomputer, and a dot matrix printer.

A total of five sensors are used in the system. These are, a load cell to monitor the axial load, and LVDT to measure the vertical displacement, and three pressure transducers to detect the chamber pressure, the effective pressure, and the volume change. The conditioned output signals of these sensors are then received by the process interface unit

which is one of the main hardware items of the system. The process interface, as a peripheral device, forms communication link between the computer and the loading system. The unit consists of a 16-loading channel, 12 bit, high speed A-D converter, 8 channels of 12-bit, high speed D-A converters and a 24-channel digital input/output port. The D-A converter channels can also configured as gain controllers to suit specific purposes of a designed system.

For the automated triaxial testing system, nine channels of the A-D converters are used. Five channels are used to monitor the signals from the five sensors equipped with the system. One is to monitor drainage conditions, the other two are used to monitor e/p valve drive signals; and other one as a zero reference to minimize the zero shift of the grounded system. The D-A converters are configured to two high resolution controllers to control the axial load and lateral pressure, respectively.

The microcomputer with disk drives and high resolution graphics serves as the brain of the whole system. It receives and stores the real time data in its memory and issues control signals to regulate the testing process accordingly. Through the keyboard and the display screen the computer provides the means for effective and convenient interaction between the operator and the testing system. The computer also performs other functions such as data reduction, data processing, etc.

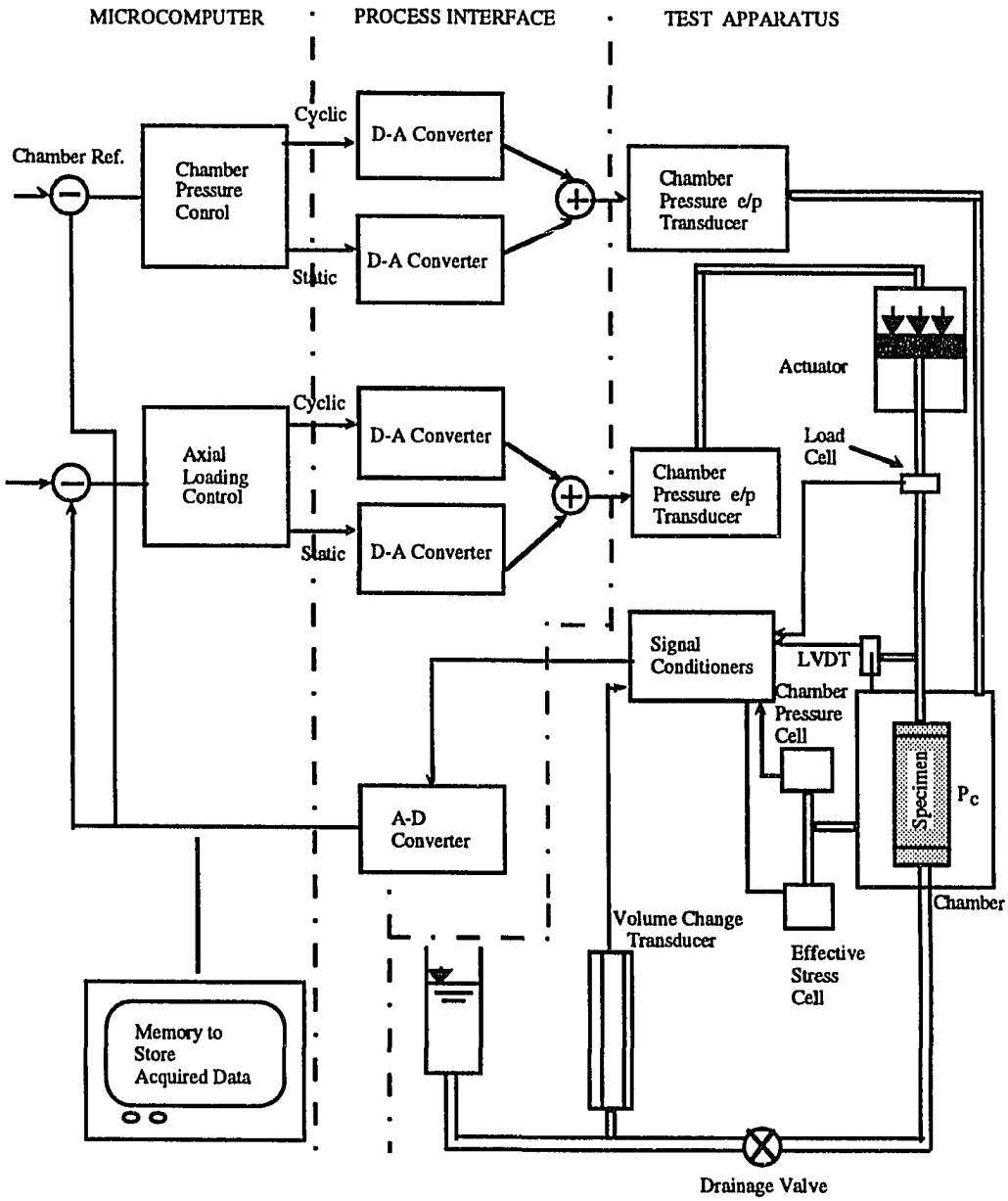

Figure 3.1 Schematic Diagram of The Automated System

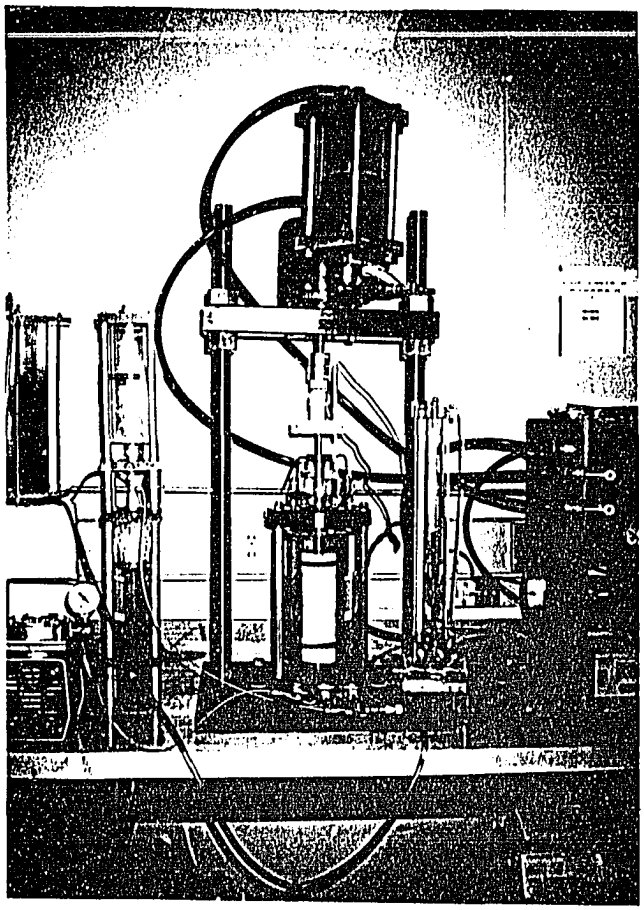

Figure 3.2 Photograph of The Automated Triaxial Device

The capabilities of the triaxial test have been fully described by Bishop and Henkel (1957) and in the volume edited by Donaghe, Chaney and Silver (1988).

3.2.2 The System

The system used for this research is an electropneumatic cyclic loading system. It uses an electronic-to-pneumatic (e/p) pressure transducer coupled with a volume booster relay to pressurize the actuator. The function generator provides an electronic signal of the desired load trace to the transducer. The e/p transducer is a force-balance instrument. The force of the output pressure balances the force produced on the input coil by the interaction of the input current and the permanent magnetic field. An increase in the current to the coil creates a downward thrust, casusing an increase in the output pressure. The output pressure is very low and is amplified by the 1:4 pneumatic amplifier. It is a pneumatic force-balance instrument that uses a 1:4 ratio of diaphragm areas. The volume booster relay further increases the pressure by a factor of two. It also relays the output pressure that now has a large flow capacity. For the push-pull mode of the operation by the actuator, the steady side is pressurized through an other volume booster relay controlled by a manual pressure regulator. The function generator controls the magnitude, the wave form and the frequency of the system. It has a gate mode that allows the operator to start and stop the test at the same preset load. The initial load is controlled by the amplitude setting, which was modified with a ten-turn potentiometer and a counter to facilitate repeatable setting.

3.2.2. Stress Conditions

During earthquakes, an element of soil is subjected to a series of cylic stresses. If the ground surface is horizontal, there is no shear stress on the horizontal plane. The total

normal stress during an earthquake remains constant on this plane. On the other hand, cyclic shear stresses may exist for the duration of the shaking. Under isotropic consolidation as shown in Fig.3.3 principal stress, σ_1 acts alternately in the vertical and horizontal directions. When $\Delta\sigma_1$ is applied, the maximum shear stress develops on a 45^0 plane in the specimen. Then, $-\Delta\sigma_1$ is applied and the shear stress reverses. This condition is simulated by triaxial test first by consolidating the soil to a required effective stress. The next stage is to create a principal stress difference on the sample by increasing the vertical stress acting on its top and bottom circular faces. This is achieved by increasing the load on the piston at the top of the sample. Stress controlled tests are run to get pore pressure, vertical load, and vertical deformation as a function of the number of cycles of load.

In addition to liquefaction characteristics of soils, dynamic properties can be obtained. Young's Modulus E, and shear modulus G, are often measured in the cyclic triaxial tests by performing strain controlled tests as seen in Fig. 3.4. Young's modulus is determined from the ratio of the applied axial stress to axial strain. For strain-controlled tests, shear modulus is computed from:

$$G = \frac{E}{2(1+\mu)} \qquad (3.1)$$

$$\gamma = (1+\mu)\varepsilon_v \qquad (3.2)$$

in which μ the Poisson's Ratio. ε_v is the single amplitude vertical strain.

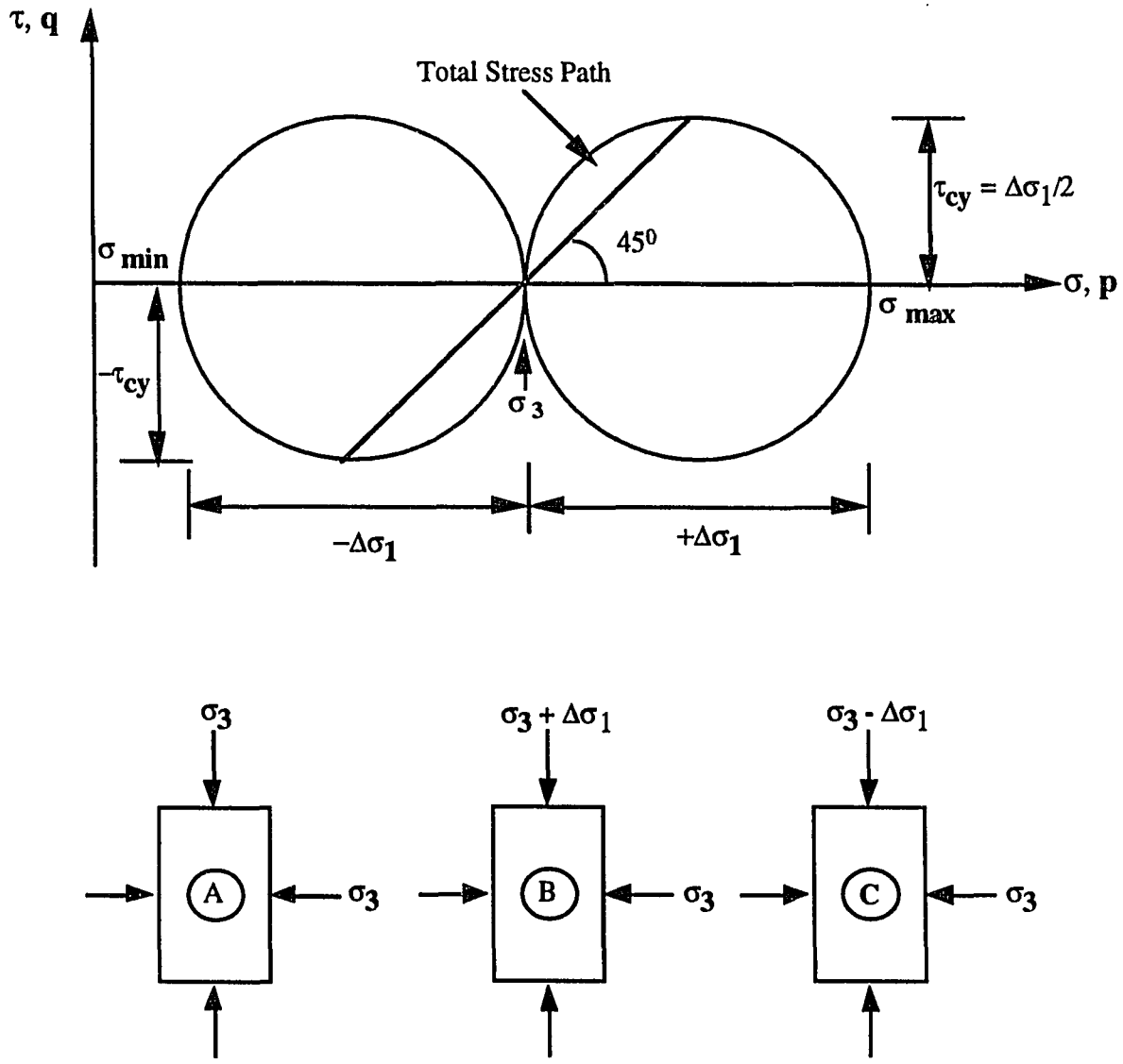

Figure 3.3 Stress Components in Cyclic Triaxial Test Specimens for Isotropically Consolidated Specimens

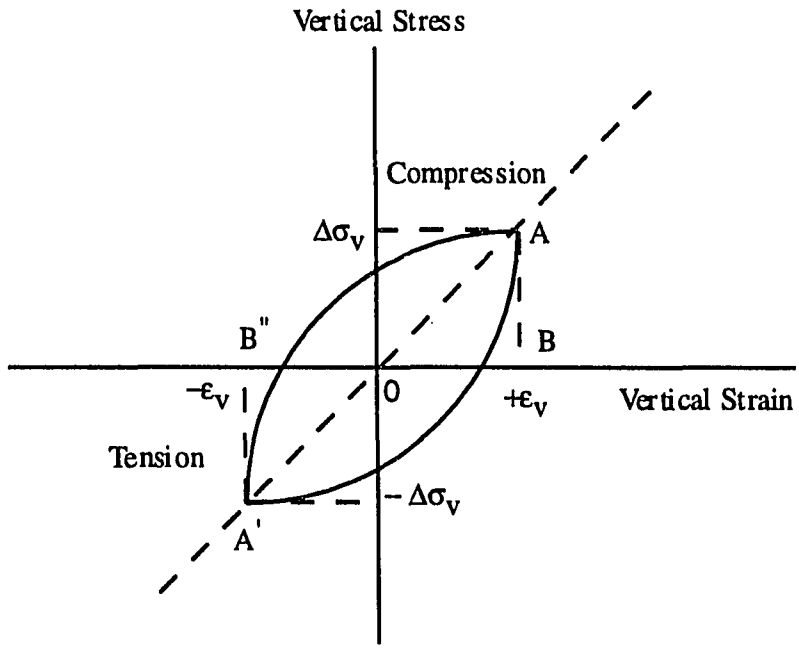

$$D = \frac{1}{2\Pi} \frac{\text{Area of Hysteresis Loop}}{\text{Area of Triangle OAB \& OA'B'}}$$

Figure 3.4 Calculating G and D

3.2.3 Preparation Of Cell And Specimen

1-) Fill the volume change device with fresh deaired water.

2-) Take a dry porous stone and a wet filter paper and place it on the base.

3-) Put vacuum grease on the mold halves and put two O-rings to the top and bottom of the mold.

4-) Attach the mold to the bottom platen. Apply a 25 cm of mercury to the mold and pull the membrane over the top.

5-) Increase the vacuum making sure that the membrane conforms to the side of the mold.

6-) Prepare the specimen using undercompaction wet tamping method.

7-) Place the top stone and filter paper. Attach the top plate of the triaxial cell locking the top platen above the specimen. Pull up membrane over the top platen. Put the O-rings on.

8-) Apply 12.5 cm mercury to the inside of the specimen, through the bottom platen line. Remove the mold.

9-) Measure the specimen height to 0.1 mm. at two locations and obtain the average.

10-) Measure the specimen diameter to 0.01 mm. at three elevations (the center, near top and near bottom) to obtain the average.

11-) Assemble the cell and insert the piston rod into the recess in the top cap.

3.3 Saturation Procedure

Specimens should be saturated in laboratory investigations in order to prevent volume change and provide pore water response during static or dynamic undrained loading. Obtaining an acceptable saturation level for specimens are very important to get meaningful results in liquefaction tests.

Saturating a specimen can be a very tedious process depending on the soil and procedures used. In majority of triaxial tests carried out in practice these difficulties are avoided by saturating the sample as the first stage of test. The "B" value is measured during back pressure application to determine the maximum allowable size of the next increment of cell pressure and to determine if saturation is complete or adequate.

3.3.1 Vacuum Procedure

Methodology for vacuum saturation procedure can be summarized as follows:

1-) Place the specimen with the membrane around it inside the triaxial cell.

2-) Fill the upper reservoir with water while the lower reservoir is kept empty.

3-) Switch the three-way valve to the vacuum side and apply vacuum into the sample from valve D (Figure 3.5). This vacuum should be around 30~50 kpa.

4-) Apply vacuum into the triaxial cell (outside the sample) from the top valve.

5-) Increase the inside pressure and outside pressure by the same amount. This increase interval should not exceed 5 minutes depending on the soil type to insure a proper equilibrium inside the sample.

6-) Initially flush the specimen with de-aired water, using the smallest pressure gradient required to achieve flow. A pressure gradient of 68.9 kPa (1.0 psi) is typically used. Maintain cell pressure during flushing at one half the final effective stress. At all times, the cell pressure should be greater than the back pressure, to prevent destruction of the specimen. Use valve D for flushing.

7-) Close the valve outside the sample.

8-) Decrease the vacuum inside the sample by adjusting the vacuum pump. Let the water penetrate to the sample by opening the upper chamber valve.

9-) Repeat step 1 to 9 until a desired level of saturation is achieved.

After the vacuum procedure is complete, the pressure valve is opened and experiment is started.

3.3.2 B-Determination

Saturation of a specimen is first achieved by evacuating the drain lines, stones and specimen under high vacuum. Deaired water is admitted to the lines. The pore pressure is increased to a level high enough for the water to absorb, all the air originally in the void spaces, into solution. At the same time confining pressure is increased, so the effective stress is maintained constant. The pore pressure in the specimen lags behind the applied backpressure and thus varies with time and location within the specimen. So, care must be taken to avoid "over consolidating" the specimen. Because of this lag in pore pressure response, the back pressure and cell pressure must be raised in increments, the size and frequency of which depend on the initial degree of saturation within and around the specimen and several other factors. It is extremely difficult to calculate the size and frequency of these back pressure increments so "B" value is monitored empirically, by periodically monitoring the degree of pore pressure equalization during the back pressuring process.

The degree of saturation is monitored during and at the end of the process by measuring the "B" value at the outset before the back pressure is raised. The required accuracy of the "B" values measured during application of back pressure is not as great as at the end of back pressuring, when "B" is being measured to determine if back pressuring is adequate.

3.3.3 Procedure

1-) Select and record σ'_{3c}, σ'_i and $\sigma'_{3max\,all}$.

$\sigma'_{3max\,all}$: Maximum allowable effective stress at any point within the specimen.

σ'_{3c}: Final desired effective consolidation stress

σ'_i: Value to which the effective stress in the specimen is initially adjusted, before raising the back pressure.

2-) Increase the back pressure to 150 kPa and the cell pressure will be increased automatically to give the desired effective consolidation stress. The cell pressure and back pressure should be increased in increments of about 34.5 kPa.

3-) Allow the specimen to reach equilibrium under the imposed stress conditions, as indicated by a relatively constant pore pressure response with time if the back pressure valve A is closed.

4-) Close the drainage valves and increase the cell pressure by an amount equal to one half the effective stress or by 69 kPa. whichever is smaller. Allow the specimen to reach an equilibrium state and note the corresponding change in pore pressure. Then check the "B" value.

5-) Repeat steps 2 through 4 until the "B" obtained in step 4 is satisfactorily high.

The value of "B" needed for accurate pore pressure measurements depends on the stiffness of the soil specimen. A minimum value about 0.95 is recommended to accept the soil as saturated.

If successive stages of back pressuring fail to produce significant increases in "B" or if the limit of the apparatus is reached, the back pressure should be left on overnight to allow

additional time for solution of air bubbles. If the "B" value is still not satisfactory, the specimen should be scrapped. In this study it was extremely difficult to get high "B" values as silt content is inreased. Values of "B" higher than 0.95 are accepted since it was impossible to achieve B=1 for some specimens.

Typical values of pore pressure coefficient "B" at 100% saturation and just below, are summarized in Table 3.1. The data are also presented in Fig. 3.6 for typical values of pore pressure coefficient "B" related to degree of saturation.

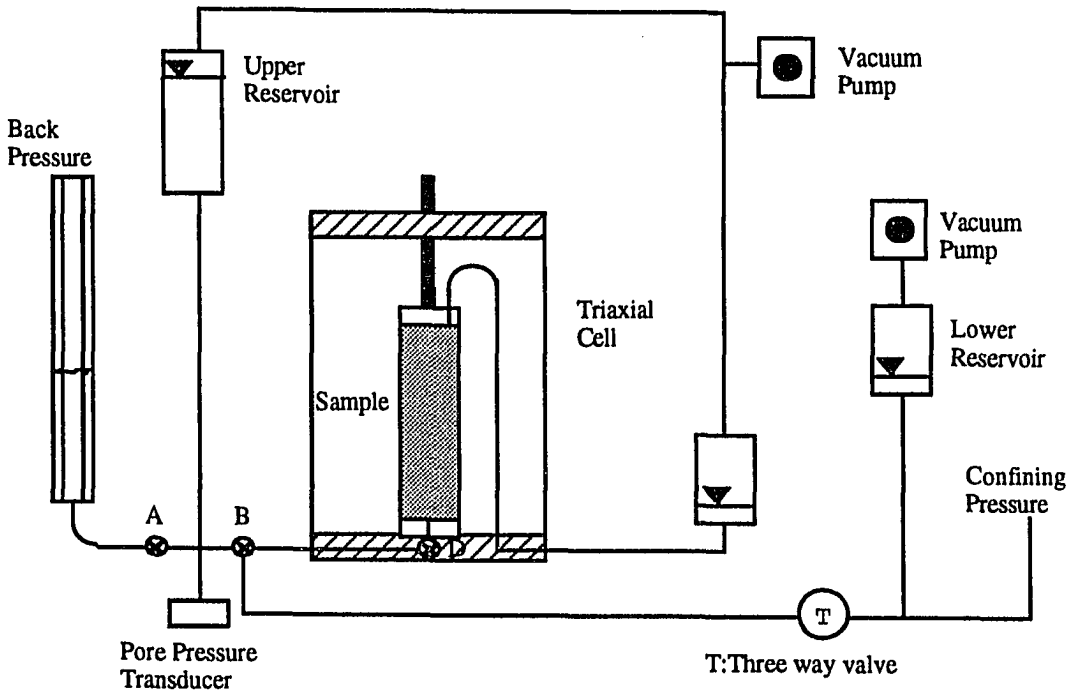

Figure 3.5 Experimental Setup For Vacuum Procedure

Table 3.1 Values of B For Typical Soils At or Near Full Saturation

Soil Category	Degree of Saturation 100%	99.5%	99.0%
Soft	0.9998	0.992	0.986
Medium	0.9988	0.963	0.93
Stiff	0.9877	0.69	0.51
Very Stiff	0.913	0.2	0.1

(after Black and Lee, 1973)

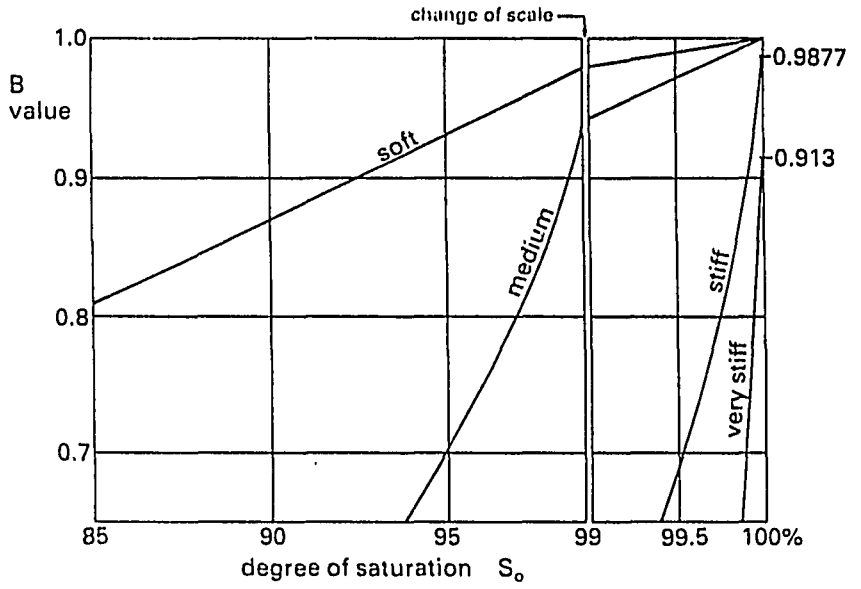

Figure 3.6 Typical Values of Pore Pressure Coefficient "B" Related to Degree of Saturation and Soil Stiffness (after Black and Lee, 1973)

3.4 Specimen Consolidation

In real life, soil consolidates and soil particles are bonded together by minerals carried in the ground water. Consolidation increases the soil's shear strength and its resistance to liquefaction and deformation. The samples used in cyclic tests are consolidated in the triaxial cell prior to testing in order to predict the deformation that would occur to a stratum of soil under similar pressures in the ground. Tests are run in isotropic condition meaning that the equal pressure is applied to all sides of the samples. Deviatoric stress was set to zero and consolidation pressure was 98 kpa all the time. Drainage of the excess pore water took place from the bottom of the sample. The coefficient of consolidation, C_v for all tests can be determined from the consolidation data by using the square root time curve fitting method.

Tests are run until primary consolidation is reached. Primary consolidation, arises when effective stress-strain properties are independent of time. The rate of generation of strain is related to the permeability of the soil skeleton. Since the amount of fines were different for each specimen, the consolidation times varied depending on the permeability changes. The specimens were compacted to a denser void ratio after consolidation is complete.

3.5 Test Parameters and Test Materials

The sand tested was Ottowa 20-30 (ASTM C-190) which has properties listed in Table 3.2 (a). Non-plastic silt used is known as Silco-Sil 125 and consists of crushed silica. Low plasticity effect is obtained by adding New Jersey silty clay to the parent material. The index properties of these soils are listed in table 3.2 (a) and (b). Silty clay is obtained from NJ and represented on the geologic map of NJ as the Kirkwood Sand, the Woodbury clay

and the Merchantville clay. It was kept in the moisture room before use and oven dried before mixing with the sand. The grain size distribution and hydrometer analysis for the tested soils are shown in the Figure 3.7.

For each of the sand-silt specimen, maximum void ratio was determined in accordance with ASTM D454-83, method B. Specific gravity, G_S tests were run for each specimen (ASTM D-854) and G_S values were determined, values ranging from 2.62 to 2.67 for each sample. Minimum densities of the soils tested were determined by compaction tests. Initially, the ASTM D4254 Method B was used; but as the fine content was increased, this test method was found unreliable because silt particles caused difficulties due to boiling and segregation. This resulted in a lower density than the true maximum density measured for each soil tested. Hence, as suggested by Head (1992) for silty specimens, minimum void ratio tests were run, by using a standard Proctor mold and hammer. The results of laboratory compaction tests on sand-silt mixtures are plotted in Figure 3.8. The general pattern of curves is roughly the same irrespective of the mixture, except for the 10% silt curve. Other curves show that as silt content is increased, the maximum dry density is increased. Since, 8% water content corresponds to the maximum dry density values, silty specimens compacted at this water content is increasing the lubrication furnished by the additional water. Because of the greater density less firm soil samples are obtained. Maximum dry unit weights determined from each test are used to calculate the minimum void ratio. Each of the above tests were run 3 times and average results were used.

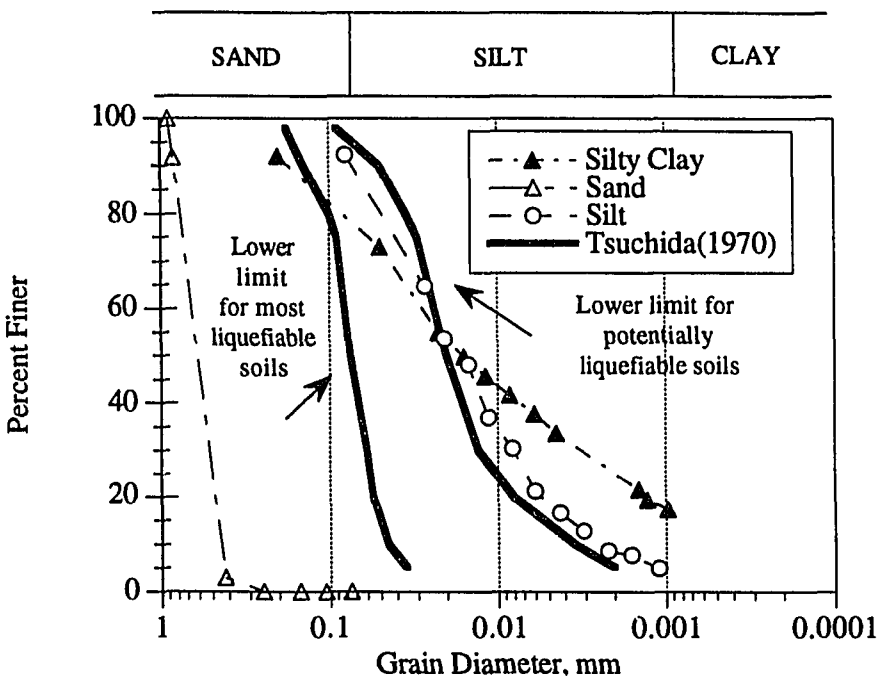

Figure 3.7 Grain Size Distributions of the Soils Tested

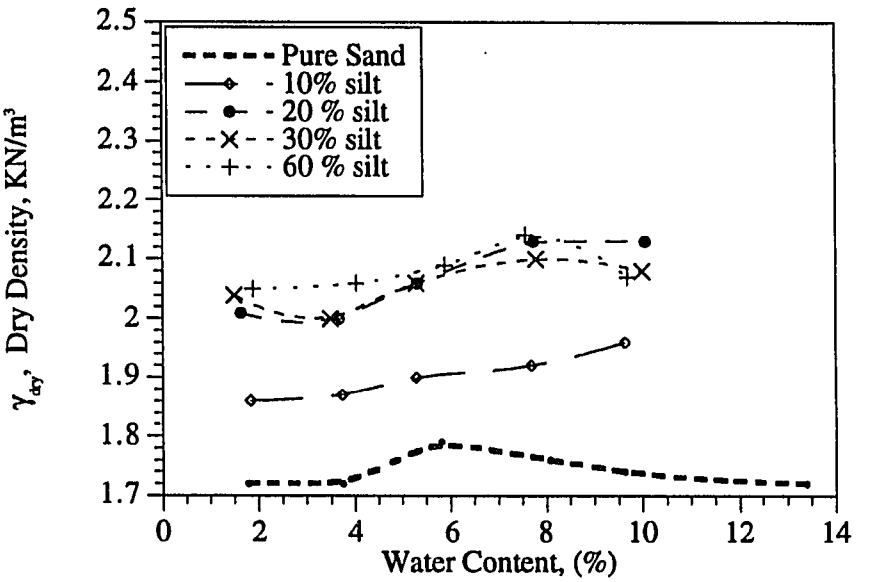

Figure 3.8 Moisture-Density Relationship for the Sand and Silty Sand

Table 3.2. The Index Properties Of the Soils Used: (a) Sand and Non-Plastic Silt, (b) Silty Clay

	Index Properties	
Type of Soil	Ottowa Sand (ASTM C-190)	Sil-Co-Sil 125
Composition	Ground Silica	Ground Silica
Specific Gravity	2.65	2.65
e_{max}	0.78	1.35
e_{min}	0.5	0.5
C_u	1	7.5
D_{10}	0.50	0.003
D_{50}	0.6	0.017
D_{90}	0.76	0.068
Liquid Limit	22	22
Plastic Limit	NP	NP
Plasticity Index	NP	NP
Particle Shape	Rounded	Rounded
Sphericity	0.85	0.85
Unified Soil Classification	SP	ML

(a)

	Index Properties
Type of Soil	Silty Clay
Specific Gravity	2.62
Liquid Limit	35
Plastic Limit	25
Plasticity Index	10
Optimum Moisture, %	26
Unified Soil Classification	ML
Maximum Density, pcf	104
Pass #4, %	100
Pass #200, %	90

(b)

The relationship between e_{max}, e_{min}, void ratio at a relative density of 50%, e_{50} and silt content , obtained from these tests can be seen from Fig. 3.9.

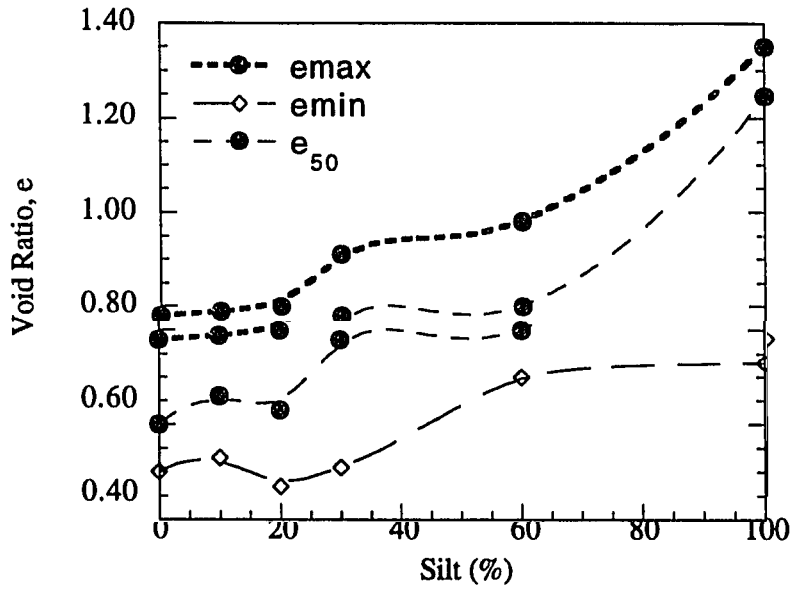

Figure 3.9 Relationship Between e_{max}, e_{min}, e_{50} and Silt Content (%)

3.6 Specimen Preparation

The method of undercompaction was used for specimen preparation. The control parameter was chosen as the void ratio because different amounts of silt were added to the sand by weight thus the maximum and minimum void ratios of the each sample was different for every placement condition. It was also recognized that the concept of relative density has some limitations with silty sands (Ishihara et al., 1980, Troncoso, 1988). The specimens were compacted in a loose and medium condition depending on the silt content. Specimens prepared by non-plastic silt could only be prepared to loose condition when fines content exceeded 30%.

The soil specimens were prepared in 10 layers, using undercompaction wet tamping method, in order to achieve a more uniform density. The concept of undercompaction (Ladd, 1978) is based on the fact that when successive layers of sand are placed without undercompaction, the compaction of each succeeding layer can further densify the sand below it. In order to avoid this difficulty, the lower layers were compacted to a lower density than desired for the final density. This lower density value was calculated by a predetermined amount defined as the percent undercompaction, U_n. The percent undercompaction of each layer linearly varied from the bottom to the top layer. The bottom layer had the maximum U_n. value. The percent undercompaction in layer being considered is:

$$U_n = U_{ni} - \left[\frac{(U_{ni} - U_{nt})}{n_t - 1} * (n-1) \right] \qquad (3.3)$$

Average percent undercompaction for layers compacted is:

$$\overline{U}_n = \frac{U_n}{n} \tag{3.4}$$

Ladd's calculation for obtaining the height of each layer in a specimen, as it corresponds to that layer's percent undercompaction is:

$$h_n = \frac{h_t}{n_t}\left[(n-1)+\left(1+\frac{U_n}{100}\right)\right] \tag{3.5}$$

where,

U_{ni} = Percent undercompaction selected for first layer

U_{nt} = Percent undercompaction selected for final layer (usually zero)

n = Number of layers being considered

n_i = First initial layer

n_t = Total number of layers (final layer)

h_n = height of the nth layer

h_t = total height of the specimen

Reconstituted specimens were compacted in a cylindrical mold 50.8 mm in diameter and 113.0 mm in height. The preliminary trials with silty sand using 6 layers with 6% water content did not work well. To get more uniform specimens, the number of layers was increased to 10. Each layer was scored after it was compacted for better bonding with the next layer. The optimum value for undercompaction was determined to be 5%.

All the specimens were prepared by tamping (lightly in a circular pattern) in an internal split mold with a tamping rod of diameter of 32 mm. The soil for each layer was weighed, placed in 10 separate containers and kept sealed until they were placed in the mold. Each layer was compacted to the required height. The diameter of the compacted specimen was

measured after a slight vacuum was applied and the mold was removed. Both the diameter and height of the specimen were measured to the nearest 0.01 mm. The specimen diameter was determined at three locations (top, bottom, middle) and the average value was used for density calculations. Triaxial membrane thickness was subtracted from the diameter to calculate the void ratio after placement. To make the calculations faster, a spreadsheet program was developed to record the specimen dimensions, weights, void ratio, etc. The spreadsheet for an actual test is shown in Table 3.3 for solid sand specimen, and easily modified for other materials and silt contents. The steps followed are carried out according to the procedure explained by Ladd (1977). The sample preparation technique was found reliable when repeated testing of duplicate samples gave uniform results. The results of the test on a standard soil specimen falls into the range with values obtained by other laboratories. Ferrito et al., (1979) compiled cyclic triaxial test data from published literature and from commercial and research laboratories involved in testing of cohesionless soils. Most of the data were for poorly graded sands (SP) and silty sand (SM).

The water content of the air dried material was adjusted so that the initial degree of saturation of the compacted specimen was between 20% and 40%. Specimens were prepared with a water content of 8%. The soil was mixed with water sixteen hours before use and sealed. The reason for this waiting period was to allow moisture to be evenly distributed throughout the soil.

The specimen was collected after each test, to determine its water content as a check for previous density calculations following the completion of the test. Based on the information given by Frydman et al., (1973) membrane correction was not performed on the results because the thickness of the membrane used was 0.2 mm. and the particle size of the soil was very fine and membrane penetration per unit area was negligible.

Undercompaction Calculations

Duygu Erten	Rutgers University	3/18/94	Test ID:	21

Input Data	Unit	Value
Water Content	%	8.00
Gs (specific gravity)		2.65
Diameter of sample	mm	50.80
Desired Ht of sample	mm	113.00
Number of layers		10.00
Minimum void ratio		0.50
Maximum void ratio		0.78
Desired void Ratio		0.64
Undercompaction	%	5.00
Membrane Thickness	mm	0.20

Output	Unit	Value
Volume of soil	cm3	137.46
Volume of Sample	cm3	225.44
Volume of voids	cm3	87.98
Relative Density	%	50.00
Dry density	g/cm3	1.62
Initial Sr	%	33.13
Diam.sample	mm	50.40
Area of the sample	mm2	1995.04
Saturated Density	g/cm3	1.75
Weight of silt	gr	0.00

Note:	PURE SAND (ASTM C-190)

Layer #	Un	Avg. Un	Hn	Layer H	Dr	In.Dens	e desired	Dry Wgt	Ht.Meas
1.00	5.00	5.00	11.87	11.87	46.00	1.6049	0.6512	37.9896	101.14
2.00	4.44	2.22	23.10	11.24	47.00	1.6076	0.6484	36.0407	89.90
3.00	3.89	1.30	34.34	11.24	48.00	1.6104	0.6456	36.1020	78.66
4.00	3.33	0.83	45.58	11.24	49.00	1.6131	0.6428	36.1636	67.42
5.00	2.78	0.56	56.81	11.24	50.00	1.6159	0.6400	36.2253	56.19
6.00	2.22	0.37	68.05	11.24	51.00	1.6186	0.6372	36.2873	44.95
7.00	1.67	0.24	79.29	11.24	52.00	1.6214	0.6344	36.3494	33.71
8.00	1.11	0.14	90.53	11.24	53.00	1.6242	0.6316	36.4118	22.47
9.00	0.56	0.06	101.76	11.24	54.00	1.6270	0.6288	36.4744	11.24
10.00	0.00	0.00	113.00	11.24	55.00	1.6298	0.6260	36.5372	0.00
								364.58	

Table 3.3 Sample Preparation and Output of A Test Data

3.7 Transducers

3.7.1 Introduction

A transducer is a device which when acted upon by a physical stimulus produces an electrical output in proportion to that stimulus. A total of five transducers are used in the system. A load cell to monitor the axial load, and an LVDT to measure the vertical displacement, and three pressure transducers to detect the chamber pressure, the effective pressure and the volume change. The conditioned output signals of these transducers are then received by the process interface unit. The transducers are calibrated monthly against known pressures in order to compare the transducer outputs against the outputs of a reference standard. Manufacturers' specifications on the axial load, LVDT and pressure transducers are given in detail by C. K. Chan in the Triaxial Manual (1988). Calibration of instruments and equipment is an essential factor in maintaining a high standard of reliability in the laboratory and re-calibration at regular intervals is equally important (Head, 1986).

3.7.2 Transducer Signal Conditioner

The model SC-5 is a 5 channel, switchable gain, A.C. transducer signal conditioning instrument. A power supply, excitation oscillator, digital panel meter and 5 channels of of signal conditioning are integrated into a signal unit. A digital panel meter is available to simplfy the setup and calibration of transducers and to display output voltages. The front panel controls are gain, zero, balance, phase, variable and channel. The gain adjusts amplitude of output signal for each channel. Zero allows the output voltage of the channel to be zeroed when the transducer is at its zero or null point. Balance is used to compensate for an imbalance in output voltage in a wheatstone bridge configuration transducer. Phase

provides compensation for phase shift the transducer output signal relative to the excitation voltage. Variable adjusts the indication on the digital panel meter when the jumper on J104 (JX04 where X is the channel number) is in the variable position. Channel selects the channel to be diplayed on the digital panel meter.

3.7.3 Calibrating the Transducers

Load transducer is calibrated with a 1500 lb. proving ring to set gain for a known load. Steady pressure is used on the upper part of the actuator. The ring is complying with a recognized standard. For a secondary check, for a 3 in. actuator, 60 kpa. is set to 1 volt. output. For a load cell of 1500 lb, 2.5 volts of output is used. The displacement transducer known as a "linear variable differential transformer" (LVDT) consists of electrical coils in a cyclinder casing, through the axis of which a metal core can slide. When a metal load moves, the inductance of the windings is measured electrically and converted to a digital display. LVDT is used to measure the axial deformation of samples in triaxial and consolidation tests. The LVDT is zeroed with no core in place. After the core is replaced, it is located mechanically to zero. Core is displaced a known amount. To do that, a slip gauge is inserted the tip of the transducer stem. Phase is set for maximum reading. Gain is set for calibrated reading for known displacement. 5.08 mm. is set to 1 volt of output.

The pressure transducers should also be calibrated. To calibrate the chamber and effective pressure transducers, the chamber pressure line is moved to steady or backpressure output. Chamber pressure outlet is plugged from oil reservoir. With no pressure, the channels are set to zero. A pressure of 552.5 kpa. is applied. Phase is set for zero reading. Reapplying the pressure to 552.5 kpa., the procedure is repeated since gain changes affects zero also.

To calibrate the volume change transducer, the evacuation chamber reservoir with a long 0.31 cm. tube is used to change the water level. Electronics are set as above for cell pressure and effective pressure using the 0 and 40 cm. on the 0.635 cm. tube to get 5 volts of output. 40 cm. of water is drawn from each combination of valve G & M and weighed for calculation of calibration factor to enter into calibration portion of software.

The zero of load and pressure transducers should be adjusted prior to opening the shut valve for air pressure to the e/p loader, the program takes care of the reading of volume change without any zeroing by the user. The cell pressure and effective pressure should be around 25 kPa. when zero voltage is applied, as per reading of Le/p. The 50 kPa. should be read on the cyclic pressure as measured by the pressure gage. The zero voltage pressure reading can be adjusted by screw driver through the back of cyclic loader box.

3.8 Testing Problems

With the usual vacuum procedure technique, water is percolated through the sample by opening the necessary valves. This accelerates the saturation of the specimen. This method worked well with specimens prepared by pure sand. The same method lead to segregation of silt and sand during percolation process. As suggested by Ishihara et al.(1978), the specimens prepared by using different amounts of silt content, were divided to three layers, top, middle and bottom. The quality of the specimen in terms of segregation of grains that might have occurred during percolation process was checked. After every test, specimen was divided in three layers. Each layer was oven-dried and grain size analysis tests were performed for each layer. It is observed from the results of grain size analysis that segregation is more pronounced for specimens prepared by

percolating water (Fig. 3.10). So these test results were discarded. The results of tests run with or without water percolation are shown in Tables 3.4 (a) and (b). Test 85 which uses a specimen with 30% silt content has acceptable results. The maximum loss in a layer is 4.26% which is less than 5%. On the other hand, the loss of fines when water is percolated during vacuum procedure, is unacceptable for all layers of test 74.

Table 3.4 Tables for different saturation methods

(a) Saturation acquired by applying back pressure only

30% Silt (Test 85)	TOP	MIDDLE	BOTTOM
Mass of Sample+Can	117.44	102.32	163.19
Mass of Can	10.87	10.91	11.24
Mass of Sample	106.57	91.41	151.95
Mass of Sand+Sieve#60	373.13	373.03	373.08
Mass of Sand Retained	74.95	64.57	108.16
Mass of Silt + Pan	714.13	709.62	726.49
Mass of Pan	682.87	682.79	682.85
Mass of Silt Retained	31.26	26.83	43.64
% Sand	70.33	70.64	71.18
% Silt	29.33	29.35	28.72
% Lost	2.23	2.16	4.26

(b) Saturation acquired by water percolating through the specimen

10% Silt (Test 74)	TOP	MIDDLE	BOTTOM
Mass of Sample+Can	62.32	107.2	120.14
Mass of Can	10.84	11.1	11.31
Mass of Sample	53.48	96.1	108.83
Mass of Sand+Sieve#60	426.22	464.87	460.03
Mass of Sieve #60	372.97	372.98	373.1
Mass of Sand Retained	53.25	91.89	86.93
Mass of Silt + Pan	683.04	686.82	704.85
Mass of Pan	682.88	682.81	682.86
Mass of Silt Retained	0.16	4.01	21.99
% Sand	99.57	95.65	79.8
% Silt	0.3	4.17	20.20
% Lost	97	58.3	200

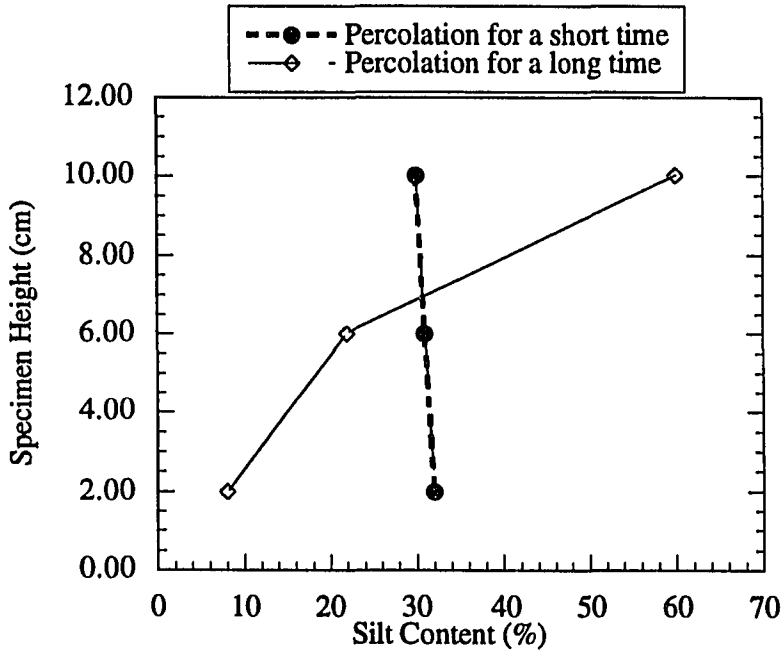

Figure 3.11 Silt Distribution Through The Height Of Specimens Saturated By Different Percolation Times

3.8 Testing Limitations

The stress acting on an element has six independent components, which may be represented by as three normal and three shear stress components. No apparatus has been devised to have a control over all six components. All tests used today apply limited range of conditions than may be experienced in the field. In the triaxial test, for example, the vertical and horizontal stresses are principal stresses and the two horizontal stresses are of equal magnitude. This constrained condition may be appropriate in some cases in order to simulate the anticipated loading. For example, an element of soil directly below a vertically loaded circular footing may experience conditions similar to those experienced in the triaxial test (O'Reilly, 1991). On the other hand, the cylic triaxial test has limitations which are:

1-) Triaxial tests can not be used for strain measurements below 10^{-2}.

2-) The extension and compression phases of each cycle produce different results, so hysteresis loops are not symmetric in strain controlled tests and samples tend to neck in stress controlled tests.

3-) There is non-uniform stress distribution on the specimen boundaries. Fig 3.12 shows contours of vertical stress expressed as a percentage of the axial load per unit sample cross sectional area of specimen with fixed ends (Hight, 1982). As can be seen, the stress non-uniformities are significant at the ends of the sample.

4-) Relative density redistribution occurs within the specimen during cyclic testing (Casagrande, 1988).

5-) The triaxial test do not permit principal stress rotation although a stress flip is possible where the major principle stress becomes a minor principle stress and vice versa.

In spite of all these shortcomings, triaxial tests if carefully conducted provide reliable data on cyclic loading characteristics up to initial liquefaction and strains of the order of about 5 percent for dense samples and 20 percent for loose samples (Seed, 1976).

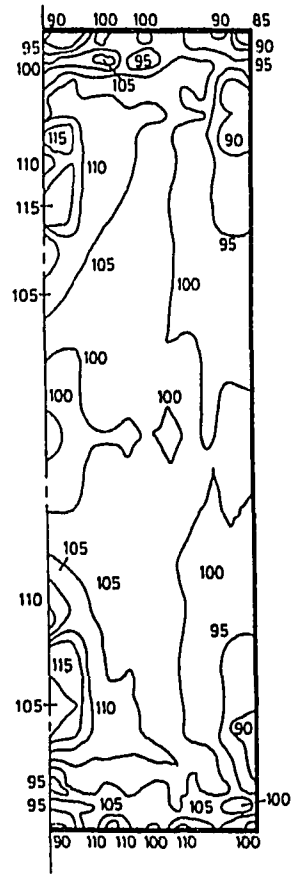

Figure 3.12 Finite Element Prediction of Contours of Vertical Stress (expressed as percentage of axial load/sample area) In Triaxial Specimen Loaded Between Fixed Ends (after Hight 1982)

IV STRESS CONTROLLED TESTS

4.1 Introduction

The laboratory measured liquefaction potential for a given soil is defined as the combination of cyclic shear stress and the corresponding number of cycles causing some degree of soil strength loss. In the performance of these tests to represent level ground conditions in the field, samples are first consolidated under an ambient confining pressure and then subjected to cyclic deviator stress applications. The results of these tests are expressed in terms of the stress ratio, which is the deviatoric stress divided by twice the confining stress and the number of stress cycles required to produce a given cyclic strain. The typical observed behavior of saturated soils in the stress controlled test is a gradual increase in the pore water pressure with increasing number of stress cycles until the effective stress first equals zero, which is termed by many as initial liquefaction (Silver and Park, 1976).

An element of soil is subjected to a series of cyclic shear stresses because of the upward propagating shear waves during earthquakes and deforms by the result of earthquake motions. If there is no surface loading, the surface has no shear stresses (Fig. 4.1).

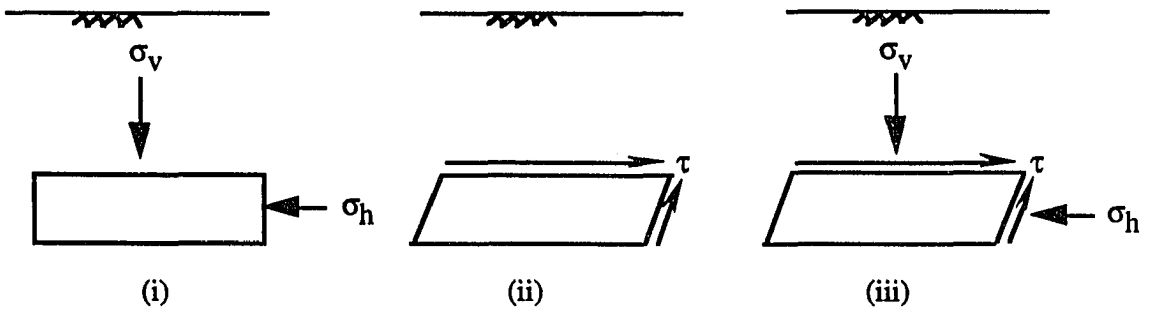

Figure 4.1 Idealized Stress Conditions for Element of Soil Below Ground Surface During an Earthquake (after Seed, 1976).

The deformations of the soil during earthquake-induced ground motions are approximated by triaxial tests. The cell pressure corresponds to the lateral pressure on the element. The axial load produces shear stresses which corresponds to the shear stresses in the field. The triaxial liquefaction tests were performed by triaxial machine in the load control mode and cycling a predetermined axial load. The magnitude of this axial load depends on the cyclic stress ratio chosen. The cyclic stress ratio is defined as:

$$S_r = \frac{\pm\sigma_{dc}}{2\overline{\sigma}_c} \qquad (4.1)$$

$$\pm\sigma_{dc} = 2\overline{\sigma}_c S_r \qquad (4.2)$$

$$P_c = \pm\sigma_{dc} A_c \qquad (4.3)$$

where:

$\pm\sigma_{dc}$ =Cyclic deviator stress (kPa.)

$\overline{\sigma}_c$ =Effective confining pressure (kPa.)

S_r =Desired cyclic stress ratio

P_c =Cyclic load (kg)

A_c =Consolidated sample area (cm^2)

The desired cyclic loading range was decided by the recommended literature values. Cyclic loading was initiated so the first half was chosen as compression. The cyclic tests were run to a double amplitude axial strain of 15%. All the tests were performed at a loading rate of one cycle per minute to ensure equalized pore pressure readings. During the test, a

constant mean normal stress is maintained by varying the chamber pressure while the axial stress or the axial strain is cycled using a sinusoidal wave form. Cyclic strain requires oil actuator to be entered, in the test initiation process. The chamber water is lowered to 1/2" from the top of the cell all the time. This allows the piston rod to move in and out of the cell without materially affecting the actual chamber pressure.

4.2 Results of Typical Stress Controlled Tests

Typical test results from a stress controlled test on medium Ottowa sand can be seen in Fig. 4.2. The specimen is consolidated isotropically to a stress of 98 kPa. and confining stress during the tests is maintained at 98 kPa. This confining pressure is approximately equivalent to an overburden pressure at a depth of 8 m. The main parameters observed during the tests were, applied cyclic axial load, pore pressure buildup with respect to cycling load, and cyclic axial displacement. The change in strain with respect to deviatoric stress can be observed from Fig. 4.2 (a). As can be seen from hysteresis loops, the stress strain curve becomes gradually flatter. As loading proceeds, the generated pore pressure increases up to the level of confining pressure as can be seen from Fig. 4.2 (c) and reduction of effective stress takes place which is accompanied by the softening of the specimen. It may be seen from this figure that excess pore water pressures were generated more rapidly as the strain levels are increased. Large shear strains are associated with stress paths approaching the phase transformation line under effective confining stress of 98 kPa. as shown in Fig. 4.2 (e). The concept of phase transformation line is first introduced by Ishihara et al., 1975. The points at which various stress paths change direction abruptly are assumed to lie on a line called the phase transformation line and the stress path model in its basic form is assumed to apply only for the region of stress space between the phase transformation lines in compression and extension. The phase

transformation lines are assumed to correspond to initial liquefaction and any cyclic loading beyond this stage quickly results in very low effective stresses and complete liquefaction (Ishihara et al., 1978). After each cycle, effective confining pressure is reduced with an increase in residual pore pressure. The gradual buildup in pore pressure causes the stress path for each cycle to progress toward the failure lines. The failure line is reached in the extension phase of a cycle, pore pressure and strain development accelerate. The stress paths run up and down the failure lines passing through or near the origin twice each cycle. This behavior corresponds to the contraction-dilation phases in densification and explains the fluctuation of pore pressure before reaching the zero effective stress condition (NRC, 1985).

The double amplitude axial strains of 2.5% and 5.0% are calculated from Fig. 4.2(b). In the first 30 cycles of stress applications, there is no strain development. Peak pore water pressure increases to 40 kPa. After the 30th cycle the specimen starts to develop shear strains, gradually increasing up to a double amplitude strain of 15% which is the limit set before starting the experiment. At the 40th cycle, the confining pressure becomes equal to the pore water pressure which is the condition of initial liquefaction. 2.5% strain occurred on the 32th cycle, 5.0% occurred on the 33rd cycle and 10.0% strain occurred on the 34th cycle. The sample was assumed to have failed when 10% strain was reached. The sample started to deform in compression on the 30th cycle. Finally, the test specimen failed in compression.

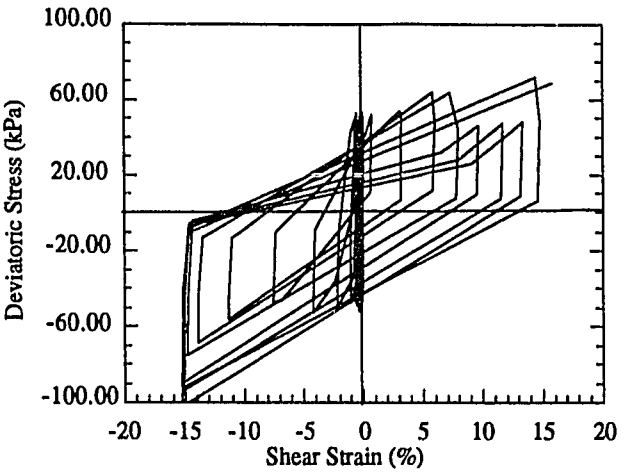

a) Deviatoric Stress vs. Shear Strain

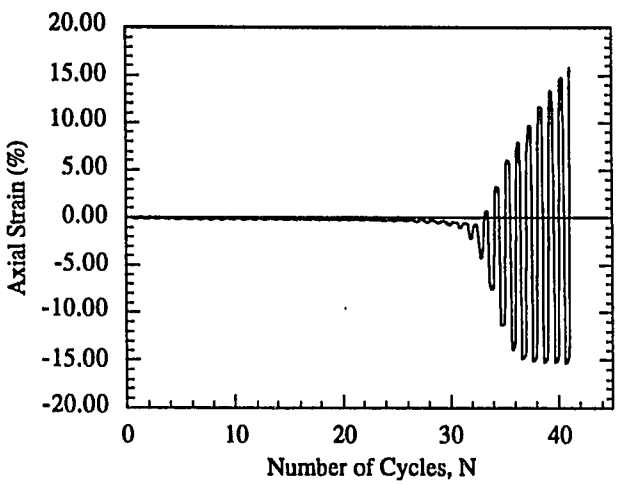

b) Axial Strain vs. Number of Cycles

Figure 4.2 Typical Results From Stress Controlled Tests

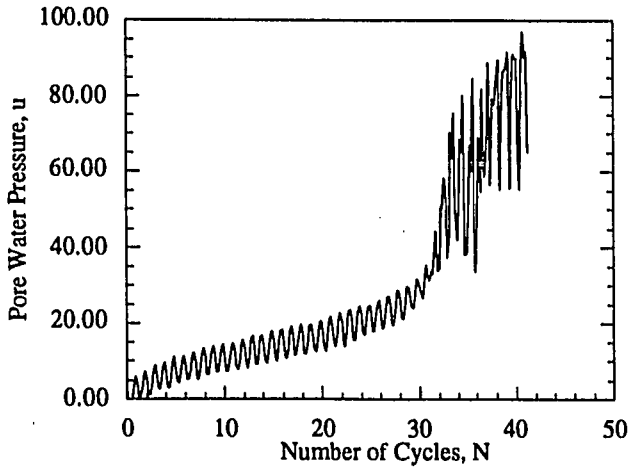

c) Pore Water Pressure vs. Number of Cycles

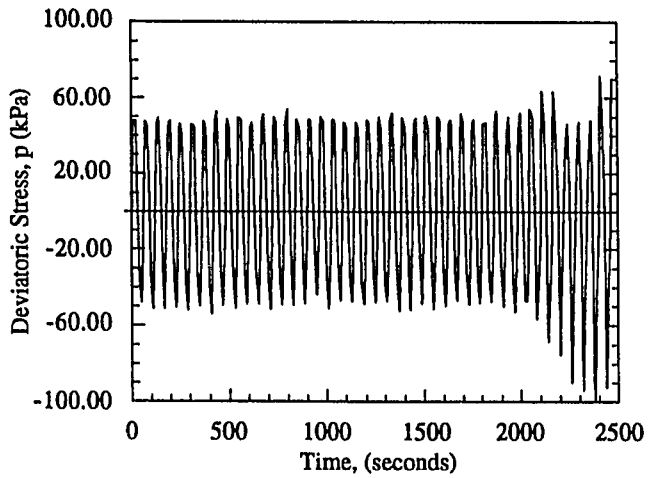

d) Deviatoric Stress Change vs. Number of Cycles

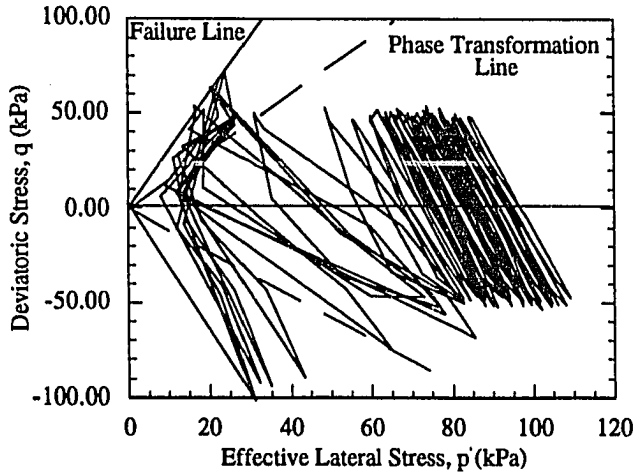

e) Changes in Effective Stress During Cyclic Loading

4.3 Liquefaction Potential of Silty Sands

The undrained response of saturated sands and silty sands to cyclic loads was evaluated in terms of the cyclic stress ratios and the number of cycles required to reach liquefaction. The basic information on how to interpret and obtain information from plots are given in the previous section. The information obtained is being used to develop plots of cyclic stress ratio vs. number of cycles for different tests having the similar void ratios. This type of approach is frequently used in the literature. The results are shown for each individual specimen, with no fines and 10, 20, 30 % fines added.

The results are plotted in terms of cyclic stress ratio versus number of cycles required to cause initial liquefaction and ±2.5 and ±5.0% axial strain. The cyclic stress ratio as defined above is the ratio of the cyclic deviatoric stress, to twice the effective confining pressure at the time of consolidation. Except for the specimens with no fines, pore water pressure never reached to the value of initial effective pressure (Fig. 4.3). Though, large amount of deformations developed for the specimens with fines even without the development of condition of initial liquefaction. So the definition of failure criteria for specimens with fines were changed. Initial liquefaction was no more accepted as a criteria for soils with fines. So as suggested by Silver and Park (1976), ±2.5 and ±5.0% axial strain were used as failure criteria. The term liquefaction here, is used to imply a certain degree of seismically induced softening of sandy soils which is commonly defined in terms of the cyclic stress ratio to cause 5% double amplitude axial strain in the course of a certain number of load application. The results of the liquefaction tests are presented in Tables of Appendix A. Fig. 4.3 shows the cyclic stress ratio vs. number of cycles on loosely constituted sand specimen. As the cyclic stress ratio decreases, the number of cycles required to induce 2.5, 5.0, 10.0 % strain and initial liquefaction almost collapse on each other. This indicates that the development of initial liquefaction almost occurs following sudden increases of cyclic strains even at the same cycles. In medium condition, as (Fig.3.4) the trends seems more or less the same but with higher stress ratios, the initial liquefaction immediately follows 10% strain faster than in loose condition. Specimens prepared by addition of 10% non-plastic silt in both loose and medium conditions, the cyclic strength curve is rather steep. For medium condition, the curves showed the same trend as loose sand and initial liquefaction occurred after couple of cycles following 10% strain. For lower stress ratios, initiation of 10% cyclic strain was immediately followed by initial liquefaction (Figs. 4.5 & 4.6). The results of cyclic tests on 10% low-plasticity fines added to sand plotted in Fig. 4.7 in terms of the cyclic stress ratio versus the number of

cycles. It may be observed that addition of both non-plastic and low-plasticity fines accelerated the pore pressure generation (Figs. 4.8 and 4.9). This effect is more pronounced with the addition of non-plastic fines. Typical relationships between the stress ratio versus cycle number for medium density conditions for all the used specimens are plotted in Figs. 4.10 through 4.12. It is apparent from the data presented in figures that, for a given cyclic stress ratio, significantly less cycles of load are required to cause 2.5, 5.0 or 10.0 % strains. The decrease in resistance to liquefaction derives mainly from the lubrication effect of fines. The cyclic resistance curves showing cyclic stress ratio, $\sigma_d / 2\bar{\sigma}_{3c}$, to cause liquefaction (5.0% double amplitude criterion in 20 stress cycles) versus void shown in Fig. 4.13.

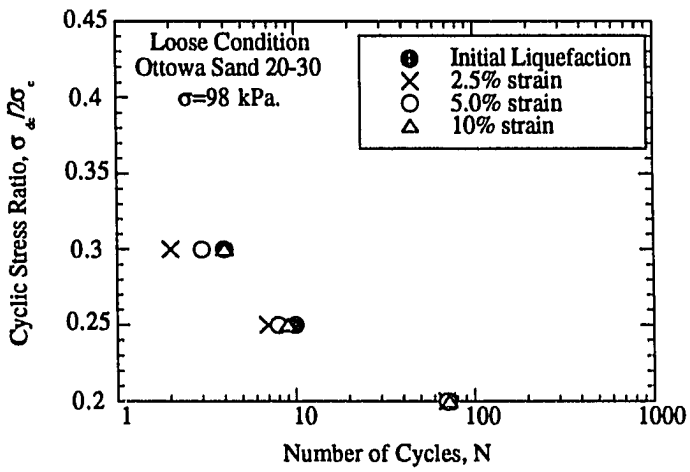

Figure 4.3 Cyclic Stress Ratio vs. Number of Cycles

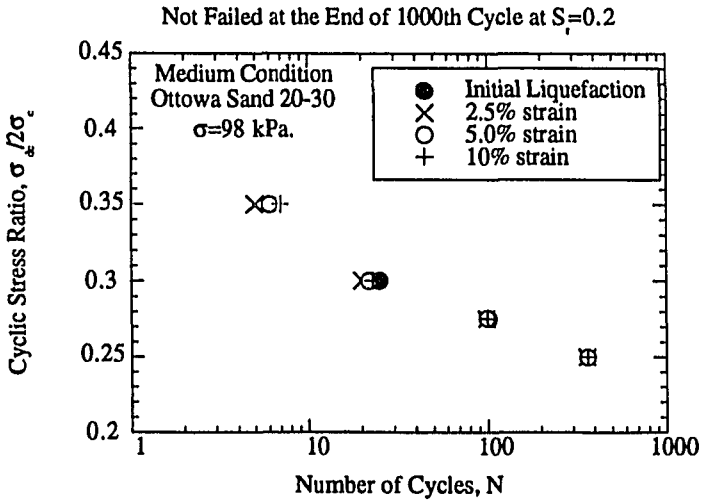

Figure 4.4 Cyclic Stress Ratio vs. Number of Cycles

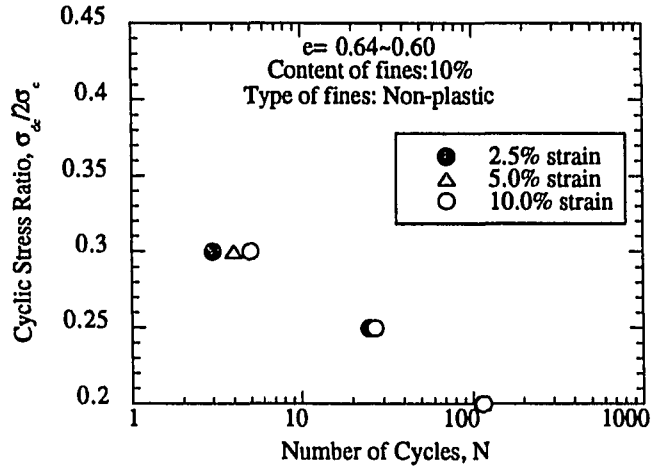

Figure 4.5 Cyclic Stress Ratio vs. Number of Cycles

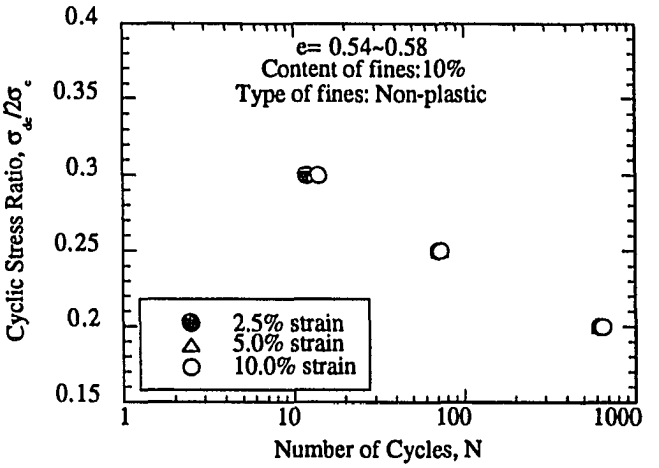

Figure 4.6 Cyclic Stress Ratio vs. Number of Cycles

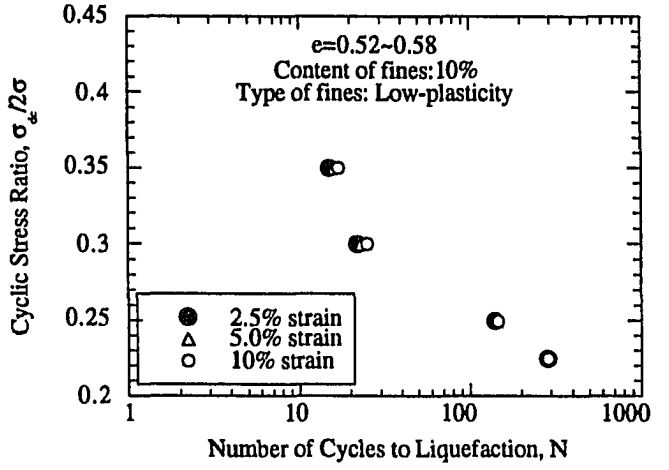

Figure 4.7 Cyclic Stress Ratio vs. Number of Cycles

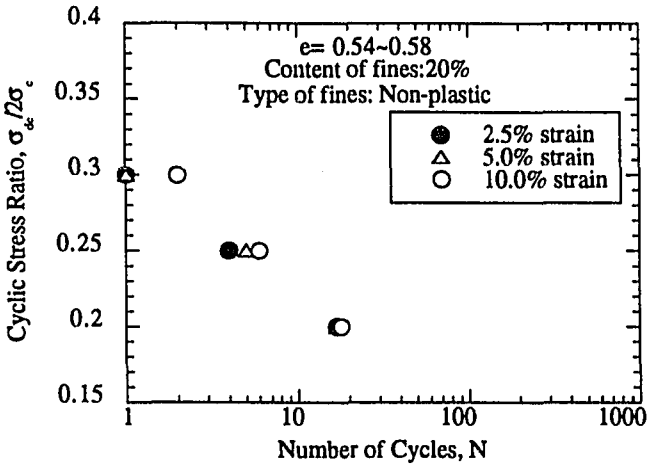

Figure 4.8 Cyclic Stress Ratio vs. Number of Cycles

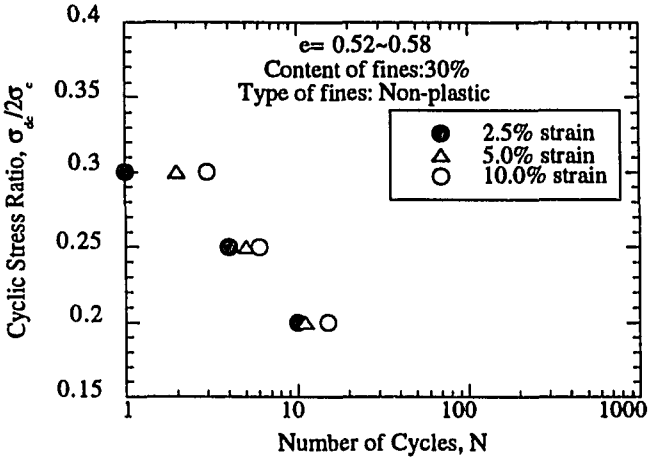

Figure 4.9 Cyclic Stress Ratio vs. Number of Cycles

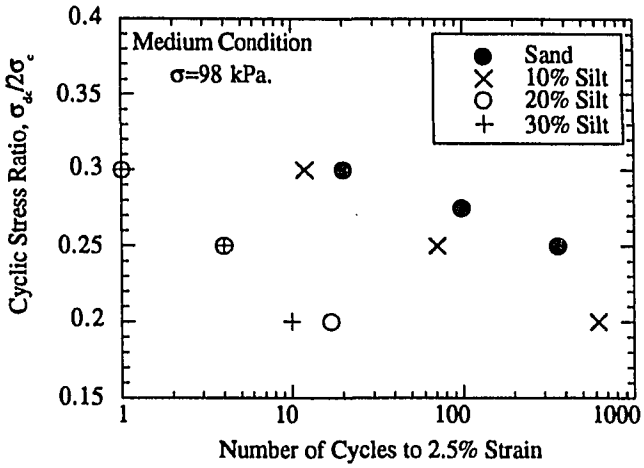

Figure 4.10 Cyclic Stress Ratio vs. Number of Cycles

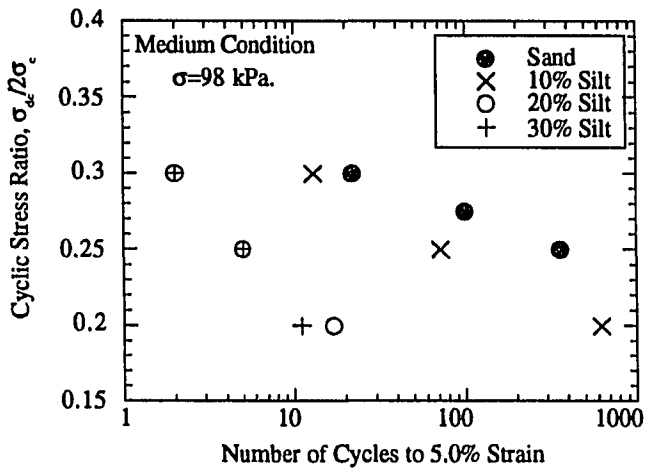

Figure 4.11 Cyclic Stress vs. Number of Cycles

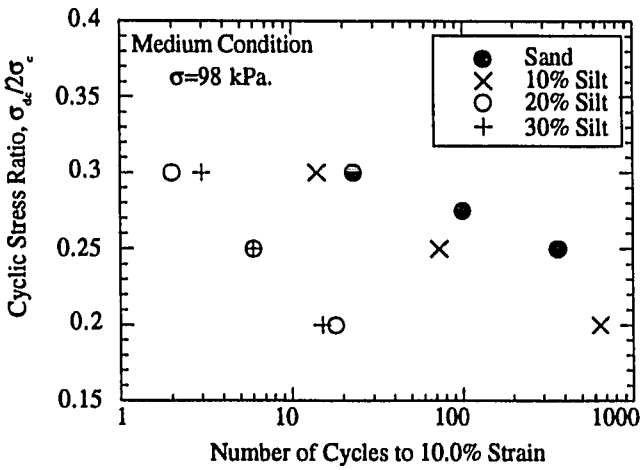

Figure 4.12 Cyclic Stress Ratio vs. Number of Cycles

As silt content increases, the resistance curves shift towards the lower void ratios. The cyclic resistance at a given void ratio decreases with increases in silt content. As can be seen from the plot, some void ratios are not attainable by some amounts of silty sands. It can be said that as the amount of silt increases, the soil becomes more susceptible to liquefaction and the effect of changes in cyclic stress ratio is more pronounced. It must be added here, preparing medium condition specimens with more than 30% silt was impossible. Void ratios attained were in the range of 0.75~0.8 for 60% silt specimens and much higher for the pure silt. The increase in cyclic resistance for the same decrease in void ratio is not same for all the specimens. As the silt content increases up to 30% the specimen is more effected from void ratio changes. Hence this proved to be wrong for higher silt contents. Changes in void ratio in specimens prepared by adding more than 60% fines have less effect on the results compared to specimens prepared by lower percentages of fines. It can be said that loose silty sands show similar cyclic strengths regardless of silt content. Higher percentage of fines are not included in Fig. 4.13 because of void ratio discrepancies.

There are many practical approaches to define resistance to liquefaction potential for a particular number of stress applications. The liquefaction resistance of silty sands for a given number of cycles can be plotted with the values of cyclic stress ratio causing 5% double amplitude strain, versus silt content is shown in Fig.4.14. From this figure, it is possible to predict the potential for 5% double amplitude strain of a soil under earthquake loading by comparing the value of stress ratios and the number of cycles as a function of silt content. All the test are carried out using a constant confining stress of 98 kPa. From the figure, it is clear that the required stress ratio to cause 5% double amplitude strain is decreased which is shown in the cycle number range of 5 to 30, as the silt concentration increases. The significance of failure in 10 and 30 cycles is that they correspond to the

duration of significant stress cycles produced by earthquakes having magnitudes of 7 and 8 respectively. The resistance to liquefaction starts increasing with the addition of 30% fines compared to previous silt contents. Since controlling the void ratio becomes a major problem for silt additions following 30%, this value is accepted as a threshold value. Previously by several researchers threshold value for silt was found as 15% (Vrymoed, 1971), 10~20% (Kaufman, 1981), 35% (Sherif et al., 1983). The difference may be attributed to the testing methods, difference in soil types, sample preparation methods etc.

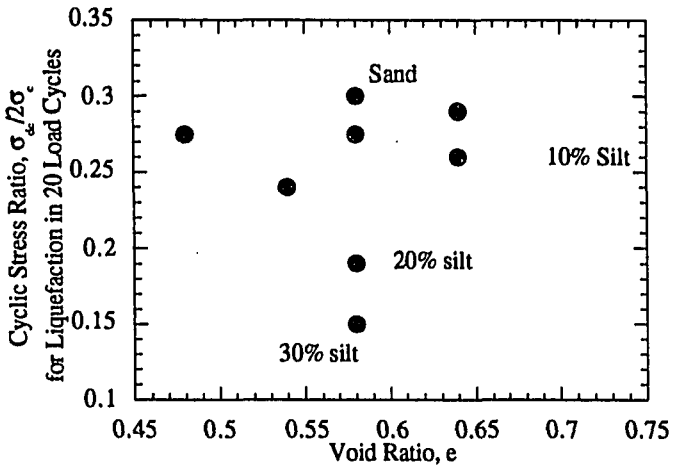

Figure 4.13 Relation Between Cyclic Strength, Void Ratio and Silt content

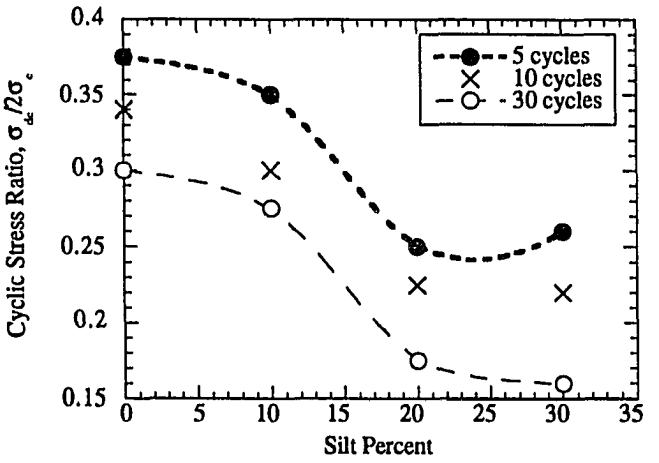

Figure 4.14 Silt percent vs. Cyclic Stress Ratio

4.2.1 Sand Skeleton Void Ratio

The equation 4.4 is used to calculate the sand skeleton void ratios as mentioned by Kuerbis et al., (1988) and Carrier (1988).

$$e_s = \frac{e_t(SFR+1)+1}{SFR} \qquad (4.4)$$

e_t = total void ratio (conventional definition)

SFR = sand-to-fines ratio, by dry weight.

Table 4.1 Sand Skeleton Void Ratio vs. ASTM Void Ratio

Type of Soil	ASTM (e)	Sand Skeleton (e)
Sand	0.58	0.580
10%	0.58	0.755
20%	0.58	0.975
30%	0.58	1.250
60%	0.58	1.630

Table 4.1 shows the sand skeleton void ratio values for the amount of fines used. As can be seen from the table, sand skeleton void ratio increases as silt content increases. This may explain the decrease in resistance to liquefaction as more silt is added to sand. Since, silty sand is gap graded, e_s controls the behavior of sand (Carrier, 1988). This why it is extremely important to consider that before construction of fills. Using silty sands, may cause segregation of fines and slides. And as the fine percentage increases, the behavior of the soil is no longer controlled by the parent material but the fines.

4.3.1 Effect of Fines

The presence of fines (passing #200 sieve), has substantial effect on cyclic undrained behavior of sands. The difference in behavior between pure sand specimens and specimens prepared by adding 10% non-plastic silt is not significant. The effect is more pronounced when the silt content exceeds 10%. The addition of fines change the fabric and grain structure of the compacted specimens. The weakening effect of the fines may also be attributed to the compaction water content. For 20 and 30% silt, specimens prepared with 8% water corresponding to the optimum moisture content. For pure sand specimens, 8% water creates specimens prepared on the wet side of the optimum. Under cyclic stress loading, the undrained shear strength decreases with increasing silt content up to a limiting value of 30%.

4.3.2 Effect of Initial Void Ratio

The state of compactness of several sand and silty sand mixtures is extremely hard to control. It is almost impossible to prepare these mixtures to the same void ratio. Small differences in void ratio for lower percentages of fines lead to wider discrepancies in state of compactness. The cyclic strength is decreasing as the void ratio of the specimen increases. When specimens are compacted to the same void ratio, the cyclic strength of silty sands is found to be lower than that of the sands. The test results also indicate that as the silt content increases (~60%), the results are less effected by of void ratio discrepancies.

4.3.3 Effect of Plasticity of Fines

The data from the cyclic triaxial tests with 10% non-plastic and 10% low-plasticity silt with 90% sand, at an initial consolidation pressure of σ=98 kPa. and specimens with void ratio of 0.58, are plotted in Figs. 4.6 and 4.7. From the observation of results, the liquefaction resistance of sands decreases with addition of low plasticity fines (PI~10). This effect is more pronounced for fines which have no plasticity. These results are consistent with the previous researches done on the effect of plasticity, Puri (1984), Sandoval (1989).

4.4 Stress Approach

The results from stress controlled tests can be used to evaluate liquefaction potential in the field. Seed and Idriss, 1971 introduced a simplified procedure to evaluate the induced shear stresses during an earthquake. For practical purposes, the average cyclic shear stress may be determined by:

$$\tau_{av} \approx 0.65 \frac{\gamma h}{g} a_{\max} r_d \qquad (4.5)$$

where a_{max} is the maximum ground surface acceleration, h is the depth of soil column considered, g is the acceleration due to gravity and γ is the unit weight of the soil. The appropriate number of significant stress cycles N_C will depend on the duration of ground shaking and thus on the magnitude of the earthquake. The use of number of equivalent stress cycles, N_C with equation 4.5 provides a simple procedure for evaluating the stresses induced at different depths by any given earthquake for which maximum ground surface acceleration is known.

The cyclic stress ratio, $\tau_h / \overline{\sigma}_c$ causing liquefaction under multi-dimensional shaking conditions in the field is related to the cyclic stress ratio causing liquefaction of a triaxial test sample in the laboratory by the expression (Seed, 1979):

$$\left(\frac{\tau_h}{\overline{\sigma}_c}\right)_{l-field} \approx C_r\left(\frac{\sigma_{dl}}{2\sigma_c}\right)_{l-triaxial} \qquad (4.6)$$

where values of C_r are approximately 0.57 for K_O=0.4 and 0.9 for K_O=1.

4.5 Test Results and Discussion

1) It is really difficult to prepare specimens to the same void ratio when different amount of fines are used. As the fines content increase, it is impossible to reach the lower void ratios so comparison of cyclic strengths becomes a problem. After consolidation, the void ratio also varies depending on the amount of fines due to the differences in permeabilities of soils.

2) Soils with different amounts of fines have different pore pressure generation characteristics. So, large amounts of axial strains developed, even before the initial liquefaction occurs. This is why the failure criteria based on 10% axial strain is selected. Initial liquefaction can not be used as a failure criteria when using silty soils.

3) The scatter of the data from stress controlled tests make the stress controlled test results unreliable to predict the liquefaction potential of silty soils. During the extension cycle, segregation of fines from sand causes weaker specimens and soil fails faster. Using natural soils might help segregation during extension phase of the tests.

4) Addition of non-plastic and low-plasticity (PI~10) fines to sand decreases the liquefaction potential of sands. This effect is less pronounced for low plasticity fines.

5) As silty soils move from medium to loose state, they demonstrate similar levels of cyclic resistance.

V. NUMERICAL MODEL FOR PORE PRESSURE GENERATION

5.1 Introduction

The influence of fines on the liquefaction potential of sandy soils has been studied by conducting isotropically consolidated stress controlled triaxial tests. Ottowa silica sand is used as the parent material. The amount of fines added to the sand was varied from 10% to 30% by dry weight. Experimental results are compared with predictions using the theory developed by Nasser and Shokooh (1977) which is based on energy considerations. The theory is based on the fact that densification and liquefaction of the soils involve rearrangement of the grains, requiring a release of certain amount of energy which is related to changes in void ratio and pore water pressure. The theory determines the excess pore water pressure in terms of the number of cycles N, the dimensionless shear stress amplitude τ_0, and the initial and minimum values of the void ratio. Model parameters are modified for the results of the tests. The comparisons with the results of this research show good agreement between experimental data and model predictions for the pore water generation under cyclic loading for both loose and medium sands and medium silty soils.

5.2 Theory

Conventional analyses of liquefaction potential uses parameters such as equivalent stresses and equivalent number of cycles to determine the dynamic pore pressure increases. In contrast to the stress based approach, a unified approach to the densification and liquefaction of homogeneous sands is formulated by Nemat-Nasser and Shokooh. They suggested that the dynamic pore pressure increase depends on the density of dissipated energy during cyclic loading. By means of a simple dimensionless analysis and several

assumptions based on the results of experimental findings, explicit expressions are obtained for the changes in void ratio and pore pressure. These changes are functions of the number of cycles, confining pressure and other relevant parameters.

The theory is based on an observation that the densification of sand involves rearrangement of its grains in which the process requires a certain amount of energy. This energy increases as the void ratio approaches its minimum value which in turn, depends on the confining pressure, shape distribution of sand particles and the size of the particles. If the saturated sand is undrained, there is a tendency toward densification induced by cyclic loading; this results in an increase in the pore pressure. Corresponding energy required to decrease the pore volume, decreases with increasing pore pressure. A simple differential equation is proposed which relates the energy loss in cyclic loading to the consequent increase in the pore pressure in the saturated undrained case. The theory is then applied in its simplest form to predict some of the existing experimental results for liquefaction phenomena (Nasser and Shokooh, 1977). The theory, in the case of liquefaction involves two parameters, one of which is fixed by the densification consideration and the other one is expressed explicitly as a function of initial void ratio, the minimum void ratio and other relevant parameters. During cyclic shearing, to change void ratio from e to $e+de$, a certain energy is needed. This energy is an increasing function of $e-e_m$ and a decreasing function of the excess pore pressure. Void ratio can not be decreased below its minimum e_m, without the expenditure of an infinite amount of energy. For the undrained case, as e decreases, p increases. It is known that for a soil mass at equilibrium, there is a balance among all interparticle forces, the pressure in the water and the applied boundary stresses. When the pressure in the water increases, it causes a reduction in the inner particle forces and therefore, decreases the required energy. Since, the particles rearrange themselves

more easily, this causes further increase in the pore pressure. The above observations can be quantified as:

$$dW = \tilde{v}\frac{de}{f(1+p)g(e-e_m)} \tag{5.1}$$

dW is the amount of energy required to change the void ratio e to $e+de$. For the undrained condition,

$$de = \frac{dV_p}{V_s} = \frac{dV_p}{V_p}\frac{V_p}{V_s} = -\frac{1}{\eta_w}\left(-\eta_w\frac{dV_p}{V_p}\right)e = -\frac{e}{\eta_w}d\bar{p} = -\frac{e}{\eta_w}dp\sigma_c \tag{5.2}$$

when placed in equation 5.1,

$$dW = \frac{v}{\eta_w}\frac{edp}{f(1+p)g(e-e_m)} \tag{5.3}$$

Here η_w is bulk modulus of water and $dp = d\bar{p} / \sigma_c$. $v = \tilde{v}\sigma_c / \eta_w$ is a positive parameter. Usually the confining pressure used for experiments is in the order of 10 psi, and the bulk modulus of water is about 300 000 psi, the volumetric strain and the corresponding work per unit volume per unit confining pressure is extremely small and can be ignored. Without a loss of accuracy, it can be said that $e = e_o$. The formula for the amount of energy required for the corresponding change for liquefaction is obtained by integrating equation 5.3;

$$\Delta W = \frac{ve_0}{\eta_w g(e_0 - e_m)}\int_0^p \frac{dp'}{f(1+p')} \tag{5.4}$$

However the energy loss ΔW, should be expressed more explicitly in terms of the number of cycles and the shear stress amplitudes. For the energy loss, it is very hard to obtain a single expression because during straining, the area confined by the hysteretic loop narrows as the loop elongates because of the increasing strain amplitude (Fig. 5.1).

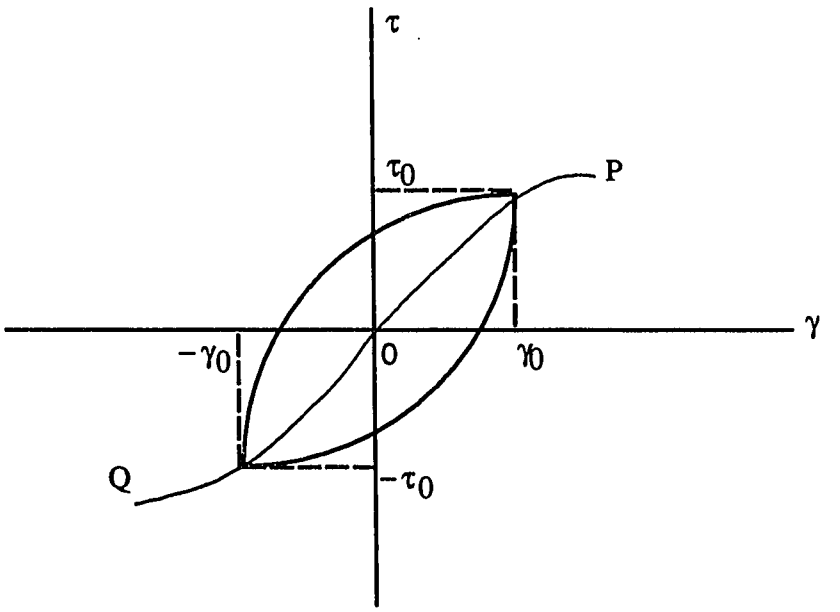

Figure 5.1 A typical maximum shear stress-maximum shear strain curve in cyclic shearing

For a cyclic shearing with a maximum shear stress amplitude $\hat{\tau}_0$, ΔW, after N cycles of loading, may be approximated by:

$$\Delta W = \sum_{i=1}^{N} h_i \tau_0^{\alpha_i+1} \tag{5.5}$$

$\hat{\tau}_0$ is normalized by dividing it by the confining pressure, $\tau_0 = \hat{\tau}_0 / \sigma_c$. The parameters h_i and α_i are parameters which, depend on the history of the deformation, confining pressure

and the initial value of the relative density. For a cyclic shearing, the hysteretic loop narrows as the number of cycles increase. This is why it is difficult to develop a single expression for the energy loss that will give exact results. A rough approximation is made, for equation 5.5 by using average quantities for α and h. It can be said that since dimensionless stress amplitude is very large, then one may assume h_i and α_i , is essentially independent of the number of preceding cycles. As a first order approximation, the average values for α and h are used.

$$\Delta W \approx hN\tau_0^{\alpha+1} \tag{5.6}$$

The value of α is determined from the experimental results. The procedure may be followed from Fig. 5.2, where in the σ, ε coordinates, the curve OA is approximated by:

$$\varepsilon = \hat{K}\sigma^{\alpha} \tag{5.7}$$

and the total energy used for densification per cycle is estimated to be proportional to:

$$\Delta W = 4\int_0^{\sigma_0} \sigma d\varepsilon = 4\hat{K}\left(\frac{\alpha}{\alpha+1}\right)\sigma_0^{\alpha+1} \tag{5.8}$$

Transferring back to the τ, γ coordinates, and combining all the resulting coefficients into one parameter, one obtains:

$$\Delta W = h\tau_o^{\alpha+1} \tag{5.9}$$

Equation 5.4 now can be written as follows:

$$hN\tau_0^{\alpha+1} = \frac{ve_0}{\eta_w g(e-e_0)}\int_0^p \frac{dp'}{f(1+p')} \tag{5.10}$$

where the left hand side is the work performed and the right hand side is the work required for the corresponding test. h is a material parameter depending on the initial value of relative density, the structure of the sand and confining pressure. It is reasonable to expect that, h should increase with increasing confining pressure and with increasing density. When D_r, exceeds 80% a non-linear relation between h and D_r takes place. This proves that dense sands follow a different deformation pattern.

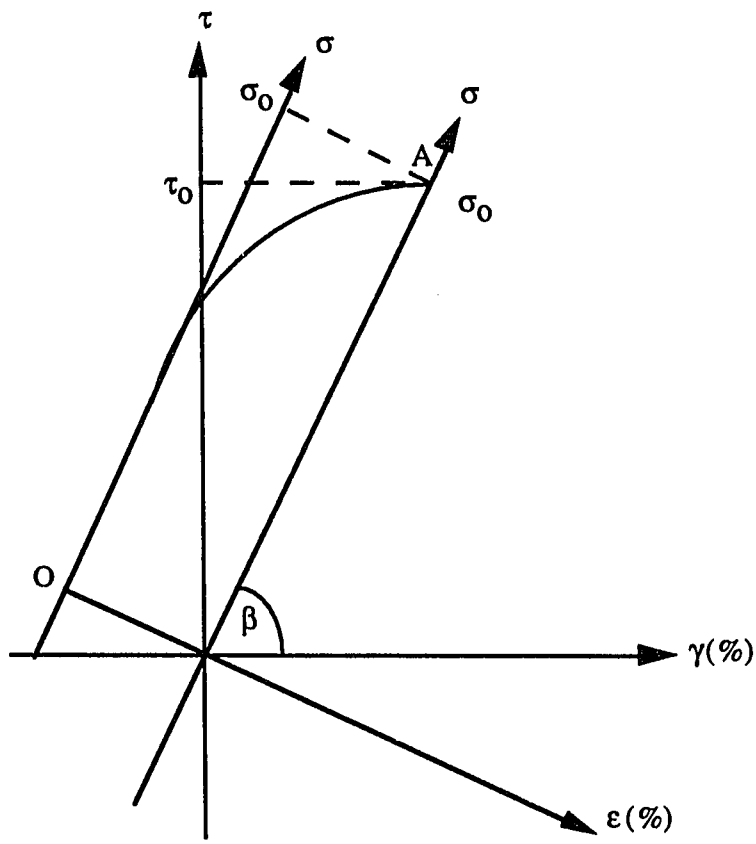

Figure 5.2 1/4 Of A Typical Hysteretic Loop

5.3 Application of the Theory

The simplest theory corresponds to the following elementary forms for the functions f and g in equation 5.4 are as follows:

$$f(1+p) \equiv (1+p)^r, \qquad r>0 \tag{5.11}$$

$$g(e_o - e_m) \equiv (e_o - e_m)^n, \quad n>1 \tag{5.12}$$

Substitution of these functions into 5.10 and integration, equation 5.13 is obtained,

$$hN\tau_0^{\alpha+1} = \frac{\hat{v}e_0}{(e-e_0)^n}[1-(1+p)]^{1-r} \tag{5.13}$$

where, $\hat{v} = v/(r-1)\eta_w$.

Nasser and Shookoh tested the validity of the above equation by setting p=1 and η and introducing $\hat{\hat{v}} = \hat{v}/h$ as follows:

$$\eta \equiv N_l \tau_0^{\alpha+1} \frac{(e-e_0)^n}{e_0} = \hat{\hat{v}}(1-2^{1-r}) \tag{5.14}$$

For a given sand with grain size and shape distribution known, $\hat{\hat{v}} = \hat{v}/h$ depends on the relative density and confining pressure. Here, N_l is the number of cycles to initial liquefaction which is the state where pore pressure equals the confining pressure. Since for silty soils, the definition of failure is changed, N_l is no more used for this research. Instead, number of cycles to cause 10% strain is used. The test results on silty sands indicated values of p smaller than 1, depending on the type of soil. So, the equation is

modified for each test. From the densification analysis made by the above writers, n is set to 3.5 and from liquefaction analysis α is set to 4. They used r as 2.5. When these values are placed in equation 5.14, it is observed that the effect of initial relative density and confining pressure is included in the parameter η. It is observed from the test results, the value of η is a constant for relative densities 54% and 68% (Table 5.1). Fig. 5.3 also shows how experimental results from De Alba et al., (1975) are compared with the theory by Nasser and Shookoh.

When p is set equal to 1, the liquefaction equation 5.14, by using the values of the parameters above can be set to:

$$N_l \tau_o^5 (e_o - e_m)^{3.5} / e_o = 0.87 x 10^{-6} \qquad (5.15)$$

From the above equation, for a given shear stress magnitude, number of cycles to liquefaction can be determined for a given sand. The two lower curves in Fig. 5.4 are plots of equation 5.15. The geometrical marks are the corresponding experimental results.

Table 5.1 Value of η For Different Relative Densities (after Nasser and Shookoh, 1978)

D_r (%)	σ_c(psi)	N_l	τ_o	$\eta * 10^{6(*)}$
54	8.07	8	0.155	0.859
	8.03	3.25	0.185	0.846
	4.53	12.5	0.144	0.929
	8.02	16	0.135	0.861
	8.14	63	0.104	0.92
68	8.09	15	0.171	0.79
	7.99	4	0.230	0.927
	8.08	53	0.134	0.824
	8.06	6	0.211	0.903

$$*\eta = \frac{(e_o - e_m)^{3.5}}{e_o} N_l \tau^5 \text{ with } e_m = 0.564$$

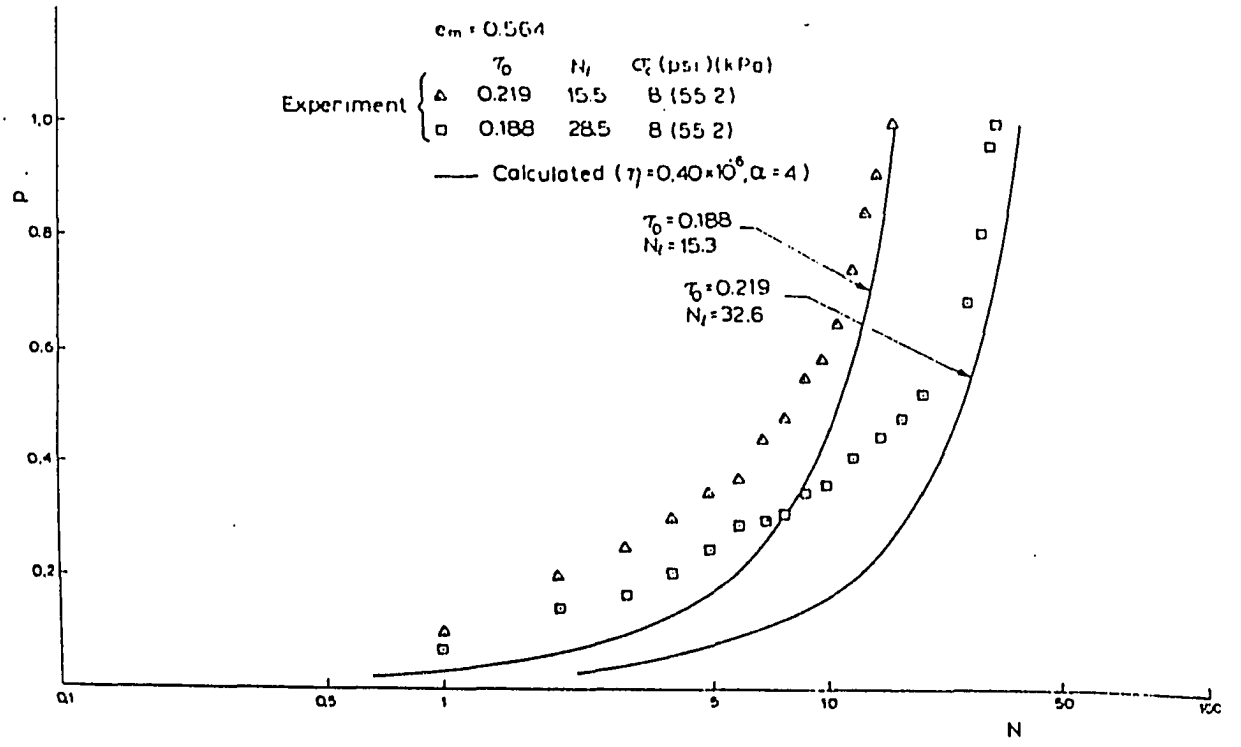

Figure 5.3 Normalized Excess Pore Pressure vs. Number of Cycles In Cyclic Shearing of Undrained Saturated Sand, (Data from De Alba et. al., 1975) τ_o=Normalized Maximum Shear Stress Amplitude, N=Number of Cycles

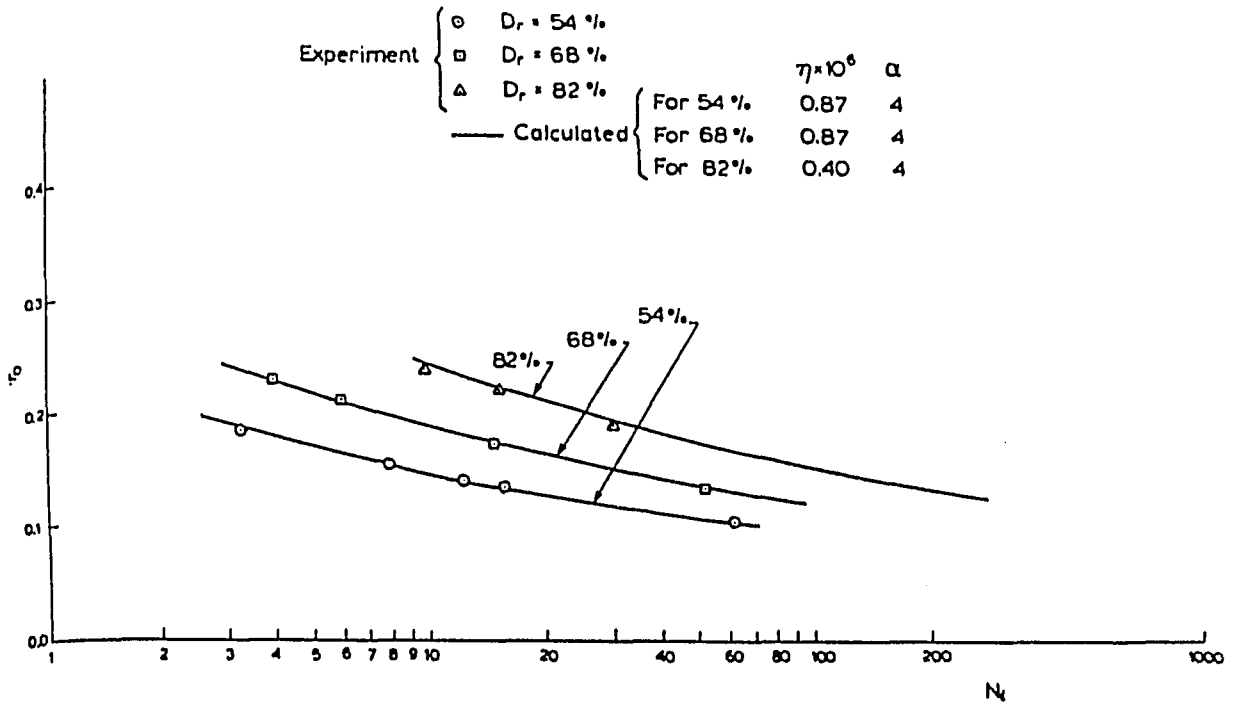

Figure 5.4 Normalized Maximum Shear Stress Amplitude vs. Number of Cycles To Liquefaction (Data from De Alba et al., 1975)

5.3.1 Comparison With Experimental Results

Equation 5.16 gives the excess pore water pressure in terms of the number of cycles N, the dimensionless shear stress amplitude τ_o, and the initial and minimum values of the void ratio.

$$p_M = \left\{1 - N\tau_o^{\alpha+1}(e_o - e_m)^n / \hat{\hat{\nu}} e_o\right\}^{1/1-r} - 1 \qquad (5.16)$$

The results of this equation have been compared by several sets of experimental data. As a start, the values of constants given by Nasser and Shookoh based on the experimental results reported by De Alba are used. The Ottowa sand used in this research has a minimum void ratio of 0.5 and maximum void ratio of 0.78. The experiments performed on sand samples with 50% and 70% relative densities for a confining pressure of 98 kPa. and for various fixed shear stress amplitudes. The excess pore water pressure and the shear strain amplitude have been reported in terms of the number of cycles for the above stated values of the initial relative density.

Theoretical results based on basic equation 5.1, for the densification of dry sand have been obtained from extensive experimental data reported by Youd (1970, 1972) and from a first order approximation, n=3.5 was found to fit all the results. This value is used as given. Assigning a positive even value to α, $\alpha = 4$ yielded results that are compatible with experimental observations in the liquefaction of cohesionless sand. In Nasser's work, the value of r is chosen to fit the experimental data. Similarly, the value of r best representing the experimental results of this research has to be determined. However this is not a straightforward task since equation 5.16 does not involve r in a simple manner. In addition to the exponent $1/(1-r)$, $\hat{\hat{\nu}} = \hat{\nu}/h$ with $\hat{\nu} = \nu/(r-1)\eta_w$ is a function of r. Hence, the

following iterative scheme is utilized to obtain a value of r that best fits the data for a particular experiment.

1) Guess a value for r, r_{guess}.
2) Calculate $\hat{\hat{v}} = \hat{v} / h$ using r_{guess}.
3) Regress $\log\left(p_{experimental} + 1\right) = \alpha \log\left(1 - N\tau_o^{\alpha+1}(e - e_m)^n / e_o \hat{\hat{v}}\right)$
4) Calculate $r_{regress}$ from $\alpha = 1/(1 - r_{regress})$.
5) Compare r_{guess} and r_{out}. If the discrepancy is too large go to step 2 until $r_{guess} = r_{out}$.

r for each type of specimen is calculated from iterations are given in Table 5.2. Calculations reveal that r must be greater than 1 and from the iterations, it must range between 2 and 6 for clean sand. r is taken as 3.7 in this research. For a given sand with a given grain size and shape distribution, $\hat{\hat{v}} = \hat{v} / h$ should depend on the confining pressure and on the initial value of the relative density. Since for clean sand the liquefaction is identified as pore pressure reaching the value of confining pressure, p is set equal to 1. The effect of the initial relative density and confining pressure is included in the parameter η. To further stress this point, η is calculated for loose and medium samples.

Table 5.4 shows the values of η. From the test results it can be concluded that the value of η is a constant for relative densities 50% and 70%. The value of h in the expression for work may tend to become larger for higher relative densities. Since η is inversely proportional to h, its value decreases as relative density gets higher. Indeed, as Nasser and Shookoh did, here η is accepted as a constant (within experimental error) for relative densities 50% and 70%. So, η can be set to 0.3 x 10^{-6} or $\hat{\hat{v}} = 0.46x10^{-6}$ for this sand with relative densities smaller than 70%. Figures 5.5 and 5.6 represent the loose and

medium sand where the solid lines correspond to the equation 5.16 and the curve with marks correspond to the pore pressure buildup curves for experiments. Both curves correspond to a confining pressure of 98 kPa.

The pore pressure buildup predictions from the results, show excellent agreement with the results of the tests. Figures 5.7 through 5.14 represent comparisons for soils, where the solid lines correspond to the theoretical results and marks correspond to the theoretical results. All the results correspond to the 98 kPa. pressure.

Table 5.2 Value Of η For Different Relative Densities for Ottowa Sand

D_r (%)	σ_c(kPa.)	N_l	τ_o	$\eta * 10^{6(*)}$
~50	98	4	0.35	0.337
	98	11	0.30	0.428
	98	17	0.25	0.333
	98	76	0.20	0.390
~70	98	26	0.30	0.125
	98	365	0.25	0.336
	98	393	0.20	0.210

$$*\eta = \frac{(e_o - e_m)^{3.5}}{e_o} N_l \tau^5 \text{ with } e_m = 0.5$$

Table 5.3 Value Of η For Different Void Ratios of Medium Silty Sand

Silt (%)	σ_c(kPa.)	N_l	τ_o	η*
10	98	13	0.30	$1.59*10^{-6}$
	98	75	0.25	$3.55*10^{-6}$
	98	629	0.20	$2.09*10^{-6}$
20	98	4	0.30	$8.32*10^{-6}$
	98	15	0.25	$7.11*10^{-6}$
	98	19	0.20	$4.54*10^{-6}$
30	98	3	0.30	$6.76*10^{-7}$
	98	8	0.275	$7.53*10^{-7}$
	98	15	0.20	$8.01*10^{-7}$
10p[1]	98	22	0.30	$2.57*10^{-6}$
	98	143	0.25	$6.72*10^{-6}$
	98	289	0.225	$8.03*10^{-6}$

$$*\eta = \frac{(e_o - e_m)^{3.5}}{e_o} N_l \tau^5 \text{ with } e_m = \text{varies with silt \%.}$$

[1]Low Plasticity Silt

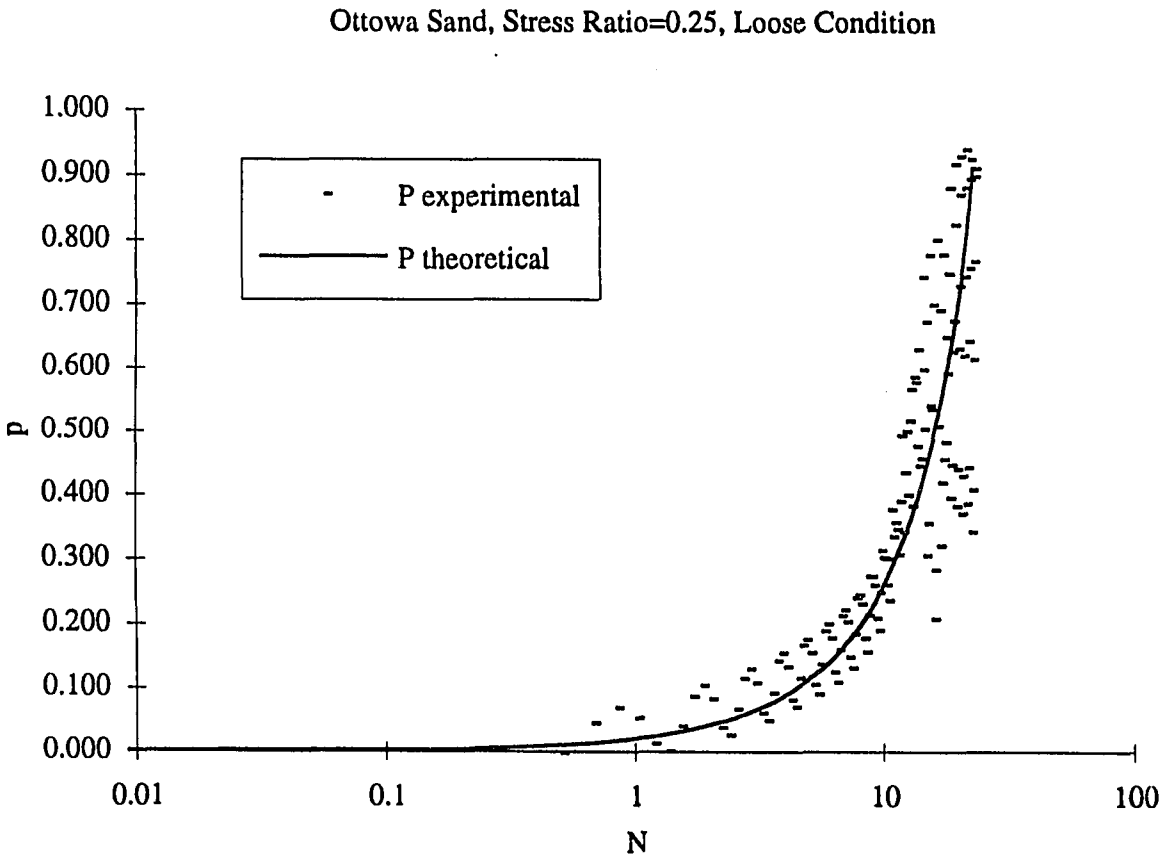

Figure 5.5 Normalized Excess Pore Pressure vs. Number of Cycles in Cyclic Shearing of Loose Sand

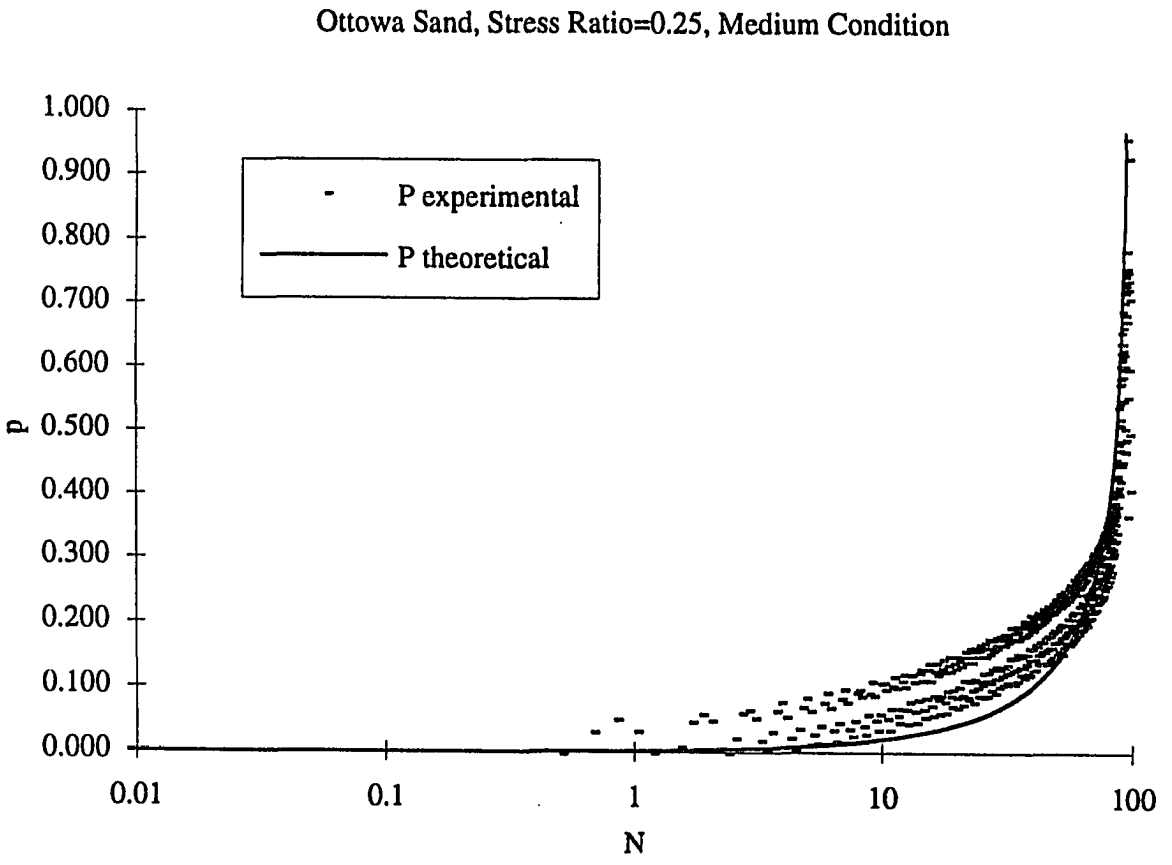

Figure 5.6 Normalized Excess Pore Pressure vs. Number of Cycles in Cyclic Shearing of Medium Sand

When n is set to 3.5 and if arbitrarily one experimental point is chosen in order to fix the parameter η, one can plot the variation of shear stress amplitude $\hat{\tau}_0$ with void ratio for the indicated confining pressure for a certain number of cycles. Since η is a material parameter, for each silt content it is different. From Table 5.4, values of η can be placed in equation $N_l \tau_o^5$ =constant, for each soil type. And for different shear stresses, number of cycles to liquefaction is calculated. As an example, the case of 30% is taken below. When the value of η is placed in equation 5.13, it becomes:

$$N\tau_0^5 = 7.4 * 10^{-7} e_o / (e_o - e_m)^{3.5} * \left[1 - (1+p)^{-1.5}\right] \qquad (5.17)$$

which relates the number of cycles for a given τ_o to the corresponding pore water pressure. There are no free constants in this equation. Its validity against experimental results are tested and presented on figure 5.15. The same procedure is repeated with the other η values and the results are presented in the plots of Figures 5.15 and 5.16. As can be seen from the above Table 5.4, the value of η, decreases as the soil gets weaker which is an indication of failure in less cycles.

Table 5.4 Values Of r and η From the Results of Iterations For Different Soil Types for Medium Condition.

	Sand	10% silt	20% silt	30% silt
Range	2<r<6	4.2<r<4.8	3.5<r<5.4	1.02<r<3.6
r	3.7	4.5	4.7	2
η	$3.8*10^{-5}$	$1.62*10^{-6}$	$6.65*10^{-6}$	$7.4*10^{-7}$

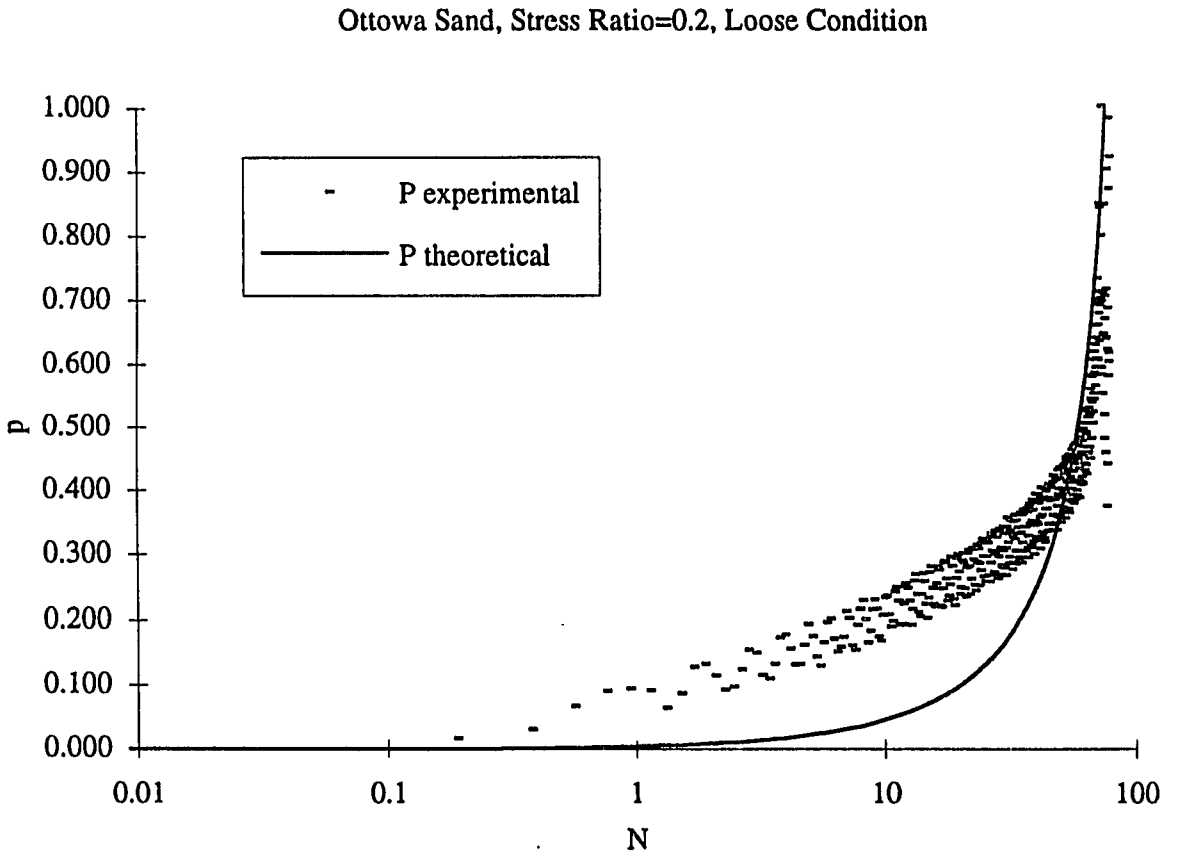

Figure 5.7 Normalized Excess Pore Water Pressure p versus number of cycles in cyclic shearing of undrained saturated loose sand

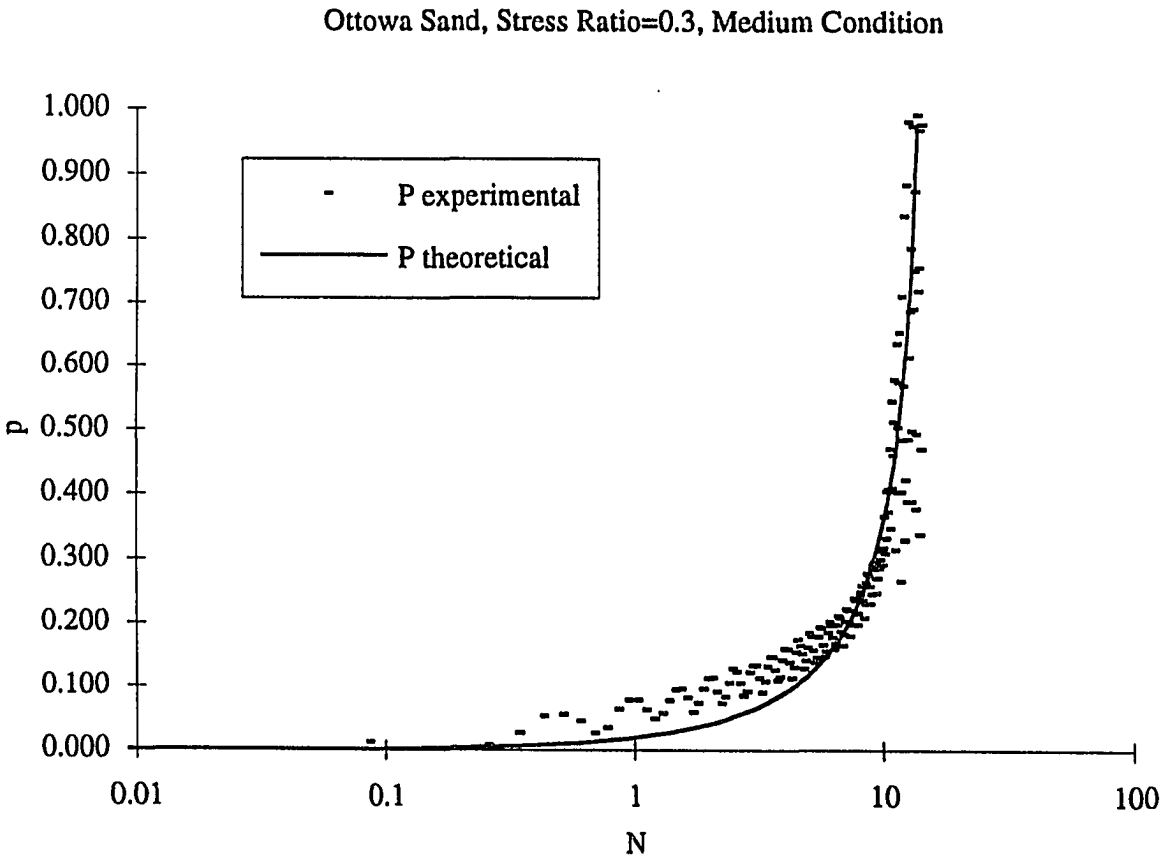

Figure 5.8 Normalized Excess Pore Water Pressure p versus number of cycles in cyclic shearing of undrained saturated medium sand

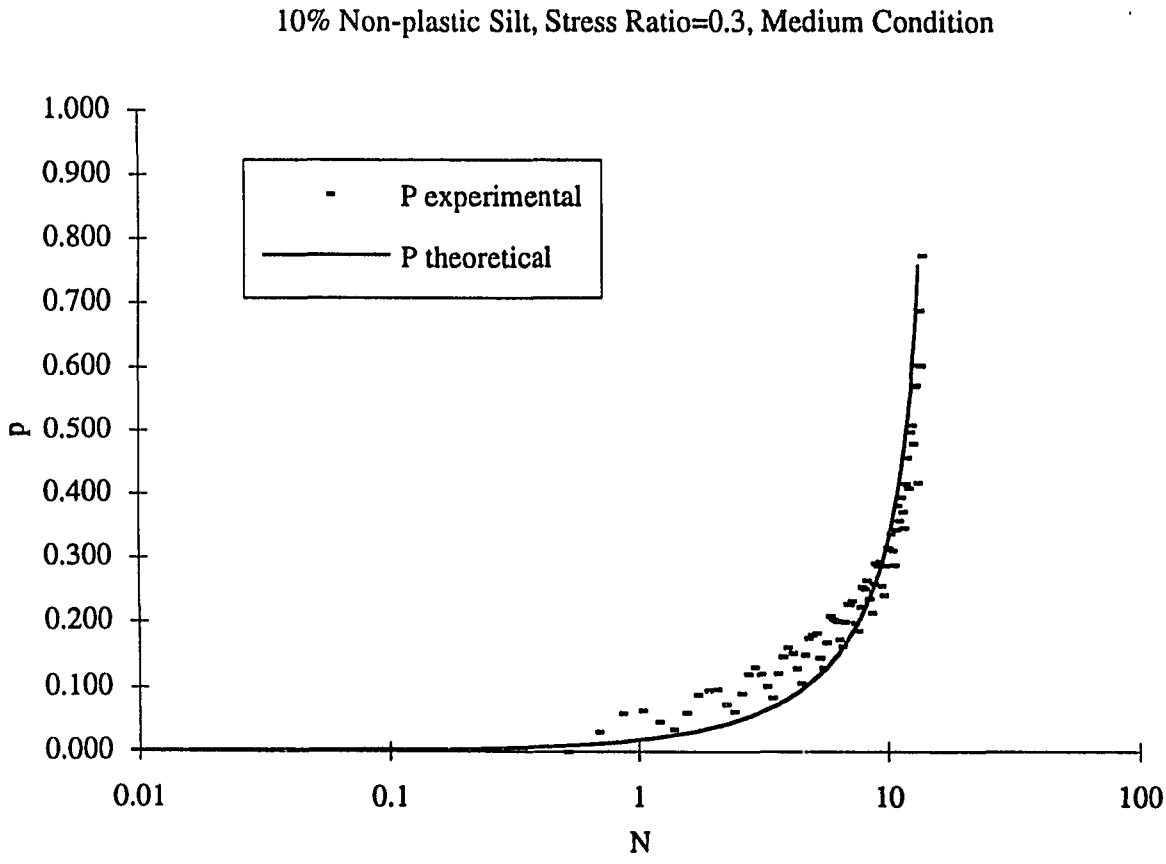

Figure 5.9 Normalized Excess Pore Water Pressure p versus number of cycles in cyclic shearing of undrained saturated medium silty soil (10% Silt)

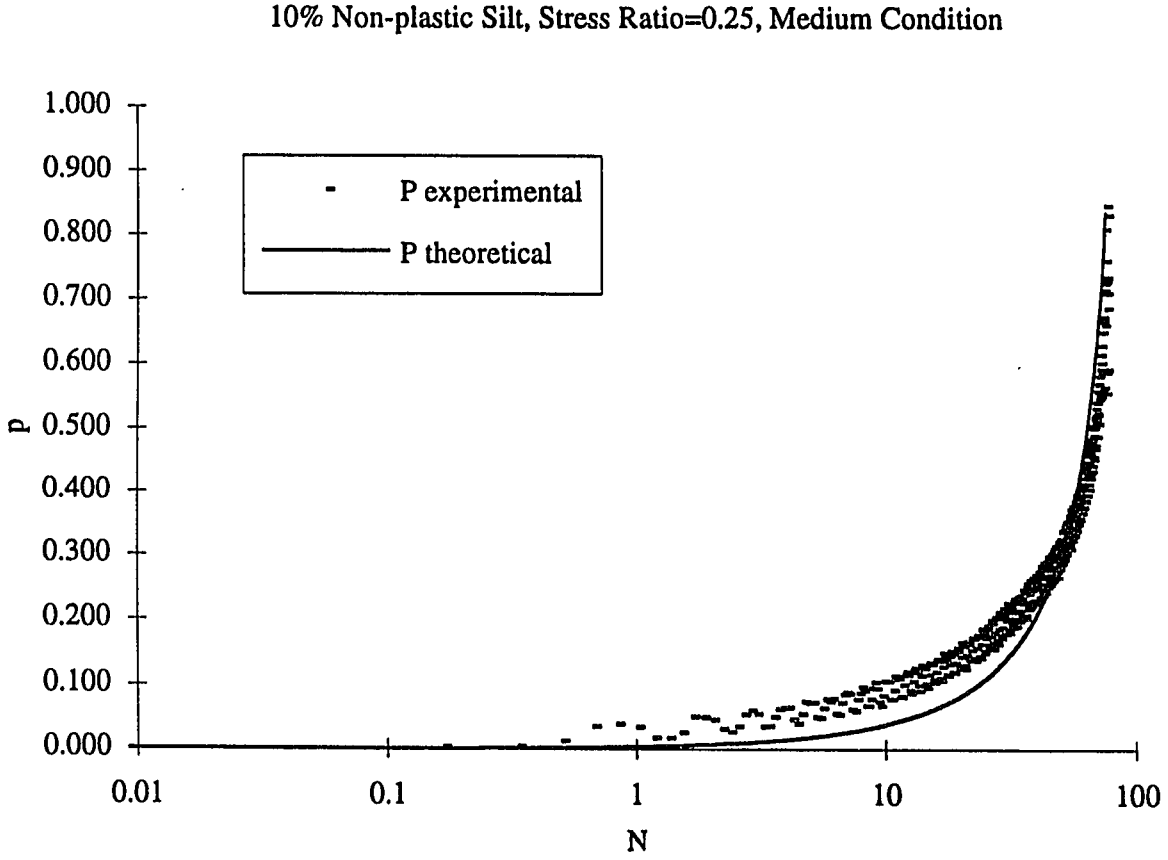

Figure 5.10 Normalized Excess Pore Water Pressure p versus number of cycles in cyclic shearing of undrained saturated medium sand (10% Silt)

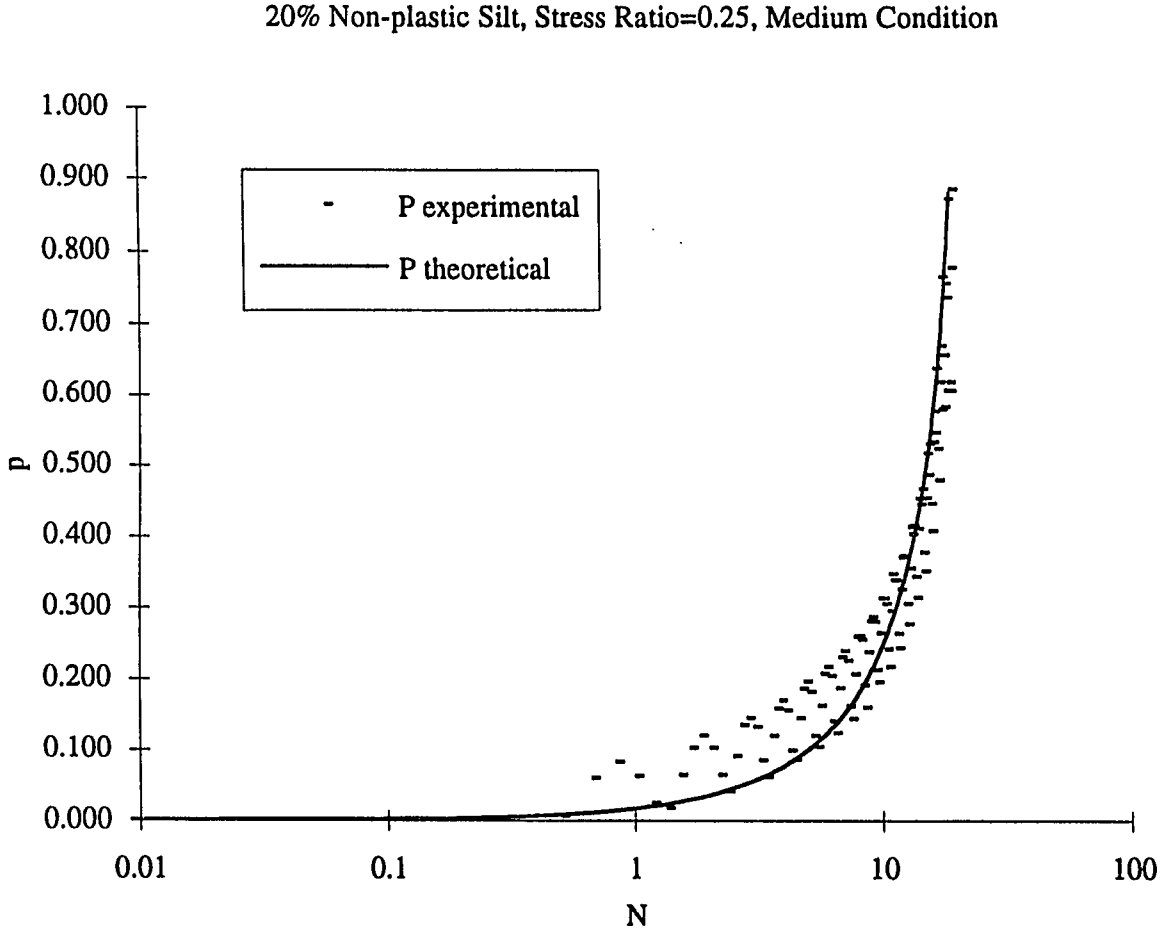

Figure 5.11 Normalized Excess Pore Water Pressure p versus number of cycles in cyclic shearing of undrained saturated medium sand (20 % Silt)

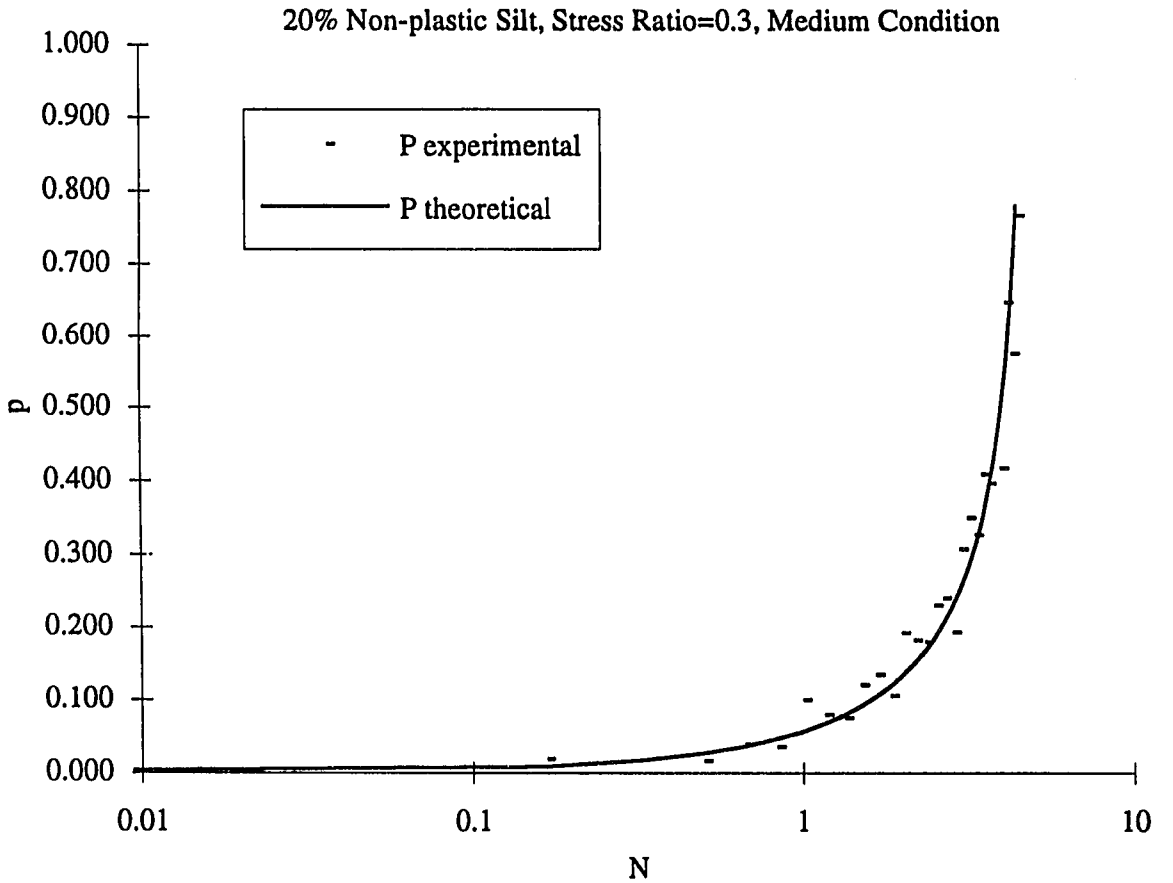

Figure 5.12 Normalized Excess Pore Water Pressure p versus number of cycles in cyclic shearing of undrained saturated medium soil (20% Silt)

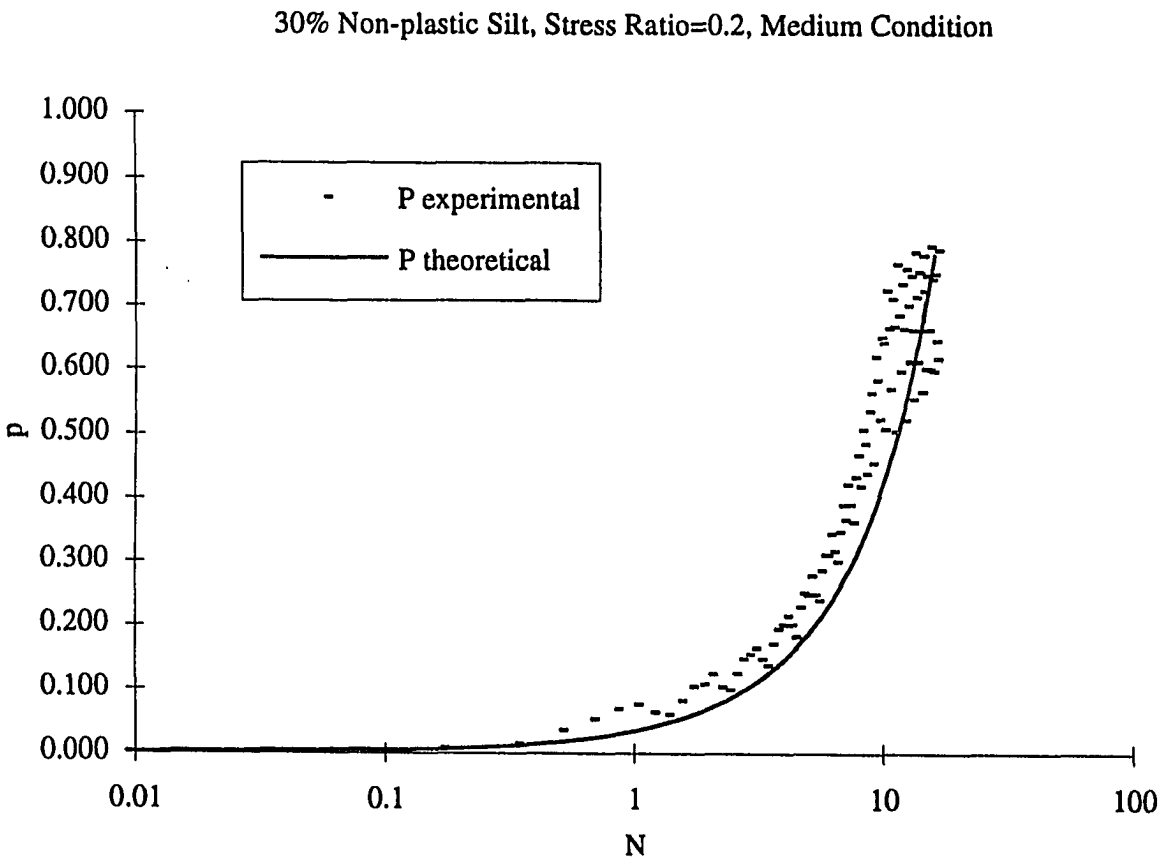

Figure 5.13 Normalized Excess Pore Water Pressure p versus number of cycles in cyclic shearing of undrained saturated medium sand (30% Silt)

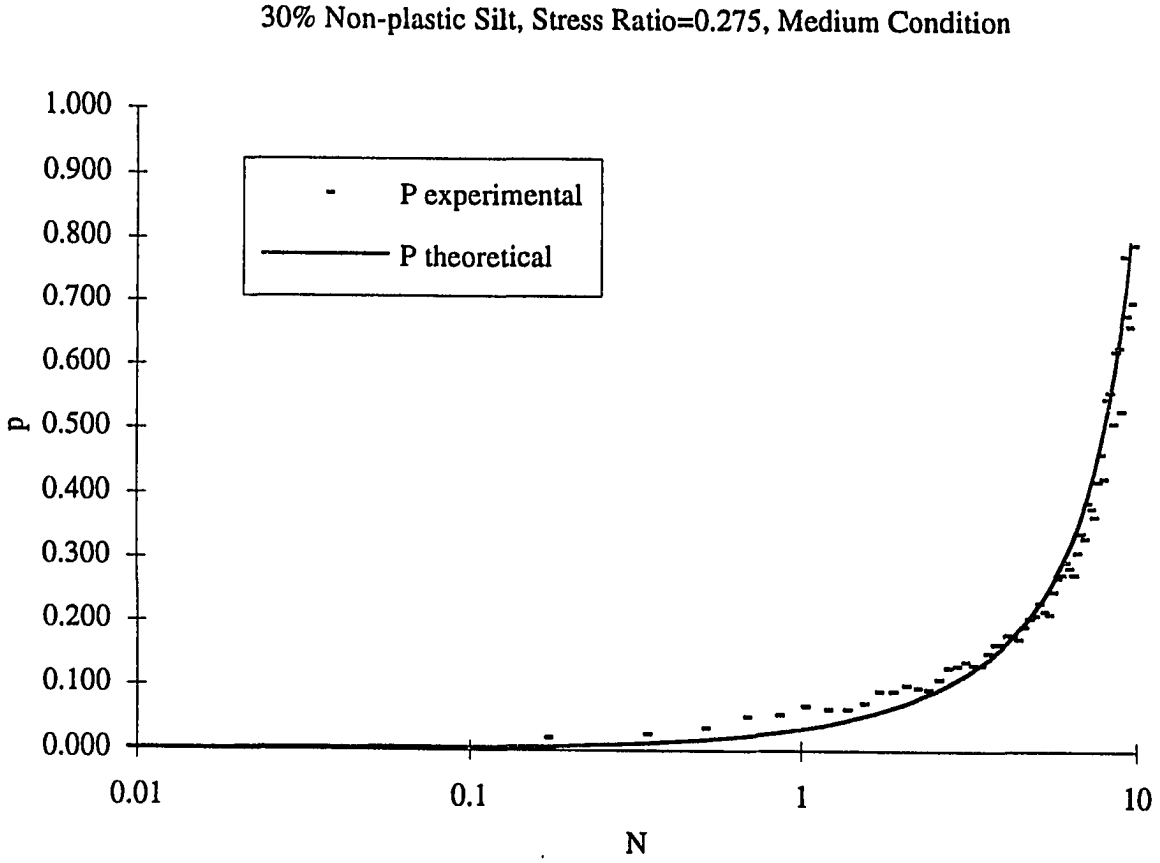

Figure 5.14 Normalized Excess Pore Water Pressure p versus number of cycles in cyclic shearing of undrained saturated medium soil (30% Silt)

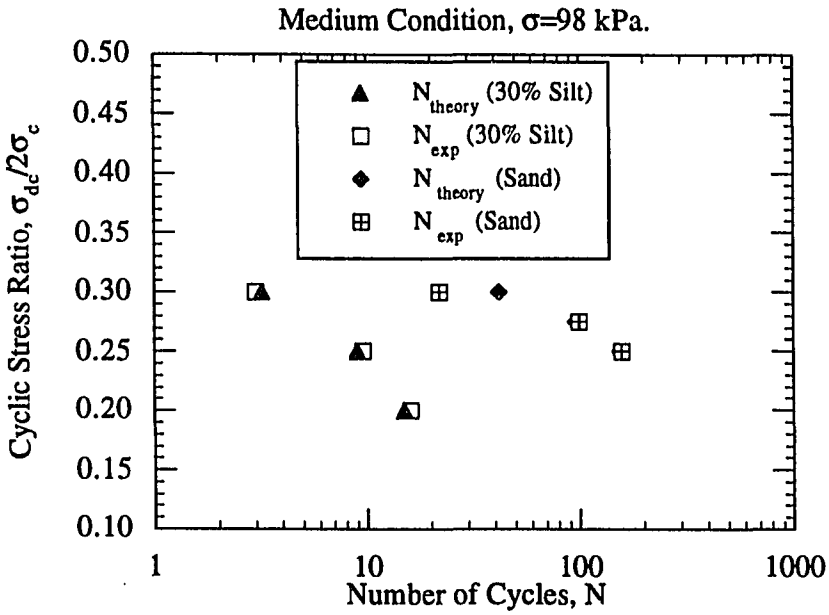

Figure 5.15 Normalized Shear Stress Amplitude vs. Number of Cycles to Liquefaction

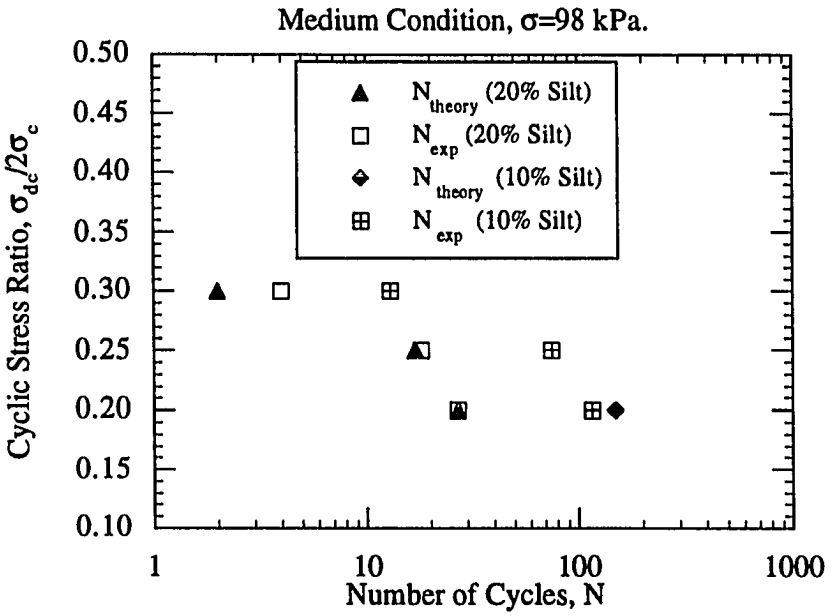

Figure 5.16 Normalized Shear Stress Amplitude vs. Number of Cycles to Liquefaction

5.4 Conclusions

The following conclusions can be drawn from the results:

1) A material model may only be deemed to be satisfactory when with its aid, it is possible to determine the behavior of the material at hand in one piece of testing equipment (e.g., in triaxial tests), and then to predict the observed behavior of the same material in some other type of testing equipment (e.g., in simple shear tests) (Prevost, 1987). This model parameters were originally set by the results from simple shear tests. And the model successfully predicted the results from triaxial test results.

2) It is obvious that, dissipated energy may be a more convenient parameter than equivalent stresses and equivalent number of cycles for characterization of actual earthquake loading.

3) The proposed liquefaction equation can successfully predict the pore pressure generation in sand and silty sand. The parameter η, seems to be insensitive to relative densities less than 70%.

4) The difference between the experimental and analytical curves is overcome by iterating the value of r, to find the best fit. After, a better agreement between the measured and calculated pore water pressures are obtained, the value of η, is used to predict the test results.

VI STRAIN CONTROLLED TESTS

6.1 Introduction

Obtaining good quality laboratory data is very important since many design methods rely on laboratory test results. Because of the unacceptable scatter of test data from stress controlled tests, strain controlled tests were run for the second stage of the testing program. The other reason was to find the threshold shear strength for silty soils.

Tests have been performed with a cyclic shear strain range of 0.015% to 1.5% to investigate the effect of fine content on the pore pressure generation in sand. These tests were carried to 1000 cycles or to initial liquefaction, whichever occurred first. Triaxial tests were performed on pure sand and silt specimens and specimens with silt additions of 10, 20, 30, and 60 % by weight. Two types of silt, a non plastic silt and a low plasticity silt (PI≈10) were used as control materials. The main parameters varied in this study were the amount of silt, the plasticity index of silt, and the void ratio where the observed parameter was the pore pressure generation. The cyclic results presented and analyzed are normalized with respect to the confining stress, σ_c.

6.2 Strain Approach to Liquefaction

Data collected from stress controlled tests from several researches show that there are many factors effecting the results of stress controlled tests and data obtained is usually scattered. The stress approach is originally based on the fact that pore pressure buildup is a function of relative density, initial effective stresses acting on the sand, method of specimen preparation, lateral earth pressure coefficient, overconsolidation ratio and increased time

under pressure (Dobry et al., 1982). These findings raised several questions about the practice of using stress-controlled tests for predicting pore pressure buildup.

Silver and Seed (1971), showed that cyclic shear strain $\gamma_c = \frac{\tau_c}{G}$ (G=secant shear modulus) rather than cyclic shear stress controls the densification and liquefaction of sands. The pore water pressure buildup is controlled mainly by the magnitude of cyclic shear strain. This leads to the conclusion that shear modulus, rather than relative density, D_r is the main parameter controlling the pore pressure buildup. Unlike relative density or sand fabric, the shear modulus at small strains, G_{max} can be directly measured in the field by means of shear wave propagation velocity.

The advantages of running cyclic strain tests is also shown by Castro (1975). Near the end of the cyclic triaxial tests, there is a substantial redistribution of water content within the specimen when the cyclic strain becomes large. So this redistribution ceases to represent the field situation. In this case the strains measured in the laboratory are so large which makes the test results unusable as a design tool. Also the fabric effect on pore pressure buildup is practically nonexistent if strain-controlled tests are performed. Cyclic strain controlled tests or strain approach assumes that cyclic shear strain amplitude is the fundamental governing cyclic loading parameter.

One other reason for using strain approach is the repeatability of the strain controlled tests. Using the same parameters for two specimens, almost same results were obtained from strain controlled tests in this research. The scatter of the test data which is the basic problem of stress controlled testing did not occur in strain controlled testing.

6.3 Threshold Shear Strain

Cyclic strain approach recognizes the existence of a threshold cyclic shear strain, γ_t. Based on cyclic test results on dry sands, Drnevich and Richart (1970), Youd (1972) and Pyke (1973) concluded that there's a threshold cyclic shear strain, γ_t of the order of 10^{-2} percent below which, no densification occurs. Dobry, defines threshold strain as the strain amplitude needed to initiate a pore pressure buildup in a saturated cohesionless soil. The existence of a threshold level at which pore water pressure buildup starts is obviously very important for liquefaction prediction.

Dobry et al., (1982), Ladd et al., (1989), Dyvik et al., (1984) studied the strain effects on the pore pressure generation in saturated clean sands using undrained cyclic triaxial tests by strain approach to evaluate the threshold shear strain level. Regardless of the number of cycles, confining stress and fabric, below threshold strain, neither volume changes nor significant pore pressure changes occur in the soil. This value is in the order of 10^{-2} % strain for clean sands (Fig. 6.1).

6.4 Soil Elasticity

The results of the cyclic triaxial tests were measured in terms of axial deviatoric load (σ_d) and strain (ε_v) and converted to cyclic shear strain $\gamma = 1.5\ \varepsilon_v$ and shear stress $\tau = 0.5\ \sigma_d$ using conventional theory of elasticity. The principal strain tensors for an element under triaxial conditions can be seen from Fig. 6.2.

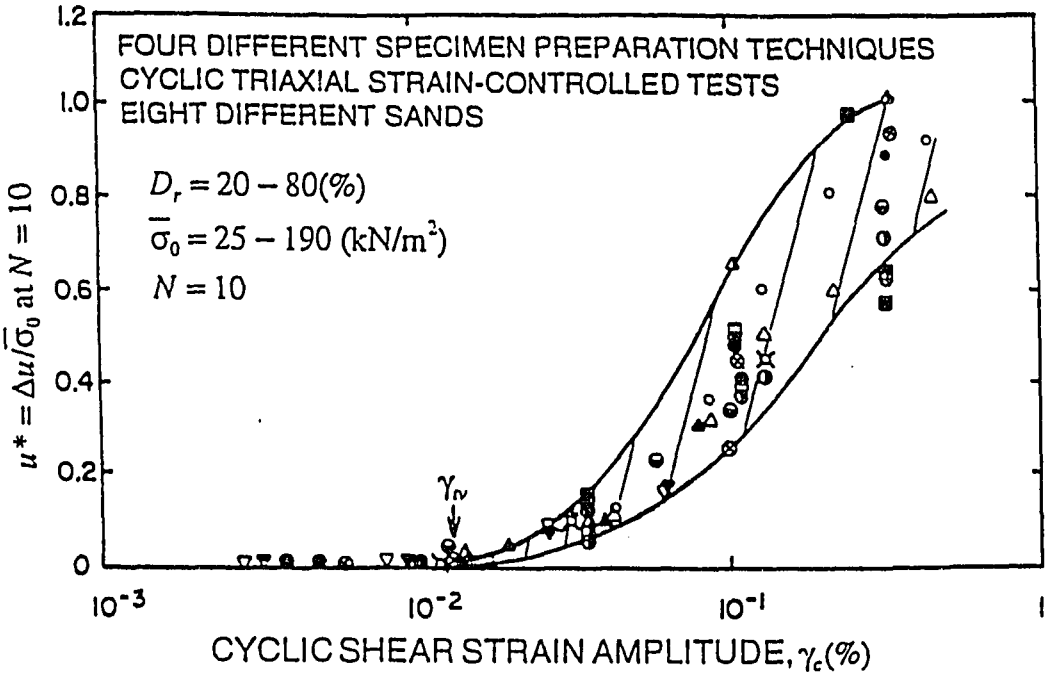

Figure 6.1 Buildup of Residual Pore Water Pressure in Different Sands in Cyclic Triaxial Strain Controlled Tests (Dobry, 1985)

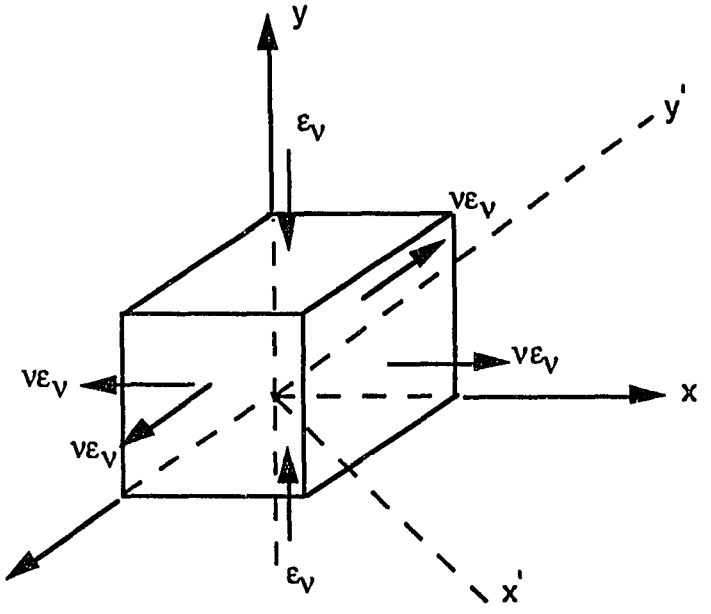

Figure 6.2 Components of Principal Strain

The transformation from axial strain, ε_v to cyclic shear strain, γ can be described by these equations:

$$\varepsilon = \begin{bmatrix} -\varepsilon_v & 0 & 0 \\ 0 & \nu\varepsilon_v & 0 \\ 0 & 0 & \varepsilon_v \end{bmatrix} \tag{6.1}$$

Transformation law applies to change the x, y, z axes to x', y', z' axes and the transformation matrix is:

$$\beta = \begin{bmatrix} 0.707 & 0.707 & 0 \\ -0.707 & 0.707 & 0 \\ 0 & 0 & 1 \end{bmatrix} \tag{6.2}$$

The rotated strain tensor can be calculated as:

$$\varepsilon' = \begin{bmatrix} 0.707 & 0.707 & 0 \\ -0.707 & 0.707 & 0 \\ 0 & 0 & 1 \end{bmatrix} \begin{bmatrix} -\varepsilon_v & 0 & 0 \\ 0 & \nu\varepsilon_v & 0 \\ 0 & 0 & \nu\varepsilon_v \end{bmatrix} \begin{bmatrix} 0.707 & -0.707 & 0 \\ 0.707 & 0.707 & 0 \\ 0 & 0 & 1 \end{bmatrix} \tag{6.3}$$

$$\varepsilon' = \begin{bmatrix} 0.707 & 0.707 & 0 \\ -0.707 & 0.707 & 0 \\ 0 & 0 & 1 \end{bmatrix} \begin{bmatrix} -0.707\varepsilon_v & 0.707\varepsilon_v & 0 \\ 0.707\nu\varepsilon_v & 0.707\varepsilon_v & 0 \\ 0 & 0 & \nu\varepsilon_v \end{bmatrix} = \begin{bmatrix} -(0.5\varepsilon_v + 0.5\nu\varepsilon_v) & (0.5\varepsilon_v + 0.5\nu\varepsilon_v) & 0 \\ (0.5\varepsilon_v + 0.5\nu\varepsilon_v) & (-0.5\varepsilon_v + 0.5\nu\varepsilon_v) & 0 \\ 0 & 0 & \nu\varepsilon_v \end{bmatrix} \tag{6.4}$$

$$\varepsilon' = \begin{bmatrix} -0.5(1-\nu)\varepsilon_v & 0.5(1+\nu)\varepsilon_v & 0 \\ 0.5(1+\nu)\varepsilon_v & -0.5(1-\nu)\varepsilon_v & 0 \\ 0 & 0 & \nu\varepsilon_v \end{bmatrix} \tag{6.5}$$

The transformed strains in xy and yz directions are:

$$\varepsilon_{xy} = \varepsilon_{yx} = 0.5(1+\nu)\varepsilon_v \qquad (6.6)$$

Cyclic shear strain is defined as:

$$\gamma_c = 2\varepsilon_{xy} = (1+\nu)\varepsilon \qquad (6.7)$$

To find the Poisson's ratio for saturated sand, under undrained constant volume condition, one can describe the general triaxial change of effective stress by the following equations (Wood, D. M. 1990):

$$\begin{bmatrix}\delta\varepsilon_v \\ \delta\varepsilon_r\end{bmatrix} = \frac{1}{E'}\begin{bmatrix}1 & -2\nu' \\ -\nu' & 1-\nu'\end{bmatrix}\begin{bmatrix}\delta\varepsilon'_v \\ \delta\varepsilon'_r\end{bmatrix} \qquad (6.8)$$

The strain increment and effective stress variables for analysis of triaxial tests are the mean effective stress p' and deviatoric stress q, and written as:

$$\begin{bmatrix}p' \\ q\end{bmatrix} = \begin{bmatrix}\frac{1}{3} & \frac{2}{3} \\ 1 & -1\end{bmatrix}\begin{bmatrix}\sigma'_v \\ \sigma'_r\end{bmatrix} \qquad (6.9)$$

and the increments of volumetric strain $\delta\varepsilon_p$ and triaxial strain $\delta\varepsilon_q$,

$$\begin{bmatrix}\delta\varepsilon_p \\ \delta\varepsilon_q\end{bmatrix} = \begin{bmatrix}1 & 2 \\ \frac{2}{3} & -\frac{2}{3}\end{bmatrix}\begin{bmatrix}\delta\varepsilon_v \\ \delta\varepsilon_r\end{bmatrix} \qquad (6.10)$$

Equation 6.8 can be written in terms of bulk modulus and shear modulus to separate effects of grain size and changing shape:

$$\begin{bmatrix} \delta\varepsilon_p \\ \delta\varepsilon_q \end{bmatrix} = \begin{bmatrix} \frac{1}{K'} & 0 \\ 0 & \frac{1}{3G'} \end{bmatrix} \begin{bmatrix} \delta p' \\ \delta q' \end{bmatrix} \qquad (6.11)$$

For a conventional undrained triaxial compression test on a soil specimen, the initial response of the soil specimen is elastic but pore pressures develop due to constant volume condition. When condition of constant volume is imposed on 6.11,

$$\frac{\delta p'}{K'} = 0 \qquad (6.12)$$

which requires $\delta p' = 0$. The relationship between bulk modulus, K Poisson's ratio ν and elastic modulus, E can be written as:

$$K = \frac{E}{3(1-2\nu)} \qquad (6.13)$$

The total stress equivalent of equation 6.11 is:

$$\begin{bmatrix} \delta\varepsilon_p \\ \delta\varepsilon_q \end{bmatrix} = \begin{bmatrix} \frac{1}{K_u} & 0 \\ 0 & \frac{1}{3G_u} \end{bmatrix} \begin{bmatrix} \delta p \\ \delta q \end{bmatrix} \qquad (6.14)$$

The distinction between elastic properties in terms of total or effective stresses is useful when the concern is undrained conditions. For an undrained constant volume condition $\delta\varepsilon_p = 0$ implies that :

$$\frac{\delta p}{K_u} = 0 \qquad (6.15)$$

The total stress undrained bulk modulus K_u must be infinite for the above equation to be valid which makes Poisson's ratio, ν_u in equation 6.13 to be 1/2. When the value of undrained Poisson's ratio is placed in equation 6.7, the equation becomes:

$$\gamma_c = (1+\nu)\varepsilon_v = (1+1/2)\varepsilon_v = 1.5\varepsilon_v \quad (6.16)$$

6.5 Discussion of the Results

Typical test results are shown in Figs. 6.3 a, b, c, d, e which are obtained from a typical test on sand with 10% non-plastic silt. In this case, a cyclic load applied to the specimen with a maximum shear strain amplitude of 1.0%. As loading proceeds, the generated pore pressure increases up to the level of confining pressure as can be seen from Fig. 6.3-d and a reduction of effective stress takes place which is accompanied by the softening of the specimen. For a constant amplitude cyclic shear strain, changes in effective stress can be seen from Fig. 6.3-e. As figure implies, after each cycle, the effective confining pressure is reduced with an increase in residual pore pressure.

An important issue of concern in this experimental program was the effect that silt content and silt plasticity might have on the magnitude of threshold shear strain. Typical value of threshold shear strain is about 0.01 percent for a wide variety of sands (Dobry et al., 1982). In Figs. 6.4 and 6.5, relationships between the shear strain and pore pressure are

presented for sand, and silty sand under both medium and loose conditions, different silt contents and silt plasticity. As shown in these figures and through the paper, for all silt contents, silt plasticity, and number of loading cycles, no significant rise in pore pressure was observed at strain levels below 0.01 percent. Therefore, silty sands have approximately the same threshold strain as sands, under both loose and dense conditions.

The effect of silt content, however, is clearly demonstrated at strain levels above the threshold shear strain. For example, for both non-plastic and low plasticity silts there is significant increase in the generated pore pressure at high strain levels. A clear trend is shown in Figures 6.6 and 6.7 for the effect of silt content on medium sand undergoing low and high amplitude loading cycles. As shown in figure 6.6, addition of up to 30 percent in non-plastic silt, while maintaining the same void ratio, results in increasing pore pressure up to a limiting value which corresponds to 30 percent in silt content. In the case of low plasticity silt, increasing silt content has no significant effect on the generated pore pressure, up to 60 percent in silt content. At silt contents above 60 percent, the pore pressure is significantly reduced, and approximately unchanged for specimens undergoing high (0.75 percent) and low (0.015 percent) amplitude loading, respectively.

It may be explained that increasing silt content, and plasticity, reduce the potential for particle rearrangement during the loading process and thus reduce the amount of generated

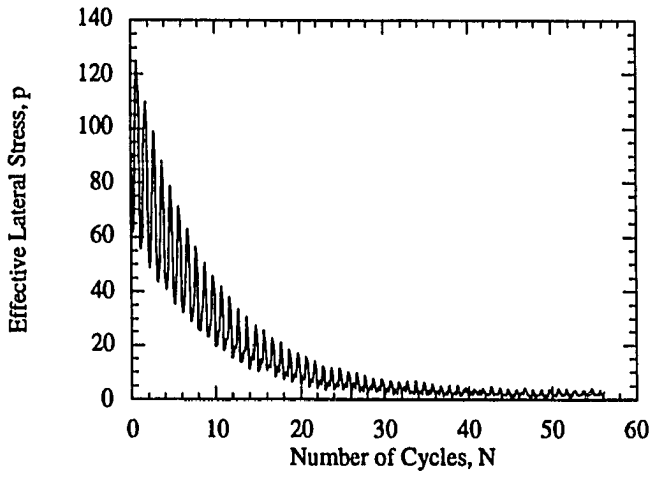

(a)

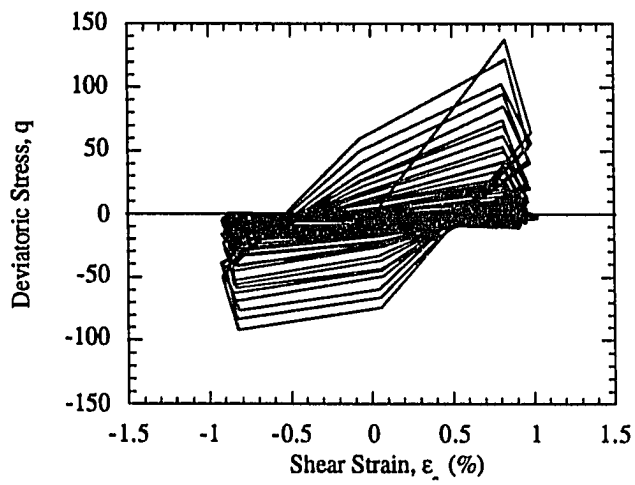

(b)

Fig.6.3 Typical Tests Results from Strain Controlled Tests a) Deviatoric Stress vs. Number of Cycles b) Pore Water Pressure vs. Number of Cycles

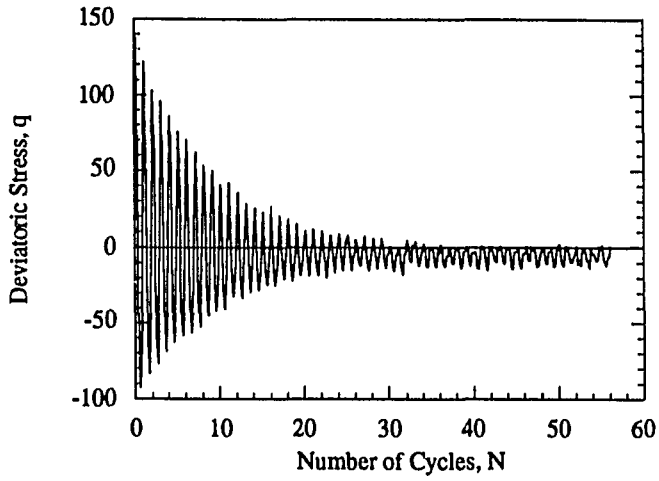

c)Deviatoric Stress vs. Number of Cycles

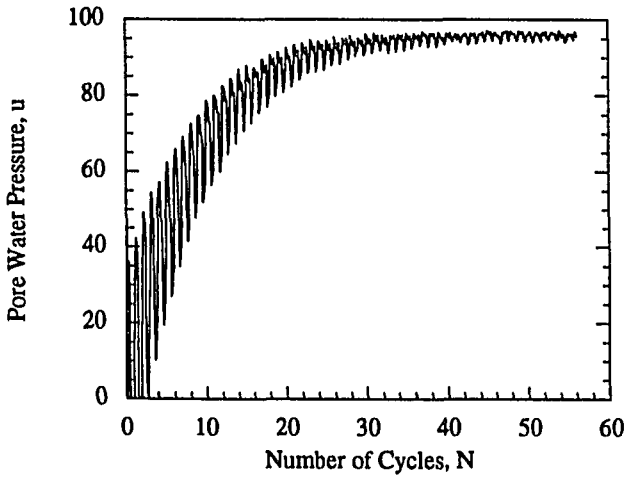

d) Pore Water Pressure vs. Number of Cycles

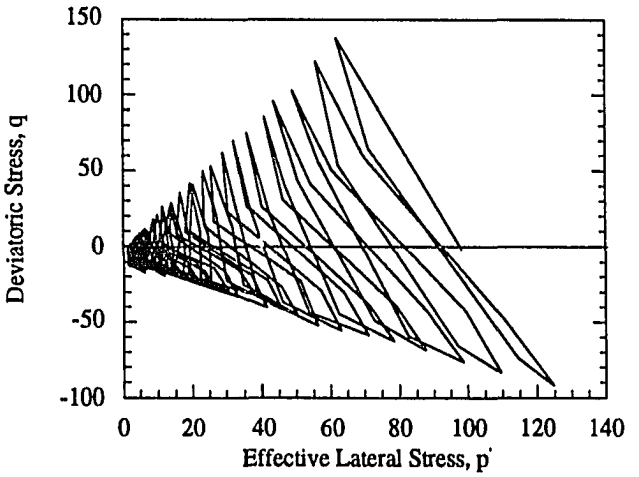

6.3 e) Deviatoric Stress vs. Effective Lateral Stress

pore pressures. The same, however, may not be said about non-plastic silts. In this case, it may be explained that presence of silt in effect helps the process of particle arrangement by acting as a pseudo lubricant. As shown in Fig. 6.6, the maximum non-plastic silt content used was 30 percent. Higher contents could not be used because of difficulties with respect to sample preparation. It was not possible to go any higher than 30 percent and maintain the same void ratio between the sand and silty sand.

The effect of number of loading cycles on the magnitude of pore pressure is basically a function of shearing strain. The number of loading cycles did not have any significant effect on the level of threshold shear strain, as shown in Figs. 6.8 and 6.10. In these figures, the effect of cycle number, which in this case is 10 and 30, on the level of threshold strain is presented. Increasing the number of cycles from 10 to 30 and even higher does not have much influence on the level of threshold shear strain, which is

approximately 0.01 percent. The magnitude of pore pressure is, however, increased significantly with increasing cycle numbers at strains higher than the threshold level. This increase is very significant from 1 to 30 cycles and reaches a limiting value at or about 100 cycles, especially at higher strain levels (Figs. 6.11 and 6.13). The increase in pore pressure generation is more rapid, or higher pore pressures are achieved at lower cycle numbers, for medium than loose silty sand. This is similar with the behavior of pure sands undergoing cyclic loads. The number of cycles required to cause particle rearrangement in denser silty sands are obviously more than that required for loose silty sand, as clearly shown in Figs. 6.11 and 6.13. The same trends can be observed for 20%, 30% and 60% silt additions (Figs. 6.12-a, b, c).

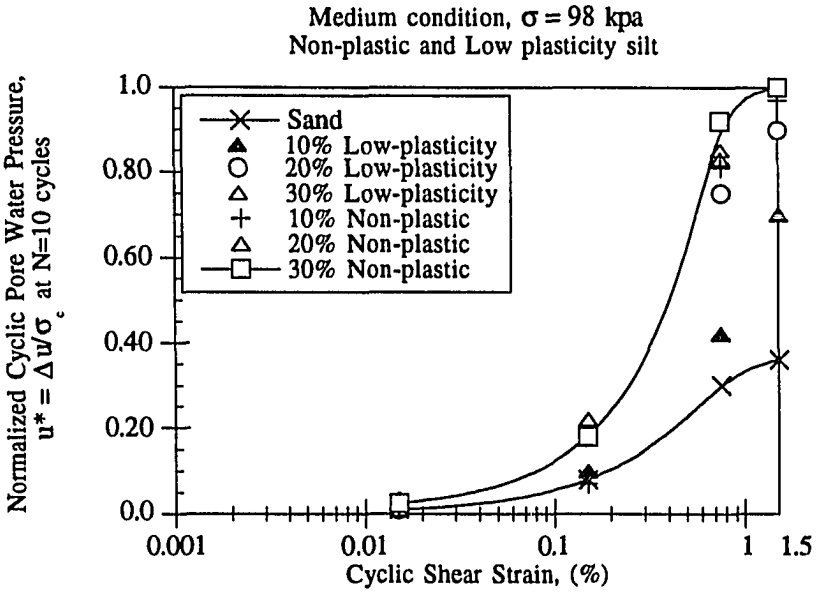

(a)

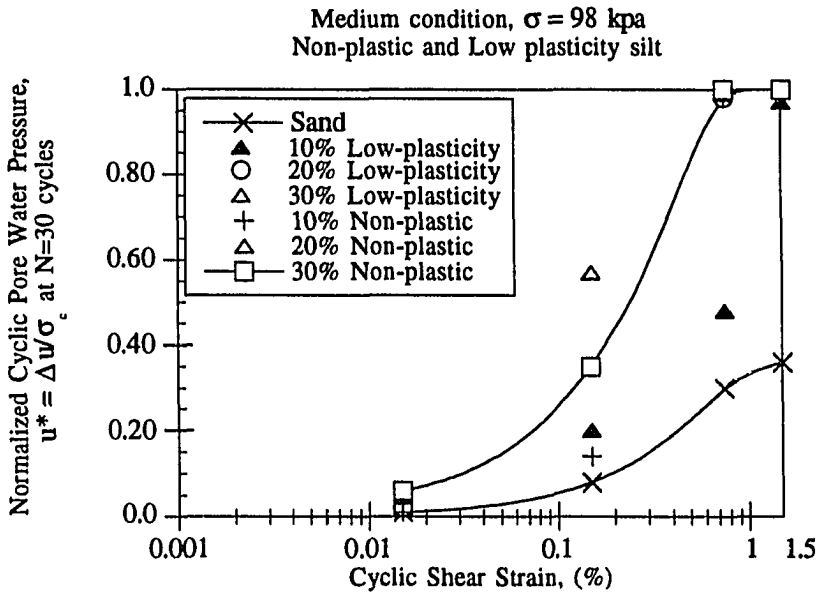

(b)

Figure 6.4. Normalized Pore Pressure Change vs. Cyclic Shear Strain at a) N=10 cycles, b) N=30 cycles

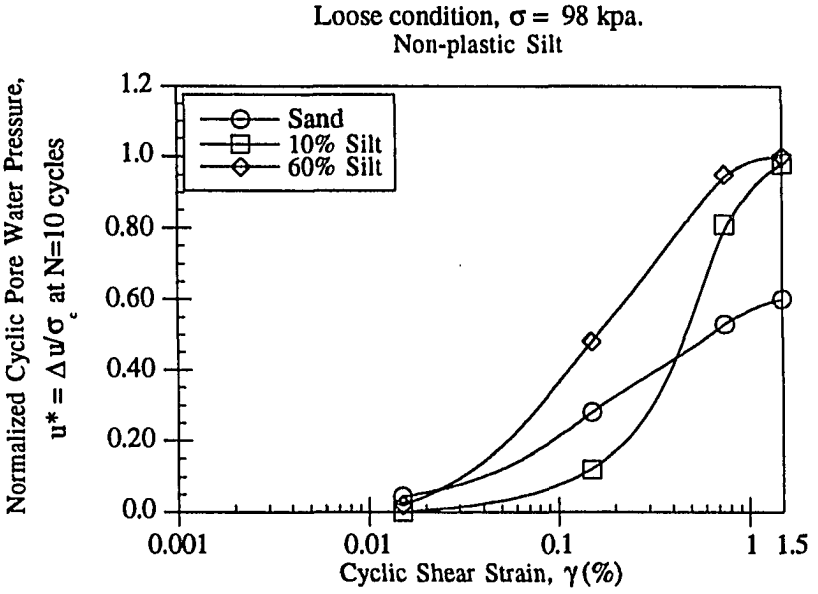

(a)

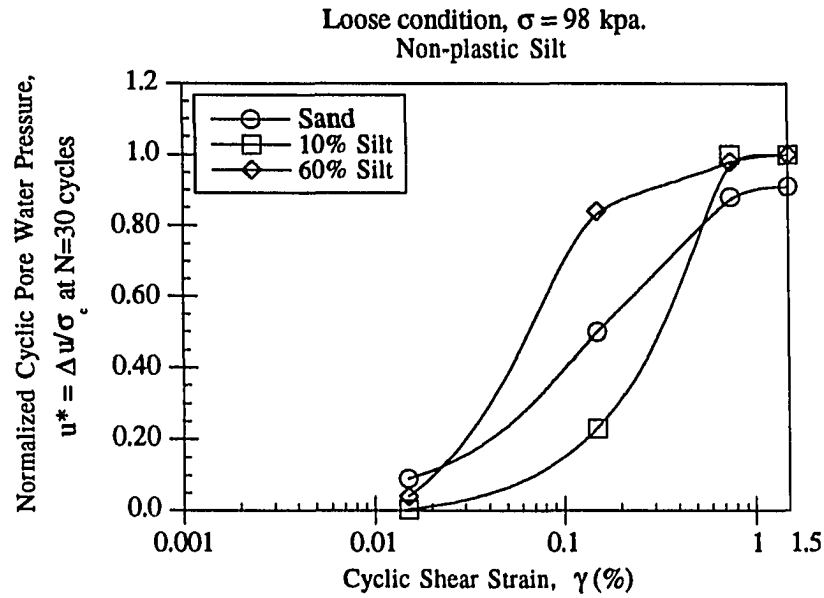

(b)

Figure 6.5. Normalized Pore Pressure Change vs. Cyclic Shear Strain for Loose Condition at a) N=10 cycles, b) N=30 cycles

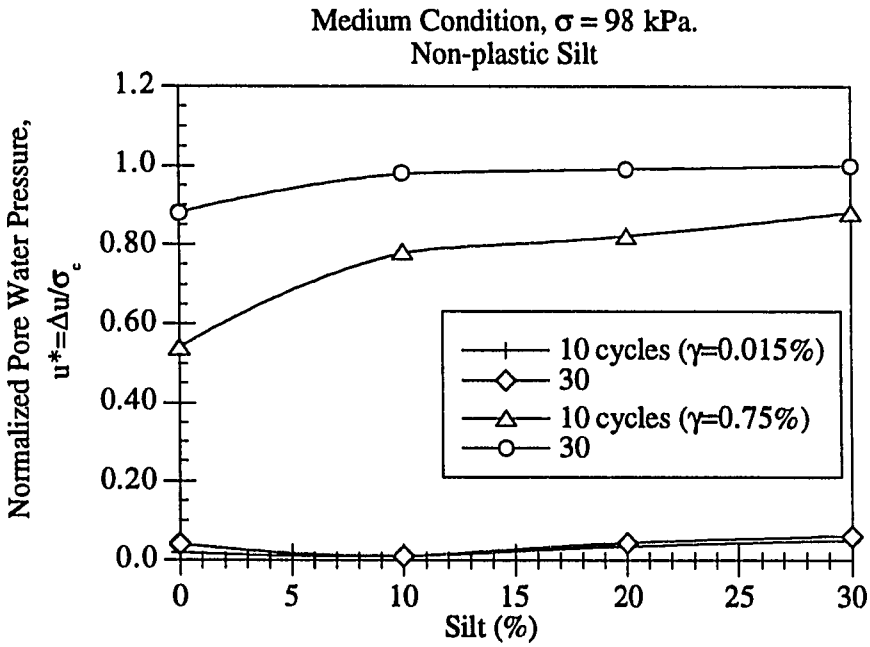

Figure 6.6. Normalized Pore Pressure Change vs. Silt % for $\gamma = 0.015\%$ and $\gamma = 0.75\%$ (Non-plastic Silt)

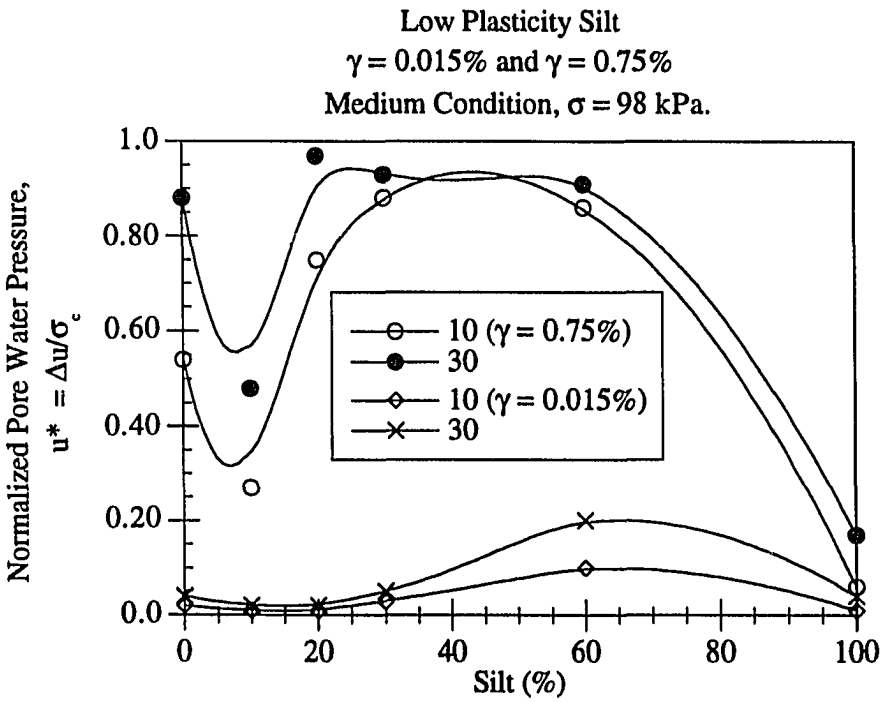

Figure 6.7. Normalized Pore Pressure Change vs. % Silt for $\gamma = 0.015\%$ and $\gamma = 0.75\%$ (Low-plasticity Silt)

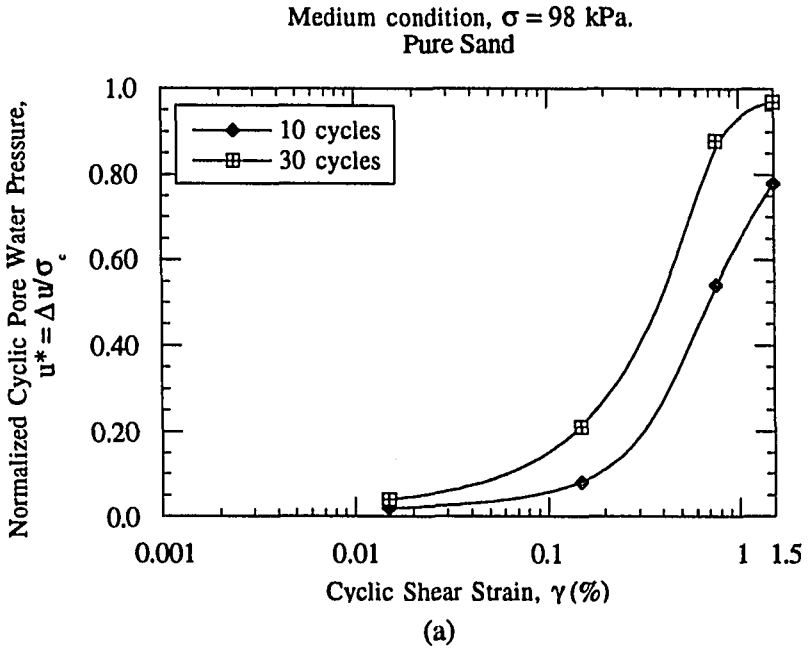

(a)

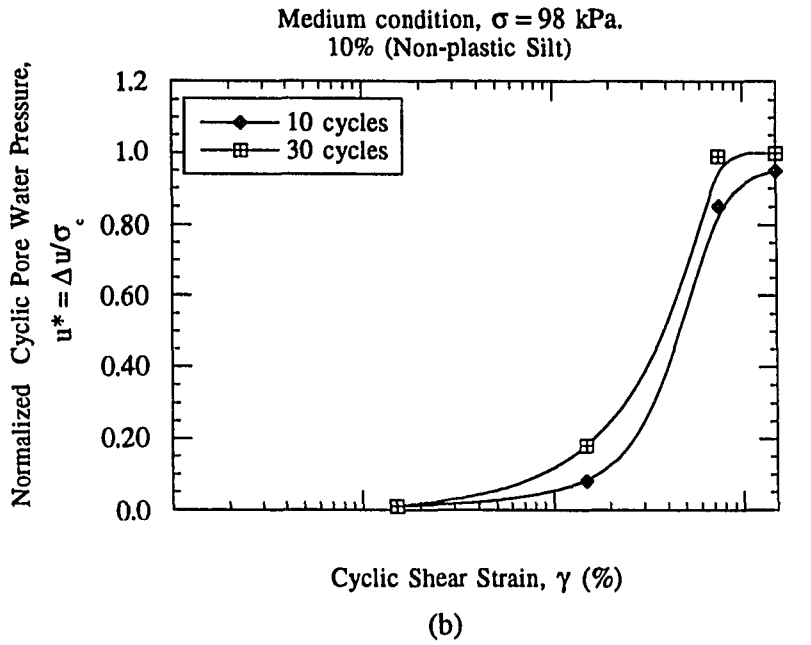

(b)

Figure 6.8. Normalized Pore Pressure Change vs. Cyclic Shear Strain for a) Pure Sand b) 10% Non-plastic silt

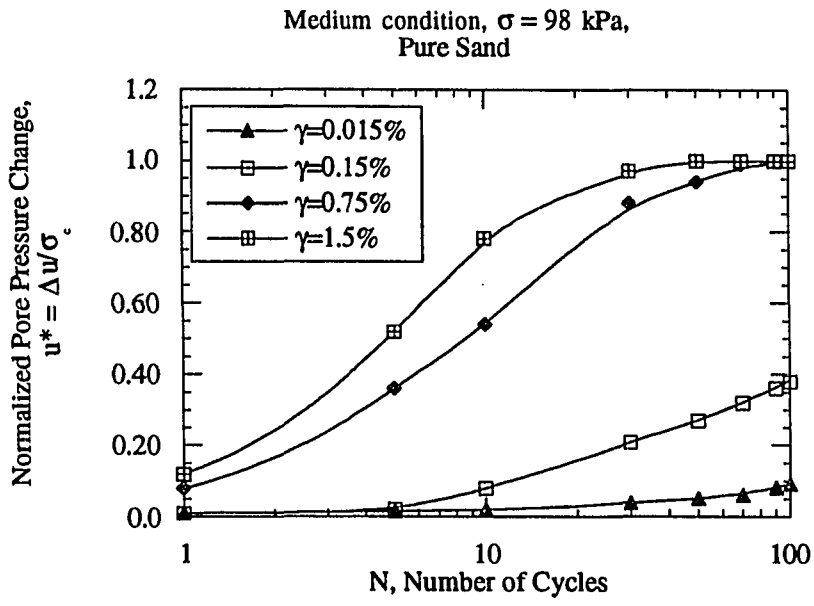

(a)

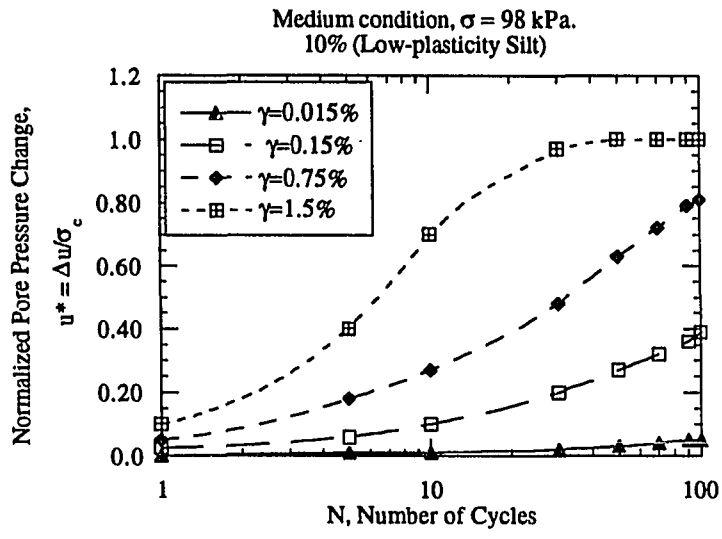

(b)

Figure 6.9. Normalized Pore Pressure Change vs. Number of Cycles for a) Pure Sand, b) 10% Non-plastic silt

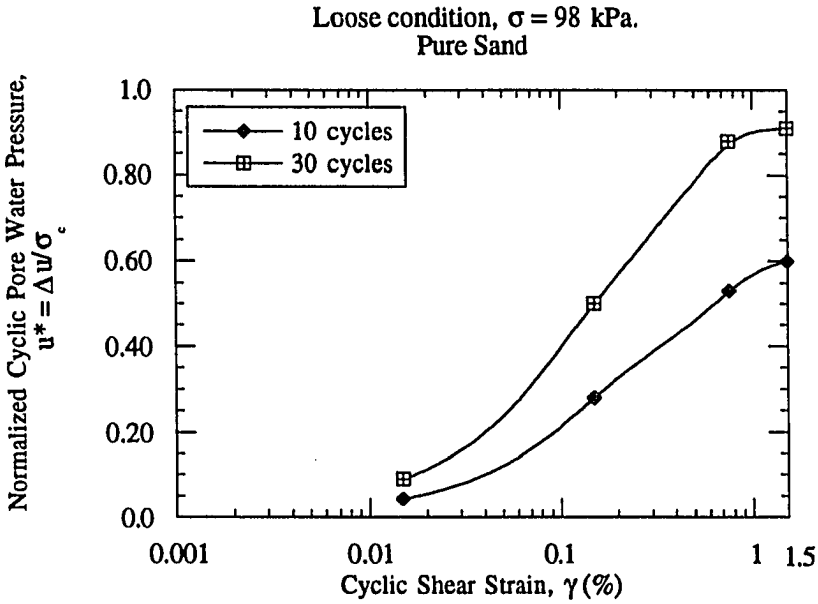

(a)

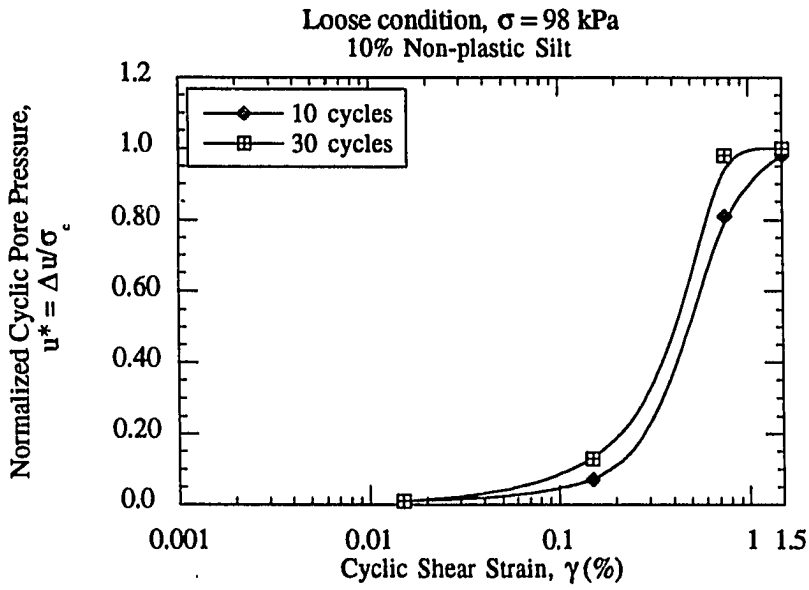

(b)

Figure 6.10. Normalized Pore Pressure Change vs. Cyclic Shear Strain for Loose a) Sand, b) 10% Non-plastic silt

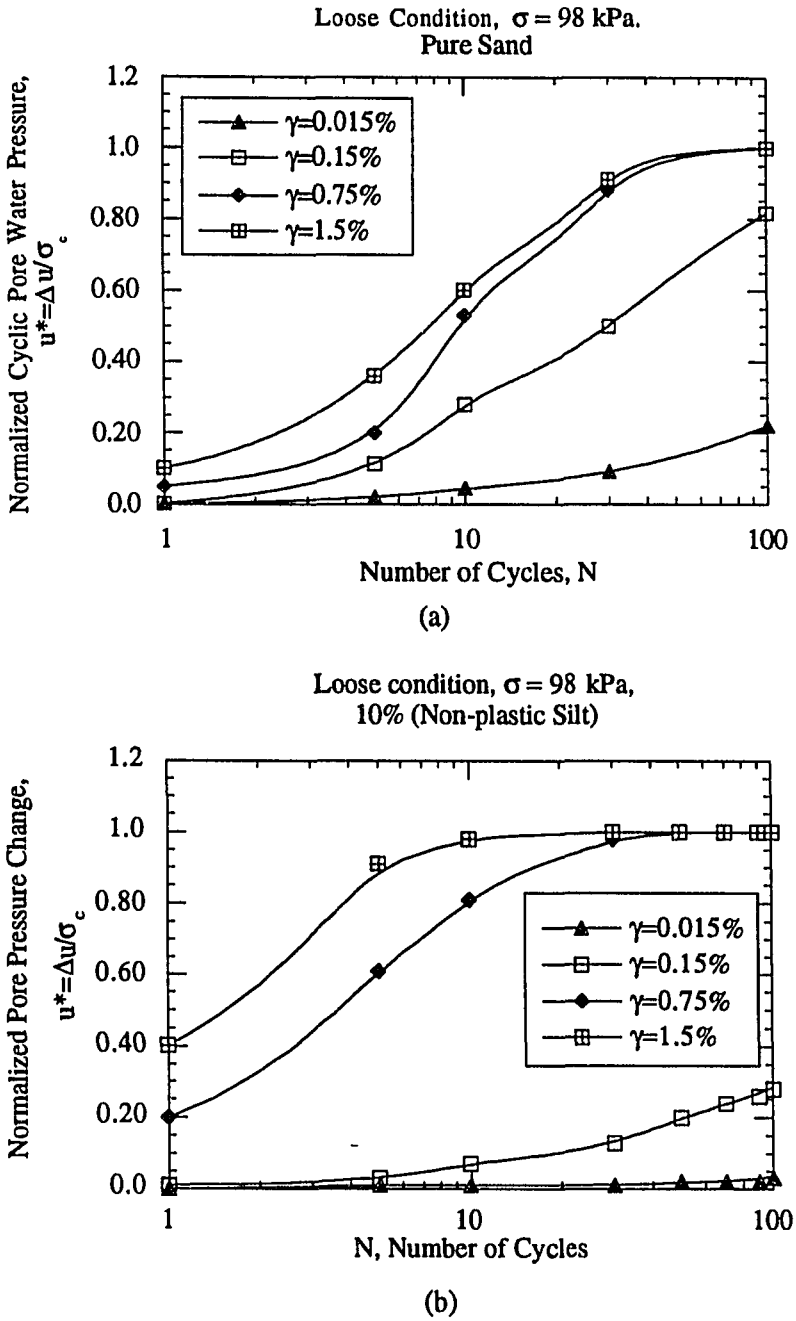

Figure 6.11. Normalized Pore Water Pressure Change vs. Number of Cycles for Loose a) Sand, b) 10% Non-plastic silt

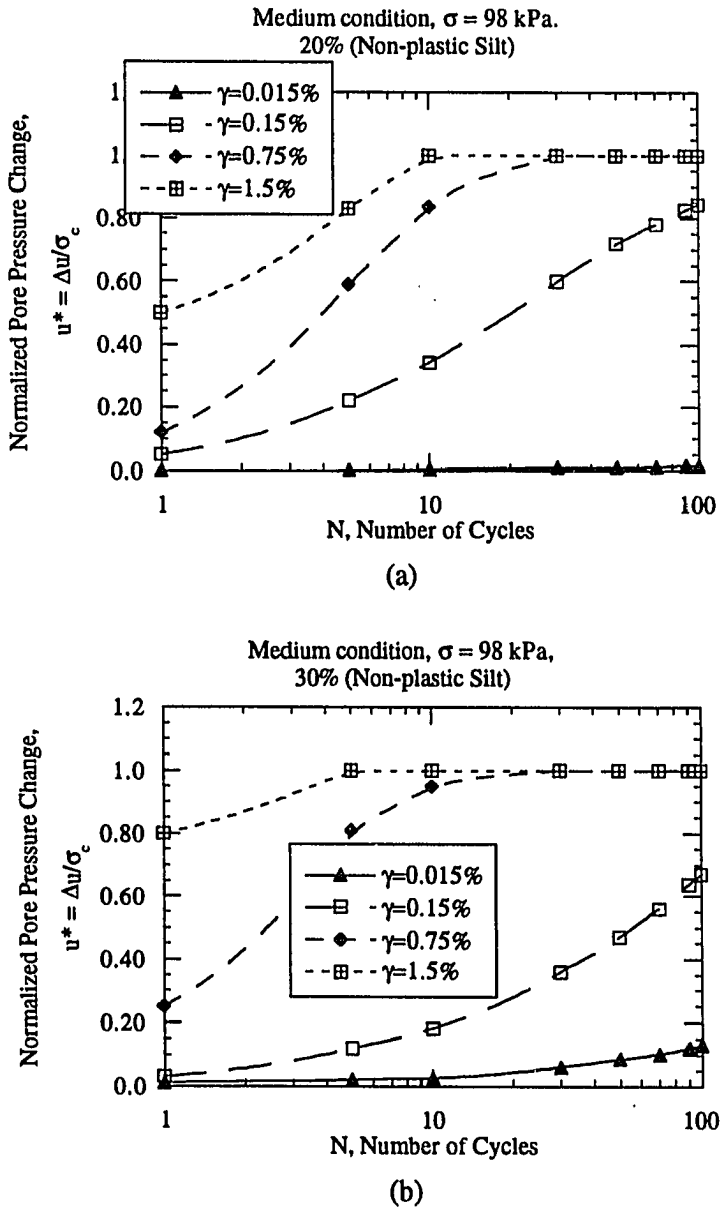

Figure 6.12 Normalized Pore Pressure Change vs. Number of Cycles for a) 20% Non-plastic Silt b) 30% Non-plastic Silt

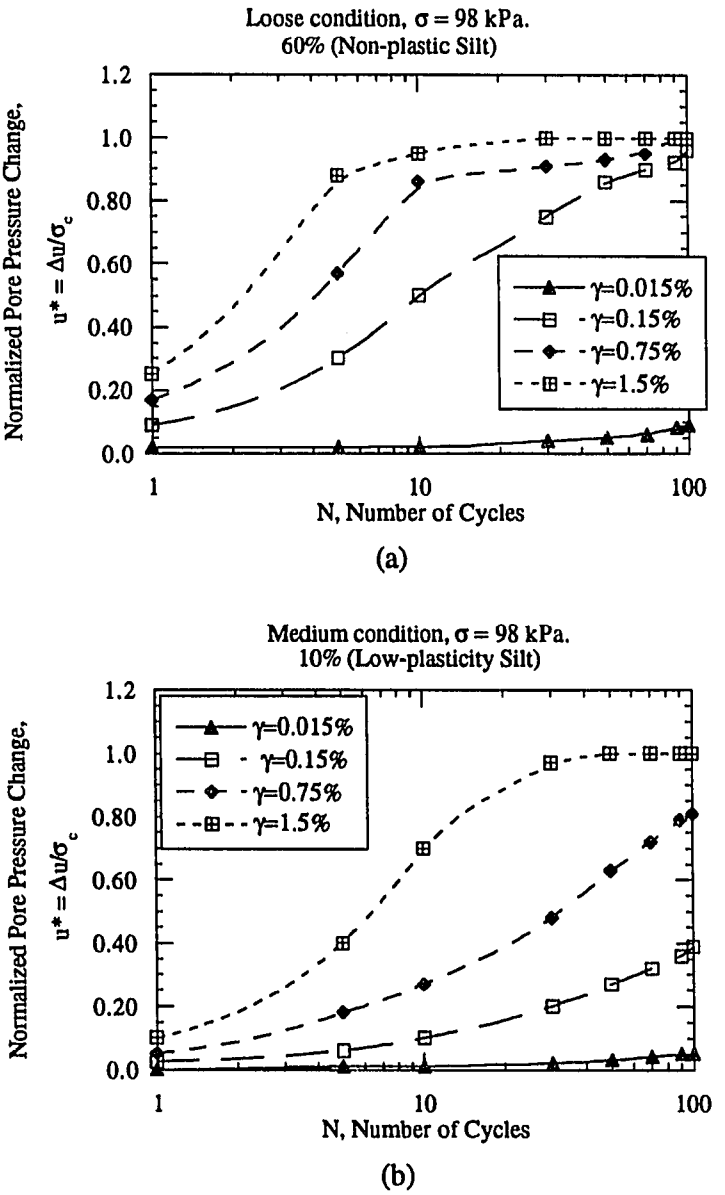

Figure 6.13 Normalized Pore Pressure Change vs. Number of Cycles for 10% Low-plasticity silt

6.6 Effect of Compaction Water

All the samples used for the testing program were prepared by an initial water content of 8%. But the maximum dry density of the samples increased as fines content increase. In order to see the effect of compacting at different water contents, the specimen prepared by 20% silt was compacted at three different water contents. The change in normalized pore pressure vs. compaction water content is plotted Fig. 6.14. 6% water content creates specimens on the dry side of optimum and the soil is flocculated. The pore pressure buildup, is retarded in case of 6% water content because compaction here results in a hard and firm soil due to capillary moisture. Particles remained individualized when their water content is less than maximum. Since, 8% water content corresponds to the maximum dry density value, for silty specimens compacted at this water content, additional water increases the lubrication. Because of the greater density, less firm soil samples are obtained. This may explain the loss of strength of specimens as the fines content is increased. As water content increases up to 10%, the soil transforms into a dispersed structure. Additional water only acts to displace the soil particles and helps to create firmer samples.

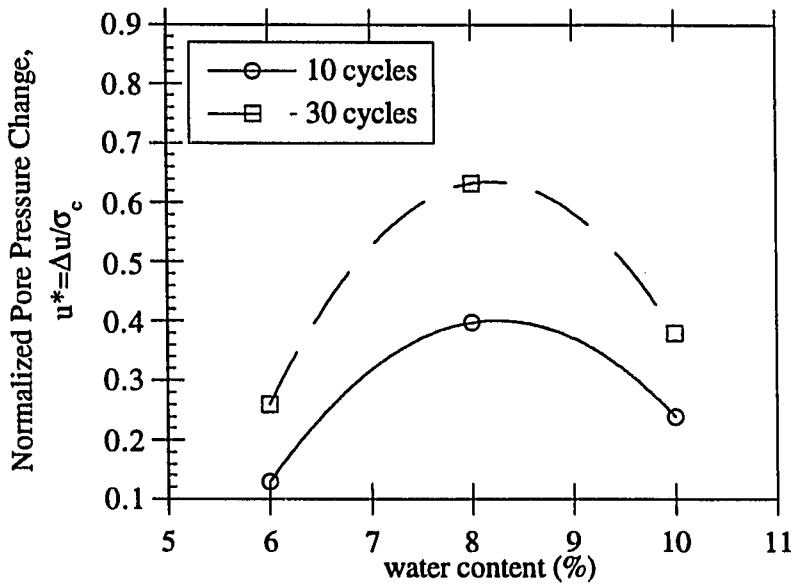

Figure 6.14 The Relationship Between Compaction Water Content and Normalized Pore Pressure Change for 20% Silt.

6.7 Evaluating Liquefaction Potential For Sites With Silty Soils

Strain approach (Dobry et al., 1982) uses seismic cyclic shear strain, γ_c to evaluate the liquefaction potential of the soil instead of using stress ratio, $\gamma_c = \tau_c / \overline{\sigma}_c$. At a given depth z, γ_c may be obtained by several methods. The method presented herein (Seed and Idriss 1971), is modified to use the equation, $\gamma_c = \tau_c / G$. The value of $\tau_c$can be computed from equation 6.16 if ground surface acceleration is known.

$$\frac{\tau_c}{\overline{\sigma}_o'} = 0.65 \frac{a_p}{g} \frac{\sigma_o}{\overline{\sigma}_o'} r \qquad (6.16)$$

a_p = horizontal peak acceleration at the ground surface,

g= acceleration of gravity = 32.2 ft/sec^2,

$\sigma_o, \overline{\sigma}_o'$ = total and effective stresses at depth z.,

$r_d = r_d(z)$= stress reduction factor varying from a value of 1 to 0.7.

The value of τ_c is then used in equation 6.17 to determine cyclic shear strain, γ_c and number of cycles, N.

$$\gamma_c = 0.65 \frac{a_p}{g} \frac{\sigma_o r_d}{G_{max} (G / G_{max})_{\gamma_c}} \qquad (6.17)$$

$(G / G_{max})_{\gamma_c}$ = effective modulus reduction factor of the soil corresponding to the cyclic strain, γ_c.

G_{max}= shear modulus of the soil at very small cyclic strains, γ_c=10^{-4}

The equivalent number of cycles N, is obtained from the earthquake magnitude M. The determined γ_c is compared with the threshold value. If it is smaller than this value, there will be no liquefaction buildup and the evaluation ends here.

If γ_c is larger than the threshold value, the values of γ_c. and N should be used together with experimental curves similar to that shown figure 6.15 to estimate the pore pressure buildup, $\Delta u / \overline{\sigma}'_o$ at the end of the earthquake. The value of $\Delta u / \overline{\sigma}'_o$ is used to decide if the site will experience initial liquefaction, ($\Delta u / \overline{\sigma}'_o$=1) or not.

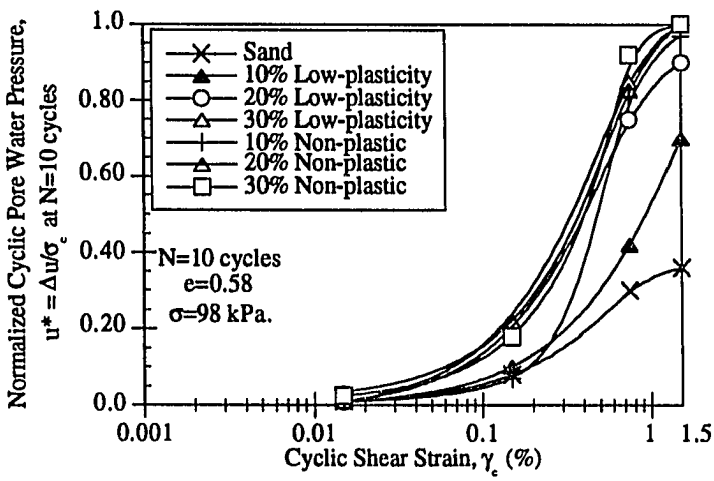

Figure 6.15 Pore Pressure Buildup in Cyclic Triaxial Strain Controlled Tests After 10 Loading Cycles, As a Function of Shear Strain for Various Amounts of Silt Contents.

6.8 Summary and Conclusions

The following conclusions may be drawn based on the experimental results.obtained from strain controlled tests on silty sands.

1. Cyclic triaxial test results demonstrate that there is a consistent relation between cyclic shear strain and pore pressure generation in silty sand. Strain controlled tests give consistent results for generation of pore water pressure in silty sand. There is a level of cyclic shear strain below which, there is little pore water pressure generation in saturated silty soils. This threshold strain level is similar to those observed in sands and is in the order of 0.01 percent.

2. For both non-plastic and low plasticity silty sands, there is significant increase in the generated pore pressure at strain levels above threshold and higher. In the case of non-plastic silt, addition of silt while maintaining the same void ratio with pure sand, results in increasing pore pressure up to a limiting value which corresponds to 30 percent in silt content.

3. Addition of low plasticity silt to sand has no significant effect on the generated pore pressures, up to 60 percent in silt content. At silt contents above 60 percent, the pore pressure is significantly reduced, and approximately unchanged for specimens undergoing high (0.75 percent) and low (0.015 percent) amplitude loading, respectively. The effect of number of loading cycles on the magnitude of pore pressure is basically a function of shearing strain. The number of loading cycles did not have any significant effect on the level of threshold shear strain, as shown in Figs 6.8 and 6.10.

4. The effect of number of loading cycles on the magnitude of pore pressure is a function of shearing strain, and its variation does not seem to have any effect on the level of threshold shear strain.

5. The effect of number of loading cycles on pore pressure generation is highly pronounced at strains higher than the threshold level. Increase in pore pressure is very significant from 1 to 30 cycles and reaches a limiting value at or about 100 cycles, especially at higher strain levels. The increase in pore pressure generation is more rapid for loose than medium silty sand, with the behavior being similar to that of pure sands undergoing cyclic loads.

VII CONCLUSIONS AND FURTHER RESEARCH

7.1 Conclusions

This research presented a systematic study of undrained response of sand with the objective of gaining an improved understanding of the behavior and performance of silty sand. The results of a series of laboratory tests are examined in an attempt to show a systematic variation in sand behavior with change in fines content. The results indicate that the physical behavior of saturated sand, having a significant percentage of fines (5~30), is less resistant to liquefaction than clean sand.

Sand with fines, depending on the fines content had different maximum and minimum void ratios. Because of that, it was believed that the relative density did not serve as a useful measure to consistently express the denseness and looseness of the materials. It should also be mentioned that, it is extremely difficult to prepare samples of the same relative density with different fines contents. Still, studies on silty soils should strictly use void ratio for comparison purposes.

7.1.1 Stress Controlled Testing

1) The presence of fines have an effect on the cyclic shear resistance of the soil. The resistance of soils with addition of 10% low plasticity and non-plastic fines compared to clean sand has small significance on the pore pressure generation of sand. Though adding 10% low plasticity fines slightly increases the resistance to liquefaction while addition of 10% non-plastic fines decrease the liquefaction potential.

2) When the presence of non-plastic fines exceed 10%, they decrease the resistance to liquefaction. The resistance to liquefaction starts increasing after fines content exceeds 30%. Seed et al., (1984) suggest a critical FC value as low as 5%, meaning that if the percentage of fines is greater than 5%, there is a distinct decrease in liquefaction potential of sands which is supporting the results of this research. It is obvious that the presence of fines should be included in evaluating the liquefaction susceptibility of a deposit.

3) As silty soils move from medium to loose state, they start to demonstrate similar levels of cyclic resistance. But it is extremely difficult to prepare loose specimens for testing. The percentage of specimens which did not fail immediately after saturation process, is so low that it is not possible to make a generalization with the same confidence as for a clean sand.

4) Stress controlled tests are found unreliable for determining the liquefaction potential of silty soils. During the extension cycle, segregation of fines from sand causes weaker specimens and specimen fails faster. Using natural soils might help segregation during extension phase of the tests.

5) Stress controlled testing is not as reliable as strain controlled testing especially when dealing with silty soils. Specimen preparation influences the results of stress controlled tests and cause scatter of the data.

7.1.2 Numerical Model

1) A material model may only be deemed to be satisfactory when with its aid, it is possible to determine the behavior of the material at hand in one piece of testing equipment (e.g., in triaxial tests), and then to predict the observed behavior of the same material in some other type of testing equipment (e.g., in simple shear tests) (Prevost, 1987). This model parameters were originally set by the results from simple shear tests. And the model successfully predicted the results from triaxial test results.

2) It is obvious that, dissipated energy is a more convenient parameter than equivalent stresses and equivalent number of cycles for characterization of actual earthquake loading.

3) The energy based model can successfully predict the pore pressure generation in sand and silty sand. The parameter η, seems to be insensitive to relative densities less than 70%.

4) The difference between the experimental and analytical curves is overcome by iterating the value of r, to find the best fit. After, a better agreement between the measured and calculated pore water pressures are obtained, the value of η, is used to predict the test results.

7.1.3 Strain Controlled Testing

1) Cyclic triaxial test results demonstrate that there is a consistent relation between cyclic shear strain and pore pressure generation in silty sand. Strain controlled tests give consistent results for generation of pore water pressure in silty sand. There is a level of cyclic shear strain below which, there is little pore water pressure generation in saturated silty soils. This threshold strain level is similar to those observed in sands and is in the order of 0.01 percent.

2) For both non-plastic and low plasticity silty sands, there is significant increase in the generated pore pressure at strain levels above threshold and higher. In the case of non-plastic silt, addition of silt, while maintaining the same void ratio with pure sand, results in increasing pore pressure up to a limiting value which corresponds to 30 percent in silt content.

3) Addition of low plasticity silt to sand has no significant effect on the generated pore pressures, up to 60 percent in silt content. At silt contents above 60 percent, the pore pressure is significantly reduced, and approximately unchanged for specimens undergoing high (0.75 percent) and low (0.015 percent) amplitude loading, respectively. The effect of number of loading cycles on the magnitude of pore pressure is basically a function of shearing strain. The number of loading cycles did not have any significant effect on the level of threshold shear strain.

4) The effect of number of loading cycles on the magnitude of pore pressure is a function of shearing strain, and its variation does not seem to have any effect on the level of threshold shear strain.

5) The effect of number of loading cycles on pore pressure generation is highly pronounced at strains higher than the threshold level. Increase in pore pressure is very significant from 1 to 30 cycles and reaches a limiting value at or about 100 cycles, especially at higher strain levels. The increase in pore pressure generation is more rapid for medium than loose silty sand, with the behavior being similar to that of pure sands undergoing cyclic loads.

6) Compaction water content effect is very important when dealing with silty soils. The behavior of the soil change greatly at dry and wet side of optimum.

7.2 Further Resarch

Based on the results of this research, potential topics and improvements may include:

1) To use natural soils for the ease of specimen preparation.

2) To extend the data to find out the response of loose silty soils and as a result continue to check the response of specimens when silt content passes 60%.

3) To investigate the effect of increasing plasticity on the behavior of silty soils.

4) To use torsional shear device to explain the effect of cyclic shear strains below and above 10^{-2} for silty sands.

BIBLIOGRAPHY

Bazant, Z. P., Krizek, R. J. (1976) "Endochronic Constitutive Law for Liquefaction of Sand," *Journal for Numerical and Analytical Methods in Geomechanics,* Vol. 2 pp. 381-404.

Black D. K. and Lee K. L. (1972) "Saturating Laboratory Samples by Back Pressure," *Journal of Geotechnical Engineering Division, ASCE*, Vol 99, No.SM1, pp. 75-93.

Brandon, T. L., Duncam, M., Cadden, A.W., (1990) "Automatic Back-Pressure Saturation Device for Triaxial Testing," Geotechnical Testing Journal, GTJODJ, Vol. 13, No.2, pp. 77-82.

Carrier, D. W. (1988), "Report on Session II," A Speciality Conference Sponsored by the Geotechnical Engineering Division of the American Society of Civil Engineers, Fort Collins, Colorado, Geotechnical Special Publication No.21, pp.208-210.

Casagrande, A. (1936) "Characteristics of Cohesionless Soils Affecting the Stability of Slopes and Earth Fills," *Journal of the Boston Society of Civil Engineers,* reprinted in *Contributions to Soil Mechanics, 1925 to 1940,* Boston Socity of Civil Engineers, Oct. 1940, pp. 257-276.

Casagrande, A. (1975) "Liquefaction and Cyclic Deformation of Sands-A Critical Review," Proceedings of the Fifth Pan American Conference on Soil Mechanics and Foundation Engineering. Buones Aires, Argentina; also published as Harvard Soil Mechanics Series No.88, January 1976, Harvard University, Cambridge, Massachusetts.

Castro, G. (1975) "Liquefaction of Cyclic Mobility of Saturated Sands," *Journal of Geotechnical Engineering Division, ASCE* 101(GT6), pp. 552-569.

Castro, G., and Poulos, J.S. (1976), "Factors Affecting Liquefaction and Cyclic Mobility," ASCE, Preprint 2752, Liquefaction Problems in Geotechnical Engineering, Philadelphia, Pa.

Castro, G., and Poulos, J.S. (1977) "Factors Affecting Liquefaction and Cyclic Mobility," *Journal of the Geotechnical Engineering Division, ASCE* 103(GT6), pp.501-506.

Chaney, R. C., Stewens, E., Sheth, N. (1979) "Suggested Test Method for Determination of Degree of Saturation of Soil Samples by B Value Measurement," *Geotechnical Testing Journal,* GTJODJ, Vol. 2, No. 3, pp. 158-162.

Chang, N. Y., Hsieh, D. L., Samuelson, D. L., Horita, M. (1982), "Static and Cyclic Undrained Behavior of Monterey No. O Sand"

Chan, C.K., (1981) "An Electropneumatic Cyclic Loading System," *Geotechnical Testing Journal,* GTJODJ, Vol. 4, No. 4, pp.183-187.

De Alba P. A. (1975) "Determination of Soil Liquefaction Characteristics by A Large Scale Laboratory Test," Ph.D. Thesis, University of California, Berkeley.

DeGregorio V. B., (1990) "Loading Systems, Sample Preparation, And Liquefaction," *Journal of Geotechnical Engineering, ASCE* Vol. 116, No. 5, pp. 805-821.

Dobry R.R., Ladd S., Yokel F. Y., Chung R. M. and Powell D., (1982) "Prediction of Pore Water Pressure Buildup and Liquefaction of Sands During Earthquakes by the Cyclic Strain Method," *Building Science Series 138*, National Bureau of Standards, Washington, D.C.

Dobry, R. Vasquez-Herrera, A., Mohamad, R., Vucetic, M., (1982) "Liquefaction Flow Failure of Silty Sand by Torsional Cyclic Tests," Advances in the Art of Testing Soils Under Cyclic Conditions, ASCE Convention, Detroit, Michigan.

Drnevich, V. P. and Richart F. E. Jr., (1970) "Dynamic Prestarining of Dry Sand," *Journal of the Soil Dynamics and Foundation Division, ASCE* , Vol. 96, No. SM2, pp. 453-469.

Dyvik, R., Dobry, R. Thomas, G. E., and Pierce, W.G. (1984) "Influence of Consolidation Shear Stresses and Relative Density on Threshold Strain and Pore Pressure During Cyclic Straining of Saturated Sands," Miscellaneous Paper GL-84-15, Department of the Army, U.S. Army Corps of Engineers, Washington, D.C., pp. 73.

Finn , W. D., Bransby P. L., Pickering D. J., (1970) "Effect of Strain History on Liquefaction of Sand," *Journal of the Soil Mechanics and Foundation Division, ASCE,* Vol. 96, No. SM6, pp. 1917-1934.

Frydman, S., Zeitlen, J. G., Alpan, I., (1973) "The Membrane Effect in Triaxial Testing of Granular Soils," *Journal of Testing and Evaluation*, Vol. 1, pp. 37-41.

Ghaboussi, J. Dikmen, U. S. (1978) "Liquefaction Analysis of Horizontally Layered Sands,"Liquefaction Analysis of Horizontally Layered Sands," Journal of Geotechnical Engineering Division, ASCE, Vol. 104, No. GT3, March 1978, pp. 341-357.

Head K. H., (1992) "Manual of Soil Laboratory Testing", John Wiley & Sons, Inc. 2. Edition, Vol.1.

Holtz R. D. and Kovacs W. D. (1981) "An Introduction to Geotechnical Engineering," Prentice Hall.

Ishihara, K. and Yasuda, S. (1975) "Undrained Deformation and Liquefaction of Sand Under Cyclic Stresses," *Soils and Foundations* 15(1), pp. 29-44.

Ishihara K., Sodekawa M., Tanaka Y., (1978) "Effects of Overconsolidation on Liquefaction Characteristics of Sands Containing Fines," Dynamic Geotechnical Testing, ASTM STP 654, American Society of Testing Materials, pp. 246-264.

Ishihara K. , Troncoso J., Kawase Y., Takahashi Y., (1980) "Cyclic Strength Characteristics of Tailing Materials," *Soils and Foundations,* Vol.20, No.4, pp. 127-142.

Ishihara, K. (1984) "Post Earthquake Failure of a Tailings Dam Due to Liquefaction of the Pond Deposit," pp.1129-1143 in Proceedings of the International Conference on Case Histories in Geotecnical Engineering, Vol.3 University of Missouri, Rolla, Missouri.

Ishihara, K. (1985) "Stability of Natural Deposits During Earthquakes," Proceedings of the Eleventh International Conference on Soil Mechanics and Foundation Engineering, A. A. Balkema Publishers, Rotterdam, Netherlands.

Ishihara, K. Tatsuoka, F. Yasuda, S. (1975) "Undrained Deformation and Liquefaction of Samd under Cyclic Stresses," Soils and Foundations, Vol. 15, No. 1, pp. 29-44.

Ishihara, K. (1988) "Pore Water Pressure Rises During Earthquakes," Proceedings of the International Conference On Recent Advances of Geotechnical Earthquake Engineering and Soil Dynamics, St. Louis MI, Vol 3, pp.1201-1204.

Iwasaki T., (1986) "Soil Liquefaction Studies in Japan: State of the Art," *Soil Dynamics and Earthquake Engineering,* Vol.5, No. 1, pp.3-69.

Kaufman L. P., (1981) "Percentage Silt Content in Sands and Its Effect on Liquefaction Potential," *Ph.D. Thesis*, University of Colorado.

Kuerbis R., Negussey D. and Vaid Y. P. (1988), "Effect of Gradation and Fines Content on the Undrained Response of Sand," Geotechnical Special Publication No.21, pp.330-345.

Ladd, R. S. (1977) "Specimen Preparation and Cyclic Stability of Sands," *Journal of the Geotechnical Engineering Division ASCE,* Vol. 103, No. GT6 , pp. 535-547.

Ladd, R.S., (1978) "Preparing Test Specimens Using Undercompaction," *Geotechnical Testing Journal,* GTJODJ, Vol.1, pp.16-23.

Ladd, R.S., Dobry, R., Dutko, P., Yokel, F.Y., and Chung, R.M. (1989) "Pore Water Pressure Buildup in Clean Sands Because of Cyclic Straining." *Geotechnical Testing Journal,* GTJODJ, Vol. 12, No.1, pp. 77-86.

Lee, K. L. and Fitton, J.A. (1969) "Factors Affecting the Cyclic Loading Strength of Soil" ASTM STP 450, American Society of Testing Materials, pp. 71-95.

Li X.S., (1988) "An Automated Triaxial Testing System," *Advanced Triaxial Testing of Soil and Rock, ASTM STP 977,* R.T. Donaghe, R.C. Chaney and M. L. Silver, Eds., ASTM, Philadelphia, pp.95-106.

Liao, S., Streeter, V. L., Richart, F. E. (1977) " *Numerical Model for Liquefaction," Journal of Geotechnical Engineering Division, ASCE,* Vol. 103 No. 6, pp. 589-606.

Liao, S. (1985), "Statistical Analysis of Liquefaction Data," Ph. D. Thesis, Massachusetts Institute of Technology, Cambridge, Massachusetts.

Martin, G. R., Finn, D. L., Seed, H. B. (1975), "Fundamentals of Liquefaction Under Cyclic Loading,"*Journal of the Geotechnical Engineering Division, ASCE* 104(GT5): pp. 423-438

Mitchell, J.K. (1988) "Densification and Improvement of Hydraulic Fills," *Geotechnical Special Publication No.21*, pp. 606-633.

Mulilis, J. P., Chan, C. K., Seed, B. (1975) "The Effects of Method of Sample Preparation on the Cyclic Stress Strain Behavior of Sands," Earthquake Engineering Research Center, Report No. 75-18, pp. 1-138.

Mulilis, J. P., Seed, H. B., Chan, C. K., Mitchell, J. K., Arulandan, K. (1977) "Effects of Sample Preparation on Sand Liquefaction," *Journal of Geotechnical Engineering, ASCE,* Vol. 103 No. GT2, pp. 91-108.

Mulilis, J. P., Townsend, F. C., Horz, R. C., (1978) "Triaxial Testing Techniques and Sand Liquefaction," Dynamic Geotechnical Testing, ASTM, STP 654, pp. 265-279.

Nemat-Nasser, S. and Shookoh A. (1979) "A unified Approach to Densification and Liquefaction of Cohesionless Sand in Cyclic Shearing," *Canadian Geotechnical Journal 16(4),* pp. 659-678.

Nemat-Nasser, S. (1982) "Liquefaction and Densification of Granular Masses in Cyclic Shearing," keynote lecture presented at the *International Symposium on Numerical Methods on Geomechanics,* Balkema Publishers, Rotterdam, Netherlands.

National Research Council (NRC), (1985) "Liquefaction of Soils During Earthquakes," Committee on Earthquake Engineering, Report No. CETS-EE-001, Washington, D.C.

Poran, J. C., Rodriguez J. A., (1989) "Large Ground Deformations Induced by the 1985 Earthquake in Port Facilities in Chile," Proceedings from the Second U.S.- Japan Workshop on Liquefaction, Large Ground Deformation and Their Effects on Lifelines, September 26-29. Edited by: T.D. O'Rourke and M. Hamada, *Technical Report NCEER-89-0032* pp.118-130.

Poulos, S. J., Castro, G., France, J. W. (1985), "Liquefaction Evaluation Procedure," *Journal of Geotechnical Engineering, ASCE* 107(GT5), pp. 553-562.

Puri, V. K., (1984) "Liquefaction Behavior and Dynamic Properties of Loessial Soils," Ph.D. Dissertation, University of Missouri-Rolla.

Prevost, J. H., Höeg, K. (1977) "Plasticity Model for Undrained Stress-Strain Behavior," Proceedings of the 9th International Conference on Soil Mechanics and Foundation Engineering, Vol. 1, pp. 255-261, Tokyo.

Pyke, R. M., (1973)"Settlement and Liquefaction of Sands Under Multidirectional Loading," Ph.D. Thesis, University of California, Berkeley.

Pyke, R., Seed, H. B., Chang, C. K. (1975), "Settlement of Sands under Multidirectional Shaking," *Journal of Geotechnical Engineering ASCE,* 101(4), pp. 379-397.

O'Rourke T.D., Stewart H.E., Blackburn F.T., Dickerman T.S. (1990) "Geotechnical and Lifeline Aspects of The October 17, 1989 Loma Prieta Earthquake in San Francisco," Technical Report NCEER-90-0001, National Center For Earthquake Engineering Research, State University of New York, Buffalo, NY

Rad, S. N., Clough, W. G., (1984) "New Procedure for Saturating Sand Specimens", *Journal of Geotechnical Engineering,* ASCE, Vol. 110, No.9, pp. 1205-1217.

Sandoval, S. J. (1989), "Liquefaction and Settlement Characteristics of Silty Soils," Ph.D. Dissertation, University of Missouri-Rolla.

Schofield, A. N. Wroth, C. P. (1968), "Critical State Soil Mechanics," McGraw-Hill, London.

Seed H.B. and Lee K.L. (1966), "Liquefaction of Saturated Sands During Cyclic Loading," *Journal of the Soil Mechanics and Foundations Division*, ASCE 92(SM6), pp.105-134.

Seed H.B., Idriss, I. M. (1971), "Simplified Procedure for Evaluating Soil Liquefaction Potential," *Journal of the Soil Mechanics and Foundation Division, ASCE,* 97(9), pp.1249-1273.

Seed H.B. (1976), "Evaluation of Soil Liquefaction Effects on Level Ground During Earthquakes," pp.1-104 in Liquefaction *Problems in Geotechnical Engineering*, ASCE Preprint 2752, presented at the ASCE National Convention, Philadelphia PA, ASCE NY, NY.

Seed, H. B., Tokimatsu, K., Harder L. F., Chung, R. M., (1984) "The Influence of SPT Procedures in Soil Liquefaction Resistance Evaluations," Report No. UBC/EERC-84/15, Earthquake Engineering Research Center, University of California, Berkeley, California.

Shen, C. K., Vrymoed, J. L., Uyeno, C. K., (1977) "The effects of Fines on Liquefaction of Sands," Proceedings of the Ninth International Conference on Soil Mechanics and Foundation Engineering, Japan, Vol II, JSSMFE, pp. 381-386.

Sherif, M. A., Ishibashi, I. (1982) "A Rational Theory For Predicting Soil Liquefaction," Soil Dynamics and Earthquake Engineering, Vo.1, No.1, pp.20-29

Sherif, M. A., Tien, Y. B., Pan Y. W. (1983) "Liquefaction Potential of Silty Sand," University of Washington, College of Engineering, Soil Engineering Research Report No. 26.

Silver, M. L., Seed H. B., (1971) "Volume Changes in Sands During Cycling Loading," *Journal of Soil Mechanics and Foundations Division,* ASCE, Vol.97, No.239, pp. 1171-1185

Terzaghi, K. Peck, R. (1967), "Soil Mechanics in Engineering Practice," 2. Edition, John Wiley and Sons, NY.

Tokimatsu, K., Yoshimi, Y., (1983) "Empirical Correlation of Soil Liquefaction Based on SPT N-Value and Fines Content," Soils and Foundations, JSSMFE, Vol. 24 No.4, pp. 56-74.

Tokimatsu, K., Yoshimi, Y., (1983) "Field Correlation of Soil Liquefaction with SPT and Grain Size," Proceedings of the International Conference On Recent Advances of

Geotechnical Earthquake Engineering and Soil Dynamics, St. Louis MI, Vol 1, pp. 203-208.

Toncoso, J. H. (1986) "Critical State of Tailing Silty Sands for Earthquake Loadings," International Journal of Soil Dynamics and Earthquake Engineering, Vol. 5, No.3, pp. 248-252.

Troncoso, J. H., (1988) "Evaluation of Seismic Behavior of Hydraulic Fill Structures," *Geotechnical Special Publication No.21*, pp. 475-491.

Tsuchida, H., (1970) "Prediction and Countermeasure Against the Liquefaction in Sand Deposits." "Seminar Abstract. Port and Harbour Research Institute, pp.3.1-3.33

Tuttle, M., Law ,T., Seeber, L., Jacop, K., (1989) "Liquefaction and Ground Failure in Ferland, Quebec Triggered by the 1988 Saguenay Earthquake," Proceedings from the Second U.S.- Japan Workshop on Liquefaction, Large Ground Deformation and Their Effects on Lifelines, September 26-29. Edited by: T.D. O'Rourke and M. Hamada, *Technical Report NCEER-89-0032*_ pp.102-117.

Vrymoed, J. L. M. (1971), "Liquefaction Characteristics of Sandy Soil with Fines Under Cyclic Loading," MS Thesis. University of California, Davis.

Vucetic, M., Dobry, R., (1988) "Cyclic Triaxial Strain Controlled Testing of Liquefiable Sands," Advanced Triaxial Testing of Soil and Rock, ASTM STP 977, R.T. Donaghe, R.C. Chaney, M.L. Silver, Eds., American Society for Testing and Materials, Philadelphia, pp. 475-485.

Walker, A. J., Stewart, H. E., (1989) "Cyclic Undrained Behavior Of Nonplastic And Low Plasticity Silts," *Technical Report NCEER-89-0035*

Wood, D. M. (1990) , *Soil Behavior and Critical State Soil Mechanics*, Cambridge University Press.

Woods, R. D., (1978) "Measurement of Dynamic Soil Properties," Speciality Conference on Earthquake Engineering and Soil Dynamics, Vol.1, ASCE, NY, NY, pp. 91-178.

Wong, R.T., Seed, H. B., and Chan, C. K., (1975)*Journal of Geotechnical Engineering Division, ASCE*, Vol. 101, No. GT6 pp. 571-583.

Xia, H. and Hu, T., (1991) "Effects of Saturation and Back Pressure on Sand Liquefaction," *Journal of Geotechnical Engineering Division, ASCE,* Vol.117, No.9, pp. 1347-1362.

Yeh, S. T. "The Effect of Grain Size Distribution on the Liquefaction Potential of Granular Soils," Master's Thesis University of Colorado, Denver.

Youd, T. L. (1972) "Compaction of Sands by Repeated Shear Straining," *Journal of the Soil Mechanics and Foundation Division, ASCE*, Vol.98, No. SM7, pp. 709-725.

Zienkiewicz, O. C. Chang, C. T. Hinton, E. (1978) "Non-linear Seismic Response and Liquefaction," Internatinal Journal for Numerical and Analytical Methods in Geomechanics, Vol. 2, pp. 381-404.

APPENDIX A

Table A.1 Stress Controlled Tests Results For Pure Sand

Test #	w% Water Content	e Void Ratio	[1]B(%)	$\sigma_d/2\sigma_o$ Cyclic Stress Ratio	[2]IL	2.5% Double Ampl. Strain	5% Double Ampl. Strain	10% Double Ampl. Strain
13	8	0.6	0.95	0.35	3	1	2	4
18	8	0.6	0.95	0.25	50	45	47	48
21	8	0.64	0.95	0.25	10	7	8	9
22	8	0.6	0.95	0.25	70	66	67	68
24	8	0.58	0.97	0.35	8	5	6	7
25	8	0.59	0.97	0.35	3	1	2	3
28	8	0.58	0.99	0.30	13	11	12	13
29	8	0.58	0.99	0.15	[3]NF	-	-	-
30	8	0.58	0.95	0.40	6	2	3	6
32	8	0.58	0.96	0.20	NF	-	-	-
39	8	0.66	0.95	0.25	6	3	4	6
43	8	0.54	0.96	0.225	390	386	387	393
44	8	0.60	0.95	0.20	NF	-	-	-
45	8	0.64	0.95	0.20	72	70	71	72
46	8	0.6	0.96	0.25	40	32	33	34
47	8	0.64	0.95	0.30	4	2	3	4

1 Skempton's B value

2 Initial Liquefaction

3 Specimen did not fail at the end of 1000 cycles

Test #	w(%) Water Content	e Void Ratio	B(%)	$\sigma_d/2\sigma_o$ Cyclic Stress Ratio	IL	2.5% Double Ampl. Strain	5% Double Ampl. Strain	10% Double Ampl. Strain
48	8	0.64	0.96	0.25	11	9	10	11
54	8	0.58	0.95	0.25	364	363	364	365
70	8	0.62	0.96	0.25	14	12	13	14
73	8	0.58	0.95	0.25	95	90	91	95
77	8	0.58	0.95	0.275	102	99	100	101
79	8	0.6	0.95	0.25	93	88	90	93

Table A.2 Stress Controlled Tests Results For Silty Sand

Test #	w% Water Content	Silt Content (%)	e Void Ratio	B(%)	$\sigma_d/2\sigma_o$ Cyclic Stress Ratio	IL	2.5% Double Ampl. Strain	5% Double Ampl. Strain	10% Double Ampl. Strain
49	8	10	0.60	0.96	0.25	[4]ND	28	29	31
50	8	10	0.64	0.96	0.30	ND	12	13	14
52	8	10	0.50	0.99	0.25	ND	113	116	120
53	8	10	0.423	0.99	0.25	ND	260	261	263
56	8	10	0.592	0.963	0.25	ND	25	26	27
57	8	10	0.54	0.96	0.25	ND	71	72	73
66	8	10	0.40	0.95	0.30	ND	95	96	98
67	8	10	0.60	0.963	0.20	ND	44	45	46
74	8	10	0.64	0.95	0.275	ND	19	20	24
75	8	10	0.58	0.95	0.275	ND	50	52	53
76	8	10	0.50	0.95	0.20	ND	625	629	645
7	8	10	0.58	0.96	0.20	ND	51	52	53
8	8	10	0.62	0.98	0.30	ND	3	4	5
23	8	10	0.54	0.96	0.20	ND	114	115	116
1	8	20	0.54	0.97	0.20	ND	17	18	19
2	8	20	0.54	0.97	0.25	ND	4	5	6
3	8	20	0.46	0.97	0.20	ND	14	15	16
4	8	20	0.50	0.97	0.30	ND	1	1	1

4 Initial Liquefaction not developed

Test #	w% Water Content	Silt Content (%)	e Void Ratio	B(%)	$\sigma_d/2\sigma_o$ Cyclic Stress Ratio	IL	2.5% Double Ampl. Strain	5% Double Ampl. Strain	10% Double Ampl. Strain
5	8	20	0.50	0.97	0.25	ND	26	27	28
62	8	20	0.40	0.97	0.225	ND	26	27	28
82	8	20	0.35	0.98	0.30	ND	56	58	66
92	8	20	0.50	0.97	0.25	ND	14	15	16
93	8	20	0.50	0.97	0.25	ND	27	28	29
9	8	30	0.52	0.97	0.30	ND	1	1	2
10	8	30	0.58	0.951	0.20	ND	5	6	7

Table A.3 Stress Controlled Tests Results For Silty Sand

Test #	w% Water Content	Silt Content (%)	e Void Ratio	B(%)	$\sigma_d/2\sigma_o$ Cyclic Stress Ratio	IL	2.5% Double Ampl. Strain	5% Double Ampl. Strain	10% Double Ampl. Strain
83	8	30	0.424	0.951	0.3	ND	NF	NF	NF
84	8	30	0.473	0.95	0.3	ND	1	2	3
85	8	30	0.348	0.9	0.25	ND	38	46	60
88	8	30	0.52	0.78	0.275	ND	7	8	9
96	8	30	0.58	0.95	0.2	ND	10	11	15
97	8	30	0.58	0.97	0.25	ND	1	1	1
98	8	60	0.8	0.97	0.25	ND	1	2	3
99	8	60	0.7	0.99	0.25	ND	2	3	4
14	8	10p[5]	0.54	0.97	0.2	NL	NF	NF	NF
16	8	10p	0.54	0.97	0.25	ND	141	143	146
17	8	10p	0.54	0.97	0.3	ND	21	22	25
18	8	10p	0.58	0.97	0.35	ND	15	16	17
19	8	10p	0.64	0.97	0.225	ND	23	26	30
20	8	10p	0.64	0.97	0.30	ND	1	2	3
21	8	10p	0.64	0.97	0.225	ND	288	289	290
22	8	10p	0.54	0.94	0.25	ND	314	316	318

5 Low plasticity Silt

APPENDIX B

Table B.1 Strain Controlled Test Results

Test #	B value	Void Ratio	[6]D.A. Axial Strain (%)	[7] $\Delta u / \sigma_c$ at N=10 cycles	$\Delta u / \sigma_c$ at N=30 cycles	Initial Liquefaction
ST5	0.95	0.627	1.0	0.938	1.0	6
ST6	0.95	0.645	0.01	0.043	0.1	1000
ST7	0.96	0.625	0.1	0.28	0.5	236
ST8	0.96	0.632	0.5	0.53	0.91	37
ST26	0.96	0.58	0.5	0.3	0.61	110
ST27	0.96	0.59	0.01	0.02	0.04	NF
ST28	0.96	0.53	1.0	0.36	0.73	150
ST29	0.96	0.57	0.1	0.08	0.21	NF
ST34	0.96	0.58	0.5	0.54	0.88	74
ST35	0.98	0.57	1.0	0.78	0.97	46

6 Double Amplitude Axial Strain

7 All test are run with a confining pressure of 98 kPa.

Table B.2 Strain Controlled Test Results on Sand with Fines

Test #	B value	Void Ratio	Silt (%)	D.A. Axial Strain	$\Delta u / \sigma_c$ at N=10 cycles	$\Delta u / \sigma_c$ at N=30 cycles	Initial Liquefaction
ST9	0.97	0.65	10	0.1	0.08	0.18	1000
ST10	0.99	0.64	10	0.5	0.85	1.0	15
ST11	0.97	0.647	10	1.0	0.938	1.0	11
ST12	0.97	0.638	10	0.01	0.01	0.01	NF
[8]ST13	0.97	0.638	10	0.1	0.12	0.23	NF
ST30	0.97	0.58	10	0.5	0.818	0.989	34
ST31	0.955	0.58	10	0.01	0.01	0.01	NF
ST32	0.96	0.58	10	0.1	0.07	0.14	NF
ST33	0.96	0.57	10	1.0	0.97	1.0	18
ST14	0.966	0.58	20	0.5	0.836	1.0	23
ST15	0.955	0.58	20	0.01	0.035	0.044	NF
ST17	0.96	0.48	20	0.01	0.014	0.015	NF
ST19	0.96	0.58	20	0.1	0.3	0.49	306
ST20	0.96	0.58	20	1.0	1.0	1.0	3

8Prestraining

Table B.3 Strain Controlled Test Results on Sand with Fines

Test #	B value	Void Ratio	Silt (%)	D.A. Axial Strain	$\Delta u / \sigma_c$ at N=10 cycles	$\Delta u / \sigma_c$ at N=30 cycles	Initial Liquefaction
ST21	0.96	0.58	30	0.01	0.025	0.06	NF
ST23	0.96	0.58	30	0.1	0.18	0.35	550
ST22	0.955	0.58	30	1.0	0.9	1.0	22
ST24	0.96	0.60	30	0.5	0.92	1.0	16
ST25	0.98	0.58	30	1.0	1.0	1.0	4
ST44	0.978	0.60	60	0.5	0.86	0.91	550
ST45	0.961	0.66	60	0.5	0.95	0.98	90
ST46	0.98	0.64	60	0.01	0.02	0.04	NF
ST47	0.97	0.79	5	0.5	0.62	0.88	100
ST48	0.95	0.79	60	0.1	0.48	0.84	31
ST49	0.976	0.76	60	1.0	0.95	0.96	50
ST52	0.96	0.8	100	0.5	0.95	1.0	22
ST53	0.96	0.85	100	0.5	0.91	1	22
ST65	0.96	0.85	100	0.01	0.01	0.01	NF

Table B.4 Strain Controlled Test Results on Sand with Fines

Test #	B value	Void Ratio	Silt (%)	D.A. Axial Strain	$\Delta u / \sigma_c$ at N=10 cycles	$\Delta u / \sigma_c$ at N=30 cycles	Initial Liquefaction
ST36	0.98	0.58	10p	0.5	0.68	0.98	135
ST37	0.987	0.52	20p	0.5	0.75	0.938	394
ST38	0.98	0.58	30p	0.5	0.66	0.96	355
ST39	0.98	0.44	20p	0.5	0.93	0.98	278
ST40	0.98	0.58	20p	0.5	0.92	0.98	85
ST41	0.97	0.55	10p	0.5	0.71	0.91	35
ST42	0.96	0.57	10p	0.5	0.27	0.48	500
ST43	0.98	0.57	30p	0.5	0.88	0.938	182
ST44	0.98	0.57	60p	0.5	0.86	0.91	114
ST50	0.96	0.80	100p	0.5	0.06	0.17	NF
ST54	0.96	0.54	20p	0.5	0.75	0.97	58
ST55	0.97	054	30p	0.5	0.95	0.99	40
ST56	0.97	0.54	30p	0.5	0.97	0.99	38
ST57	0.97	0.54	10p	0.01	0.01	0.02	NF
ST58	0.97	0.54	10p	0.1	0.1	0.20	NF
ST59	0.96	0.45	10p	1.0	0.7	0.96	50

Test #	B value	Void Ratio	Silt (%)	D.A. Axial Strain	$\Delta u / \sigma_c$ at N=10 cycles	$\Delta u / \sigma_c$ at N=30 cycles	Initial Liquefaction
ST60	0.96	0.54	10p	0.5	0.42	0.76	98
ST61	0.97	0.58	20p	0.01	0.01	0.02	NF
ST62	0.97	0.58	30p	0.01	0.03	0.05	NF
ST63	0.97	0.95	100p	0.01	0.01	0.04	NF
ST64	0.97	0.58	60p	0.01	0.10	0.20	NF

APPENDIX C

Calibrating the Transducers

Load transducer is calibrated with a 1500 lb. proving ring to set gain for a known load. Steady pressure is used on the upper part of the actuator. The ring is complying with a recognized standard. For a secondary check, for a 3 in. actuator, 60 kpa. is set to 1 volt. output. For a load cell of 1500 lb, 2.5 volts of output is used. The displacement transducer known as a "linear variable differential transformer" (LVDT) consists of electrical coils in a cyclinder casing, through the axis of which a metal core can slide. When a metal load moves, the inductance of the windings is measured electrically and converted to a digital display. LVDT is used to measure the axial deformation of samples in triaxial and consolidation tests. The LVDT is zeroed with no core in place. After the core is replaced, it is located mechanically to zero. Core is displaced a known amount. To do that, a slip gauge is inserted the tip of the transducer stem. Phase is set for maximum reading. Gain is set for calibrated reading for known displacement. 5.08 mm. is set to 1 volt of output.

The pressure transducers should also be calibrated. To calibrate the chamber and effective pressure transducers, the chamber pressure line is moved to steady or backpressure output. Chamber pressure outlet is plugged from oil reservoir. With no pressure, the channels are set to zero. A pressure of 552.5 kpa. is applied. Phase is set for zero reading. Reapplying the pressure to 552.5 kpa., the procedure is repeated since gain changes affects zero also.

To calibrate the volume change transducer, the evacuation chamber reservoir with a long 0.31 cm. tube is used to change the water level. Electronics are set as above for cell

pressure and effective pressure using the 0 and 40 cm. on the 0.635 cm. tube to get 5 volts of output. 40 cm. of water is drawn from each combination of valve G & M and weighed for calculation of calibration factor to enter into calibration portion of software.

The zero of load and pressure transducers should be adjusted prior to opening the shut valve for air pressure to the e/p loader, the program takes care of the reading of volume change without any zeroing by the user. The cell pressure and effective pressure should be around 25 kpa. when zero voltage is applied, as per reading of Le/p. The 50 kpa. should be read on the cyclic pressure as measured by the pressure gage. The zero voltage pressure reading can be adjusted by screw driver through the back of cyclic loader box.

VITA

Duygu Erten

EDUCATION

1983	Watkins Memorial High School
1988	B.S. in Civil Engineering Boğaziçi University
1990	M.S. in Civil & Environmental Engineering Rutgers University
1994	Ph.D. in Civil & Environmental Engineering Rutgers University

EXPERIENCE

1985	Engineering Trainee, STFA-Temel Mühendislik
1987	Surveying Assistant, Boğaziçi University
1989	Research Staff, Princeton University
1990-91	Assistant Geotechnical Engineer, Parsons & Brinckerhoff Construction Company.
1991-1994	Teaching Assistant for courses, Transportation Engineering, Soil Mechanics Laboratory, Mechanics of Solids, Probability and Statistics for Engineers, Foundation Engineering, Soil Mechanics System Administrator of Civil Engineering Computer Laboratory. Instructor for the courses "Introduction to Auto CAD" and "Computer Aided Design and Drawing".

PUBLICATIONS

"Cyclic Undrained Behavior of Silty Sand", Co-author M. H. Maher, Paper accepted for publication in the "*International Journal of Soil Dynamics and Earthquake Engineering," 1994*

"Effect of Fines Content on the Cyclic Undrained Behavior of Sand," Co-author M. H. Maher, Paper accepted for *Proceedings of the Upcoming 3rd. International Conference Recent Advances on Geotechnical Earthquake Engineering, 1994*

"Effect of Fines Content on the Liquefaction Potential of Sand," Co-author M. H. Maher, Paper submitted to the *"Second International Conference on Seismology and Earthquake Engineering," Tehran, Iran, May 1995*

Liquefaction Potential of Silty Soils," Co-author M. H. Maher, Abstract submitted to the *"The International Conference on Soil Dynamics and Earthquake Engineering", Crete, Greece, May 1995.*